NPS-ME-03-003

NAVAL POSTGRADUATE SCHOOL

MONTEREY, CALIFORNIA

DAMPING MODELING STRATEGY FOR NAVAL SHIP SYSTEM

by

Professor Young S. Shin, Principal Investigator
Dr. Ilbae Ham

September 2003

Approved for public release; distribution is unlimited.

Prepared for: Naval Surface Warfare Center-Carderock Division

THIS PAGE INTENTIONALLY LEFT BLANK

REPORT DOCUMENTATION PAGE			*Form Approved OMB No. 0704-0188*
Public reporting burden for this collection of information is estimated to average 1 hour per response, including the time for reviewing instruction, searching existing data sources, gathering and maintaining the data needed, and completing and reviewing the collection of information. Send comments regarding this burden estimate or any other aspect of this collection of information, including suggestions for reducing this burden, to Washington headquarters Services, Directorate for Information Operations and Reports, 1215 Jefferson Davis Highway, Suite 1204, Arlington, VA 22202-4302, and to the Office of Management and Budget, Paperwork Reduction Project (0704-0188) Washington DC 20503.			
1. AGENCY USE ONLY ***(Leave blank)***	**2. REPORT DATE** December 2003	**3. REPORT TYPE AND DATES COVERED** Technical Report, January 2002 - September 2003	
4. TITLE AND SUBTITLE: Damping Modeling Strategy for Naval Ship System			**5. FUNDING NUMBERS** **N0016702WR50152**
6. AUTHOR(S) Young S. Shin and Ilbae Ham			
7. PERFORMING ORGANIZATION NAME(S) AND ADDRESS(ES) Naval Postgraduate School Monterey, CA 93943-5000			**8. PERFORMING ORGANIZATION REPORT NUMBER**: NPS-ME-03-003
9. SPONSORING /MONITORING AGENCY NAME(S) AND ADDRESS(ES) Naval Surface Warfare Center - Carderock Division 9500 MacArthur Blvd. West Bethesda, MD 20817 - 5700			**10. SPONSORING/MONITORING AGENCY REPORT NUMBER**
11. SUPPLEMENTARY NOTES The views expressed in this thesis are those of the author and do not reflect the official policy or position of the Department of Defense or the U.S. Government.			
12a. DISTRIBUTION / AVAILABILITY STATEMENT Approved for public release; distribution is unlimited			**12b. DISTRIBUTION CODE**

13. ABSTRACT (maximum 200 words)

The damping modeling strategy for naval ship system is presented for ship shock transient time-domain analysis. The Complex Exponential Method is used for extraction of modal parameters in time-domain. Inverse Fourier Transform of Mobility form for general viscous damping model is used to verify the calculated modal parameters. Rayleigh damping parameters are calculated using modal frequency and modal damping ratios. The statistical characteristics of Rayleigh damping parameters are quantified and evaluated in each categorized area: keel, bulkhead and deck. Then the Rayleigh damping parameters are recommended for ship shock response prediction. The damping studies were conducted using 2000 ms data based on DDG 53 Ship Shock Trial.

14. SUBJECT TERMS Underwater Explosion, UNDEX, Damping, Shock and Vibration, Ship Shock, Shock Response			**15. NUMBER OF PAGES** 157
			16. PRICE CODE
17. SECURITY CLASSIFICATION OF REPORT Unclassified	**18. SECURITY CLASSIFICATION OF THIS PAGE** Unclassified	**19. SECURITY CLASSIFICATION OF ABSTRACT** Unclassified	**20. LIMITATION OF ABSTRACT** UL

NSN 7540-01-280-5500 Standard Form 298 (Rev. 2-89)
Prescribed by ANSI Std. 239-18

THIS PAGE INTENTIONALLY LEFT BLANK

NAVAL POSTGRADUATE SCHOOL

Monterey, California

RADM David R. Ellison
Superintendent

R.S. Elster
Provost

This report was prepared by:

Young S. Shin
Professor of Mechanical Engineering

Ilbae Ham
Visiting Professor of Mechanical Engineering

Reviewed by:

Anthony J. Healey
Chairman
Dept. of Mechanical Engineering

Released by:

Leonard Ferrari
Associate Provost and
Dean of Research

THIS PAGE INTENTIONALLY LEFT BLANK

ABSTRACT

The damping modeling strategy for naval ship system is presented for ship shock transient time-domain analysis. The Complex Exponential Method is used for extraction of modal parameters in time-domain. Inverse Fourier Transform of Mobility form for general viscous damping model is used to verify the calculated modal parameters. Rayleigh damping parameters are calculated using modal frequency and modal damping ratios. The statistical characteristics of Rayleigh damping parameters are quantified and evaluated in each categorized area: keel, bulkhead and deck. Then the Rayleigh damping parameters are recommended for ship shock response prediction. The damping studies were conducted using 2000 ms data based on DDG 53 Ship Shock Trial.

THIS PAGE INTENTIONALLY LEFT BLANK

TABLE OF CONTENTS

THIS PAGE INTENTIONALLY LEFT BLANK

LIST OF FIGURES

THIS PAGE INTENTIONALLY LEFT BLANK

LIST OF TABLES

THIS PAGE INTENTIONALLY LEFT BLANK

ACKNOWLEDGMENTS

The authors are grateful for full sponsorship given by Naval Surface Warfare Center in both Carderock and Indian Head Division. The authors also extend their gratitude to Mr. Fredrick A. Costanzo in NSWC-CD and Mr. Gregory S. Harris in NSWC-IH for their supports and strong interests in ship system damping. Thanks are also due to LT Jake Didoszak, USN for his excellent job to make comparison of ship shock responses with various damping factors.

THIS PAGE INTENTIONALLY LEFT BLANK

I. INTRODUCTION

Mechanical energy transforms into heat and dissipates in all vibrating systems. There are many energy dissipation mechanisms that contribute to the damping in the structure system. Some of these mechanisms are: fluid resistance and coupling, internal friction (material damping), and friction at a joint. All of these dissipation mechanisms have been shown to be a function of many variables, including a structure's shape or geometry, its material properties, temperature, frequency, boundary conditions, and different excitation energy levels. Usually over 90 percent of the inherent damping associated with fabricated build-up structures originates in the mechanical joints (Beards and Woodwat, 1985). These mechanical joints are friction joints, which dissipate energy during the vibration of a structure. Reducing the contact force in bolted structural connections can reduce system vibration amplitudes by enhancing joint damping capacity (Shin et al., 1991).

Naval ship structure systems have mostly welded joints and all stiffeners are also welded to hull plates, decks and bulkheads. The ship system also has many energy dissipation sources such as long cable trays, hangers, snubbers, the surrounding fluid coupled with ship hull, etc. The ship system damping is measurable, but difficult to quantify (Rutgerson, 2002). In conjunction with ship-shock simulation based transient analysis, time-domain representation of system damping is desirable using the frequency-domain characteristics of damping. The damping studies used for analysis were conducted using 2 sec data from the DDG 53 Ship Shock Trials.

The goal of this study is to present the damping model in Rayleigh damping form of a naval ship system for ship shock transient time domain analysis. In this study, the Complex Exponential Method is used for extraction of modal parameters in the time domain. The Inverse Fourier Transform of Mobility form of the general viscous damping model verifies the calculated modal parameters. Two factors in the Rayleigh damping

model are calculated using modal frequency and modal damping ratios. The statistical characteristics of two Rayleigh factors are quantified in each categorized area. Then the spatially dependent Rayleigh damping model is investigated and a model to be used in shock transient analysis is recommended.

II. THEORY OF GENERAL VISCOUSLY DAMPED SYSTEM

The general equation of motion for a MDOF (Multi Degree Of Freedom) system with viscous damping and harmonic excitation is:

$$[M]\{\ddot{x}\}+[C]\{\dot{x}\}+[K]\{x\}=\{f\} \tag{1}$$

In the above equation, [M] is the system mass matrix, [K] is the system stiffness matrix, [C] is the system damping matrix, {x} is the system response vector and {f} is the forcing vector.

We consider first the case where there is zero excitation in order to determine the natural modes of the system and to this end, we assume a solution to the equations of motion which has the form

$$\{x\}=\{x\}e^{st} \tag{2}$$

Substituting this into the appropriate equation of motion gives:

$$\left(s^2[M]+s[C]+[K]\right)\{x\}=\{0\} \tag{3}$$

the solution of which constitutes a complex eigenvalue problem. In this case, there are 2N eigen values, s_r in complex conjugate pairs. (This is an inevitable result of the fact that all the coefficients in the matrices are real and thus any characteristic values, or roots, must either be real or occur in complex conjugate pairs.) There is an

eigenvector corresponding to each of these eigenvalues, but these also occur as complex conjugates. Hence we can describe the eigensolution as:

$$s_r,\ s_r^* \text{ and } \{s\}_r,\ \{s^*\}_r \quad \text{r = 1, N} \tag{4}$$

It is customary to express each eigenvalues s_r in the form

$$s_r = \omega_r(-\zeta_r + i\sqrt{1-\zeta_r^2}) \tag{5}$$

where ω_r is the 'natural frequency' and ζ_r is the critical damping ratio for that mode. Sometimes, the quantity ω_r is referred to as the 'undamped natural frequency' but this is not strictly correct, except in the case of proportional damping (or, of course, of a single degree of freedom system).

The eigen solution possesses orthogonality. In order to examine these we must first note that any eigenvalue/eigenvector pair satisfies the equation

$$\left(s_r^2[M]+s_r[C]+[K]\right)\{\psi\}_r = \{0\} \tag{6}$$

and then we pre-multiply this equation by $\{\psi\}_q^T$ so that we have:

$$\{\psi\}_q^T\left(s_r^2[M]+s_r[C]+[K]\right)\{\psi\}_r = \{0\} \tag{7}$$

A similar expression to (6) can be produced by using λ_q and $\{\psi\}_q$:

$$\left(s_q^2[M]+s_q[C]+[K]\right)\{\psi\}_q = \{0\} \tag{8}$$

which can be transposed, taking account of the symmetry of the system matrices, to give:

$$\{\psi\}_q^T\left(s_q^2[M]+s_q[C]+[K]\right) = \{0\}^T \tag{9}$$

If we now post-multiply this expression by $\{\psi\}_r$ and subtract the result from that in Equation (7), we obtain:

$$\left(s_r^2 - s_q^2\right)\{\psi\}_q^T[M]\{\psi\}_r + \left(s_r - s_q\right)\{\psi\}_q^T[C]\{\psi\}_r = 0 \tag{10}$$

and provided s_r and s_q are different, this leads to the first of a pair of orthogonality equations:

$$\left(s_r + s_q\right)\{\psi\}_q^T[M]\{\psi\}_r + \{\psi\}_q^T[C]\{\psi\}_r = 0 \tag{11}$$

A second equation can be derived from the above expressions as follows:

Multiply (7) by s_q and (9) by s_r and subtract one from the other to obtain:

$$s_r s_q \{\psi\}_q^T [M] \{\psi\}_r - \{\psi\}_q^T [K] \{\psi\}_r = 0 \tag{12}$$

These two equations - (11) and (12) – constitute the orthogonality conditions of the system and it is immediately clear that they are far less simple. However, it is interesting to examine the form they take when the modes r and q are found as a complex conjugate pair. In this case, we have that

$$s_q = \omega_r (-\zeta_r - i\sqrt{1-\zeta_r^2}) \tag{13}$$

and also that,

$$\{\psi\}_q = \{\psi^*\}_r \tag{14}$$

Inserting these into Equation (11) gives

$$-2\omega_r \zeta_r \{\psi^*\}_r^T [M] \{\psi\}_r + \{\psi^*\}_r^T [C] \{\psi\}_r = 0 \tag{15}$$

from which we obtain:

$$2\omega_r \zeta_r = \frac{\{\psi^*\}_r^T [C] \{\psi\}_r}{\{\psi^*\}_r^T [M] \{\psi\}_r} = \frac{c_r}{m_r} \tag{16}$$

Similarly, inserting (13) and (14) into (12) gives

$$\omega_r^2 \{\psi^*\}_r^T [M] \{\psi\}_r - \{\psi^*\}_r^T [K] \{\psi\}_r = 0 \tag{17}$$

from which

$$\omega_r^2 = \frac{\{\psi^*\}_r^T [K] \{\psi\}_r}{\{\psi^*\}_r^T [M] \{\psi\}_r} = \frac{k_r}{m_r} \tag{18}$$

In these expressions, m_r, k_r, and c_r may be described as modal mass, stiffness and damping parameters respectively although the meaning is slightly different to that used in the other systems.

A. FORCED RESPONSE ANALYSIS

Returning to Equation (1), and assuming a harmonic response:

$$\{x(t)\} = \{x\} e^{i\omega t} \tag{19}$$

we can write the forced response solution directly as

$$\{x\} = \left[[K] - \omega^2 [M] + i\omega [C] \right]^{-1} \{f\} \tag{20}$$

but this expression is not particularly convenient for numerical application. Define a new coordinate vector {y}, which is of order 2N, and which contains both the displacements {x} and the velocities $\{\dot{x}\}$:

$$\{y\} = \begin{Bmatrix} x \\ \dot{x} \end{Bmatrix}_{(2N\times 1)} \tag{21}$$

Equation (1) can then be written as:

$$[C : M]_{N\times 2N}\{\dot{y}\}_{2N\times 1} + [K : 0]\{y\} = \{0\}_{N\times 1} \tag{22}$$

However, in this form we have N equations and 2N unknowns and so we add an identity equation of the type:

$$[M : 0]\{\dot{y}\} + [0 : -M]\{y\} = \{0\} \tag{23}$$

which can be combined to form a set of 2N equations

$$\begin{pmatrix} C & M \\ M & 0 \end{pmatrix}\{\dot{y}\} + \begin{pmatrix} K & 0 \\ 0 & -M \end{pmatrix}\{y\} = \{0\} \tag{24}$$

which can be simplified to:

$$[A]\{\dot{y}\} + [B]\{y\} = \{0\} \tag{25}$$

These equations are now in a standard eigenvalue form and by assuming a trial solution of the form $\{y\} = \{y\}e^{st}$, we can obtain the 2N eigenvalues and eigenvectors of the system, λ_r and $\{\theta\}_r$, which together satisfy the general equation:

$$(\lambda_r[A] + [B])\{\theta\}_r = \{0\}; \qquad \text{r = 1, 2N} \tag{26}$$

These eigen properties will, in general, be complex although for the same reasons as previously they will always occur in conjugate pairs. They possess orthogonality properties, which are simply stated as

$$\begin{aligned} \{\theta\}^T[A]\{\theta\} &= \begin{bmatrix} \ddots & & \\ & a_r & \\ & & \ddots \end{bmatrix} \\ \{\theta\}^T[B]\{\theta\} &= \begin{bmatrix} \ddots & & \\ & b_r & \\ & & \ddots \end{bmatrix} \end{aligned} \tag{27}$$

and which have the usual characteristic that

$$\lambda_r = -\frac{b_r}{a_r} \qquad \text{r = 1, 2N} \tag{28}$$

Now we may express the forcing vector in terms of the new coordinate system as:

$$\{P\}_{2N\times 1} = \begin{Bmatrix} f \\ 0 \end{Bmatrix} \tag{29}$$

and assuming a similarly harmonic response and making use of the previous development of a series form expression of the response. We may write:

$$\begin{Bmatrix} x \\ i\omega x \end{Bmatrix} = \sum_{r=1}^{2N} \frac{\{\theta\}_r^T \{p\} \{\theta\}_r}{a_r (i\omega - s_r)} \tag{30}$$

However, because the eigenvalues and eigenvectors occur in complex conjugate pairs, this last equation may be written as:

$$\begin{Bmatrix} x \\ i\omega x \end{Bmatrix} = \sum_{r=1}^{N} \left(\frac{\{\theta\}_r^T \{p\} \{\theta\}_r}{a_r (i\omega - s_r)} + \frac{\{\theta^*\}_r^T \{p\} \{\theta^*\}_r}{a_r^* (i\omega - s_r^*)} \right) \tag{31}$$

At this stage, it is convenient to extract a single response parameter, say x_j, resulting from a single force such as f_k - the receptance frequency response function, α_j^k, and in this case Equation (31) leads to:

$$\frac{x_j}{f_k} = \alpha_j^k(\omega) = \sum_{r=1}^{N} \left(\frac{{}_r\theta_j \; {}_r\theta_k}{a_r (i\omega - s_r)} + \frac{{}_r\theta_j^* \; {}_r\theta_k^*}{a_r^* (i\omega - s_r^*)} \right) \tag{32}$$

or,

$$\alpha_j^k(\omega) = \sum_{r=1}^{N} \left(\frac{{}_r A_{jk}}{(i\omega - s_r)} + \frac{{}_r A_{jk}^*}{(i\omega - s_r^*)} \right) \tag{34}$$

where, ${}_r A_{jk} = \dfrac{{}_r\theta_j \; {}_r\theta_k}{a_r}$, ${}_r A_{jk}^* = \dfrac{{}_r\theta_j^* \; {}_r\theta_k^*}{a_r^*}$

Equation (34) describes the displacement response at 'j' degree of freedom under excitation at 'k' degree of freedom of general viscously damped system in frequency domain. If Fourier Transform is made onto Equation (34), we can get the Impulse Response Function $h_{jk}(t)$ of this system.

$$h_{jk}(t) = \frac{1}{2\pi} \int_{-\infty}^{\infty} \sum_{r=1}^{N} \left(\frac{{}_r A_{jk}}{(i\omega - s_r)} + \frac{{}_r A_{jk}^*}{(i\omega - s_r^*)} \right) e^{i\omega t} \, d\omega \tag{35}$$

If we let $(i\omega - s_r)$ as iz, then, by Cauchy's Integral Formula, it becomes:

$$\frac{1}{2\pi} \int_{-\infty}^{\infty} \frac{{}_r A_{jk}}{(i\omega - s_r)} e^{i\omega t} \, d\omega = \frac{{}_r A_{jk} e^{s_r t}}{2\pi i} \int_{-\infty}^{\infty} \frac{e^{izt}}{z} dz = {}_r A_{jk} e^{s_r t} \tag{36}$$

and similarly,

$$\frac{1}{2\pi} \int_{-\infty}^{\infty} \frac{{}_r A_{jk}^*}{(i\omega - s_r^*)} e^{i\omega t} \, d\omega = \frac{{}_r A_{jk}^* e^{s_r^* t}}{2\pi i} \int_{-\infty}^{\infty} \frac{e^{izt}}{z} dz = {}_r A_{jk}^* e^{s_r^* t} \tag{37}$$

From Equations (36) and (37), the Impulse Response Function of a general viscous damping system can be written as:

$$h_{jk}(t) = \sum_{r=1}^{N} \left({}_{r}A_{jk}\, e^{s_r t} + {}_{r}A_{jk}^{*}\, e^{s_r^{*} t} \right) \tag{38}$$

The forced response can then be calculated as Equation (39) in time domain.

$$x_j = \int_0^t f_k(\tau)\, h_{jk}(t-\tau)\, d\tau \tag{39}$$

THIS PAGE INTENTIONALLY LEFT BLANK

III. PROCEDURE OF DAMPING CALCULATION FROM MEASURED DATA

A. MODAL PARAMETER EXTRACTION

In Equation (34), ${}_rA_{jk}$, ${}_rA_{jk}^*$, s_r, s_r^* are called modal parameters, ${}_rA_{jk}$, ${}_rA_{jk}^*$ are called modal constants, and eigenvalues s_r, s_r^* contain information of modal properties such as modal frequency ω_r and modal damping ratio ζ_r. Calculation of damping ratio from the measured shock trial data needs utilizing modal parameter extraction methods, the simple 3-dB (half power) bandwidth measurement or logarithmic decay rate calculation can be incorrect in real cases, because, in usual cases, real measurement data not only contain noise components but also have many closely coupled frequency components.

Basically there are two groups of techniques in the field of experimental modal analysis. One is related to frequency domain analysis methods that use Frequency Response Function of measured input and output data. This group of methods is widely used, from single degree of freedom circle fitting to complex multi-degree of freedom fitting methods. And the other is related to time domain analysis techniques that use Impulse Response Function as analysis data.

In this study, the time domain method is used because the measured useful shock trial data sets are too short in time to obtain sufficient frequency resolution in the frequency domain, and there is only one event, shot data, thus the averaging process cannot be done. Complex Exponential Method (CEM), one of the effective modal parameter extraction methods in the time domain, is used to extract modal parameters.

The 2 second long measured data has been used in this study and the effective frequency span is limited from 3 Hz to 250 Hz. The original measured data has been band-pass filtered from 2 Hz to 250 Hz to avoid long-term trends in low frequencies and to remove unwanted high frequency noise components.

1. Complex Exponential Method (CEM)

In the field of experimental modal analysis, a term Receptance is widely used to describe the ratio of displacement response to excitation force, and the term Mobility is used in describing the ratio of velocity response to excitation force. The Receptance (displacement/force) $\alpha(\omega)$ of a general viscously damped system, Equation (34), can be rewritten as Equation (40), complex eigenvalue s_r is as in Equation (40.a),

$$\alpha(\omega) = \sum_{r=1}^{N} \frac{A_r}{j\omega - s_r} + \frac{A_r^*}{j\omega - s_r^*} \quad ; \quad s_r = -\omega_r \zeta_r + j\omega_r \sqrt{1-\zeta_r^2} \qquad (40.a)$$

or,

$$\alpha(\omega) = \sum_{r=1}^{2N} \frac{A_r}{j\omega - s_r} \quad ; \quad s_r \Rightarrow s_r^*, \quad A_r \Rightarrow A_r^* \quad , for \quad r > N \qquad (40.b)$$

we can get velocity $v = Ve^{j\omega t}$ by time differentiating displacement $x = Xe^{j\omega t}$, that is,

$$v = V(\omega)e^{j\omega t} = j\omega X e^{j\omega t} \qquad (\ )$$

and Mobility(velocity/force) Y(ω) can be related to $\alpha(\omega)$ (displacement/force),

$$Y(\omega) = j\omega\alpha(\omega) \tag{41}$$

The corresponding Impulse Response Function (IRF) can be obtained by taking Inverse Fourier Transform (IFT) of the Receptance $\alpha(\omega)$ as Equations (35) through (38),

$$h\ (t) = \sum_{r=1}^{2N} A_r e^{s_r t} \tag{42}$$

By time differentiating, the velocity form of IRF can be expressed as,

$$\dot{h}\ (t) = \sum_{r=1}^{2N} A_r s_r e^{s_r t} \tag{43}$$

Then the measured velocity data set sampled by Δt time steps can be expressed as follows:

$$\dot{h}_0,\ \dot{h}_1,\ \dot{h}_2, \cdots\cdots,\ \dot{h}_q = \dot{h}(0),\ \dot{h}(\Delta t),\ \dot{h}(2\Delta t), \cdots\cdots,\ \dot{h}(q\Delta t) \tag{44}$$

Hereafter, the exponential term will be simplified using the following notation.

$$e^{s_r \Delta t} \rightarrow V_r \tag{45}$$

Thus for the j-th sample data, the Equation (43) becomes,

$$\dot{h}_j = \sum_{r=1}^{2N} A_r s_r V_r^j \tag{46}$$

which, when extended to the full data set of q samples (j=1,2,….,q), gives:

$$\begin{aligned}
\dot{h}_0 &= s_1 A_1 + s_2 A_2 + \cdots\cdots + s_{2N} A_{2N} \\
\dot{h}_1 &= V_1 s_1 A_1 + V_2 s_2 A_2 + \cdots\cdots + V_{2N} s_{2N} A_{2N} \\
\dot{h}_2 &= V_1^2 s_1 A_1 + V_2^2 s_2 A_2 + \cdots\cdots + V_{2N}^2 s_{2N} A_{2N} \\
&\vdots \qquad \vdots \qquad \vdots \qquad\qquad \vdots \\
\dot{h}_q &= V_1^q s_1 A_1 + V_2^q s_2 A_2 + \cdots\cdots + V_{2N}^q s_{2N} A_{2N}
\end{aligned} \tag{47}$$

Provided that the number of sample points q exceeds 4N, this equation can be used to set up an eigenvalue problem, the solution yields the complex natural frequencies contained in the parameters V_1, V_2, etc.

Multiply each equation in (47) by a coefficient, β_j to form the following set of equations:

$$\begin{aligned}
\beta_0 h_0 &= \beta_0 A_1 + \beta_0 A_2 + \cdots\cdots + \beta_0 A_{2N} \\
\beta_1 h_1 &= \beta_1 V_1 A_1 + \beta_1 V_2 A_2 + \cdots\cdots + \beta_1 V_{2N} A_{2N} \\
\beta_2 h_2 &= \beta_2 V_1^2 A_1 + \beta_2 V_2^2 A_2 + \cdots\cdots + \beta_2 V_{2N}^2 A_{2N} \\
&\vdots \qquad \vdots \qquad \vdots \qquad\qquad \vdots \\
\beta_q h_q &= \beta_q V_1^q A_1 + \beta_q V_2^q A_2 + \cdots\cdots + \beta_q V_{2N}^q A_{2N}
\end{aligned} \tag{48}$$

Adding all equations in (48) vertically results in,

$$\sum_{i=0}^{q} \beta_i \dot{h}_i = \sum_{j=1}^{2N} (A_j \sum_{i=0}^{q} \beta_i V_j{}^i) \tag{49}$$

The coefficients β_j s are taken to be the coefficients in the polynomial equation,

$$\beta_0 + \beta_1 V + \beta_2 V^2 + \beta_3 V^3 + \cdots\cdots + \beta_q V^q = 0 \tag{50}$$

The roots are $V_1, V_2, \cdots, V_q$.

Next, the values of the β coefficients are to be sought in order to determine the roots of Equation (50) - values of V_r - and hence the system natural frequencies. Now, recalling that q is the number of degrees of freedom of the system model. It is now convenient to set these two parameters to the same value, i.e. let q = 2N .

If we find β coefficients that make Equation (50) fulfilled, then Equation (50) can be expressed as,

$$\sum_{j=0}^{2N} \beta_j V_r^j = 0 \quad ; \quad \text{r} = 1, 2\text{N} \tag{51}$$

And thus every term on the right-hand side of Equation (49) is zero.

$$\sum_{i=0}^{2N} \beta_i \dot{h}_i = 0 \tag{52}$$

Rearranging Equation (52), by moving the last term of left-hand side to right-hand side,

$$\sum_{i=0}^{2N-1} \beta_i \dot{h}_i = -\dot{h}_{2N} \qquad \text{by setting } \beta_{2N} = 1 \tag{53}$$

Repeat the process from (44) to (53) using different set of IRF data points and further choose the new data set that overlaps considerably with the first set – In fact, for all but one item.

Successive applications of this procedure lead to a full set of 2N equations:

$$\begin{bmatrix} \dot{h}_0 & \dot{h}_1 & \dot{h}_2 & \cdots & \dot{h}_{2N-1} \\ \dot{h}_1 & \dot{h}_2 & \dot{h}_3 & \cdots & \dot{h}_{2N} \\ \vdots & \vdots & \vdots & \vdots & \vdots \\ \dot{h}_{2N-1} & \dot{h}_{2N} & \dot{h}_{2N+1} & \cdots & \dot{h}_{4N-2} \end{bmatrix} \begin{Bmatrix} \beta_0 \\ \beta_1 \\ \vdots \\ \beta_{2N-1} \end{Bmatrix} = - \begin{Bmatrix} \dot{h}_{2N} \\ \dot{h}_{2N+1} \\ \vdots \\ \dot{h}_{4N-1} \end{Bmatrix} \tag{54.a}$$

or,

$$\left[\dot{h}\right]_{2N\times 2N} \{\beta\}_{2N\times 1} = -\left\{\tilde{h}\right\}_{2N\times 1} \tag{54.b}$$

The unknown coefficients {β} can be found from Equation (54). Now the values of V_1, V_2, …, V_{2N} can be determined using Equation (50) and subsequently the system natural frequencies can be found using the following relationship.

$$V_r = e^{s_r \Delta t} \tag{55}$$

Using Equation (47), corresponding modal constants A_1, A_2, …, A_{2N} can be calculated, this may be written as,

$$\begin{bmatrix} 1 & 1 & 1 & \cdots & 1 \\ V_1 & V_2 & V_3 & \cdots & V_{2N} \\ V_1^2 & V_2^2 & V_3^2 & \vdots & V_{2N}^2 \\ \vdots & \vdots & \vdots & \cdots & \vdots \\ V_1^{2N-1} & V_2^{2N-1} & V_3^{2N-1} & \cdots & V_3^{2N-1} \end{bmatrix} \begin{Bmatrix} A_1 s_1 \\ A_2 s_2 \\ A_3 s_3 \\ \vdots \\ A_{2N} s_{2N} \end{Bmatrix} = \begin{Bmatrix} \dot{h}_0 \\ \dot{h}_1 \\ \dot{h}_2 \\ \vdots \\ \dot{h}_{2N-1} \end{Bmatrix} \tag{56}$$

or

$$[V]\{A\} = \{h\} \tag{57}$$

2. Verification of Extracted Modal Parameters

The modal parameters calculated according to the mentioned procedure can be verified by comparing synthesized time histories to the originally measured time histories. Mobilities can be determined by frequency differentiation, multiplied by $j\omega$, from Equations (40) and (41),

$$\hat{Y}(\omega) = \sum_{r=1}^{N} \frac{j\omega A_r}{j\omega - s_r} + \frac{j\omega A_r^*}{j\omega - s_r^*} \quad ; \quad s_r = -\omega_r \zeta_r + j\omega_r \sqrt{1-\zeta_r^2} \tag{58}$$

or

$$\hat{Y}(\omega) = \sum_{r=1}^{2N} \frac{j\omega A_r}{j\omega - s_r} \quad ; \quad s_r \Rightarrow s_r^*, \; A_r \Rightarrow A_r^* \; , for \;\; r > N \tag{59}$$

In Equations (58) and (59), extracted modal parameters A_r, A_r^*, s_r, s_r^* are used to calculate the synthesized Frequency Response Function in frequency domain. And by inverse Fast Fourier Transform (IFFT), taking the real part of the results, synthesized IRF can be calculated and compared to original time histories. Frequency bandwidth Δf should be multiplied during calculation procedure to generate band level.

$$\left\{ \hat{\dot{h}} \right\} = \mathrm{Re}\, al \;\; Part \;\; of \;\; Inverse \;\; FFT\left(\Delta f \, \hat{Y} \right) \tag{60}$$

3. Calculation of Rayleigh Damping

Rayleigh damping is a kind of general proportional damping model. It assumes that damping matrix [C] in Equation (1) can be represented as linear combination of the mass matrix and stiffness matrix. Then the damping matrix can be easily decoupled to the modal damping matrix. Using the Rayleigh damping representation, the damping matrix can be represented as,

$$[C]=\alpha[M]+\beta[K] \tag{61}$$

or by using mass normalized modal matrix $[\varphi]$,

$$[\varphi]^T[C][\varphi]=[2\omega_r\zeta_r]_{diag}=\alpha I+\beta\left[\omega_r^2\right]_{diag} \tag{62}$$

By using Equation (62) for all 2N modes, following 2N equations can be set.

$$\begin{aligned}
&\alpha+\beta\omega_1^2=2\omega_1\zeta_1\\
&\alpha+\beta\omega_2^2=2\omega_2\zeta_2\\
&\quad\vdots\\
&\alpha+\beta\omega_{2N}^2=2\omega_{2N}\zeta_{2N}
\end{aligned} \tag{63}$$

or

$$[W]_{2N\times 2}\begin{Bmatrix}\alpha\\ \beta\end{Bmatrix}=\{Z\}_{2N\times 1} \tag{64}$$

If 2N is larger than 2, then Equation (64) becomes over-determined, with 2 unknowns and 2N equations. By post-multiplying the transpose matrix of [W] to both sides of Equation (64), we can get Equation (65).

$$[W]^T_{2\times 2N}[W]_{2N\times 2}\begin{Bmatrix}\alpha\\ \beta\end{Bmatrix}=[W]^T_{2\times 2N}\{Z\}_{2N\times 1} \tag{65}$$

Then two Rayleigh parameters α and β are calculated as,

$$\begin{Bmatrix}\alpha\\ \beta\end{Bmatrix}=\left([W]^T_{2\times 2N}[W]_{2N\times 2}\right)^{-1}[W]^T_{2\times 2N}\{Z\}_{2N\times 1} \tag{66}$$

As a final step, modal damping ratios for each vibration modes are calculated in each categorized area of ship.

$$\zeta = \alpha\frac{1}{2\omega}+\beta\frac{\omega}{2} \tag{67}$$

IV. RESULTS OF MODAL PARAMETER EXTRACTION

A. VERIFICATION RESULTS

Modal parameters for a total of 773 sets of measured data are calculated for each measuring position and direction.

The following figures show some results of the modal parameter extraction method according to the aforementioned procedure. Figure 1, Figure 3, and Figure 5 show the original measured data sets, while Figure 2, Figure 4, and Figure 6 show synthesized curves with the calculated modal parameters ω_r, ζ_r and A_r. The black line shows parts of the original signal between the 125 msec point and the 1200 msec point. The red line stands for the synthesized curve of those parts. The 125 msec parts of each of the measured data sets are not included in analysis to avoid being mixed with the effect of excitation signal. Also the latter parts that contain the secondary excitation are not included in the analysis. This secondary excitation can be seen on Figure 1, Figure 3, and Figure 5 around the 1250 msec point.

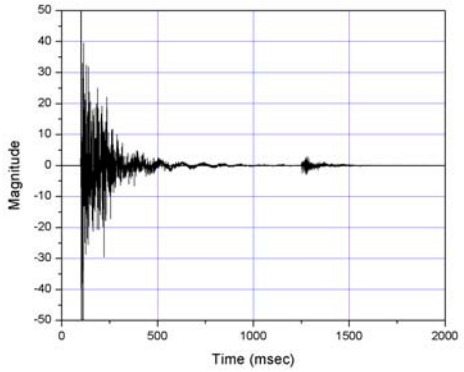

Figure 1. Measured Data at A2001AI

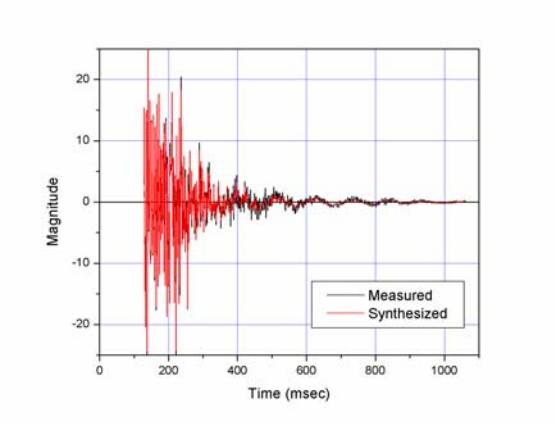

Figure 2. Synthesized Results at A2001A (between 125 msec and 1200 msec)

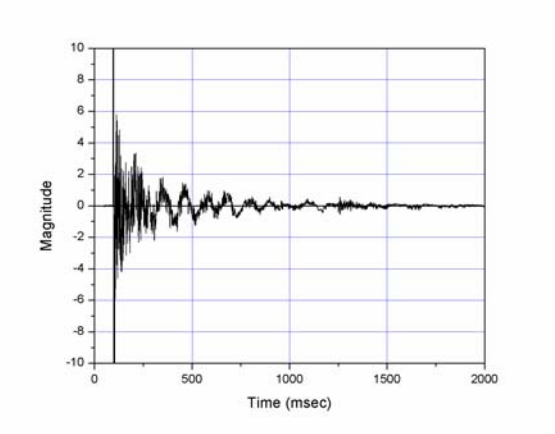

Figure 3. Measured Data at A2004A

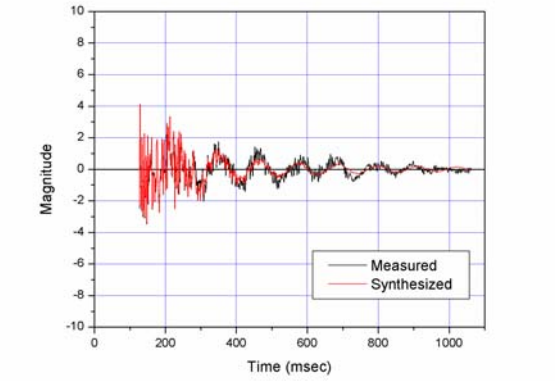

Figure 4. Synthesized Results at A2004A (between 125 msec to 1200msec)

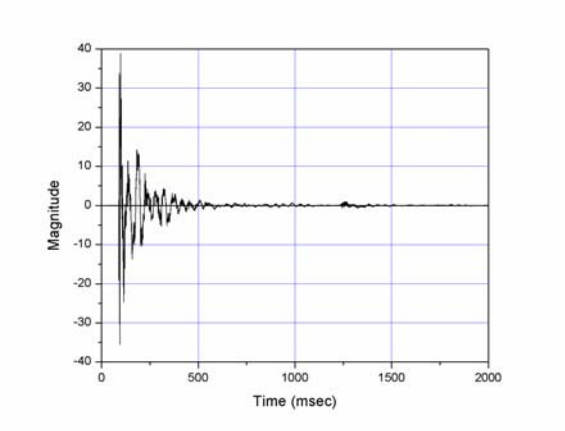

Figure 5. Measured Data at A3506V

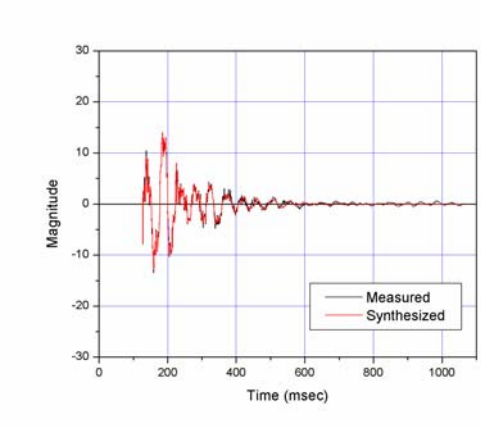

Figure 6. Synthesized Results at A3506 (between 125 msec and 1200 msec)

B. RESULTS OF RAYLEIGH DAMPING CALCULATION

A total of 773 data sets were categorized into 67 area groups, based on the location of the measuring sensor installation, as well as by the direction of measurement, which were the athwartship and vertical directions of the ship.

Figure 7 through Figure 10 show some typical results of the Rayleigh Damping coefficients calculated according to the aforementioned procedure, using Equations (61) through (67). Each black square point is a mode. The red lines represent the regenerated modal damping ratio using α and β calculated in least-square sense.

Each figure tagged as 'Original' in caption is from the initial step results, whereas the others are of the final results, which have been modified by eliminating the unrealistic and noisy components. From the 'Original' figures, we can identify that some of the results are scattered and contain damping ratios, which cannot be regarded as reasonable against the physical sense. Some modifications to the above results have been made. The unreasonable damping data points have been removed from curve fitting α and β. The modes of which modal constants A_r are seriously less than one thousandth of the maximum value in each measuring position have been removed. The modes that contain damping ratios, which are greater than 0.5 have been removed. Likewise, the modes with damping ratios that contain a great deal of scattered from the initial curve-fitted have been also removed. The final results are shown in both of linear scales and logarithmic scales.

The figures presented in Appendix A illustrate the damping calculation results for the remaining areas that were studied.

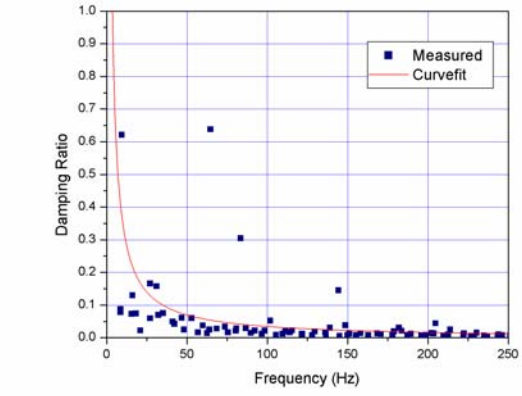

Figure 7. Modal Damping Ratio at Area 6, Athwartship Direction (Original)

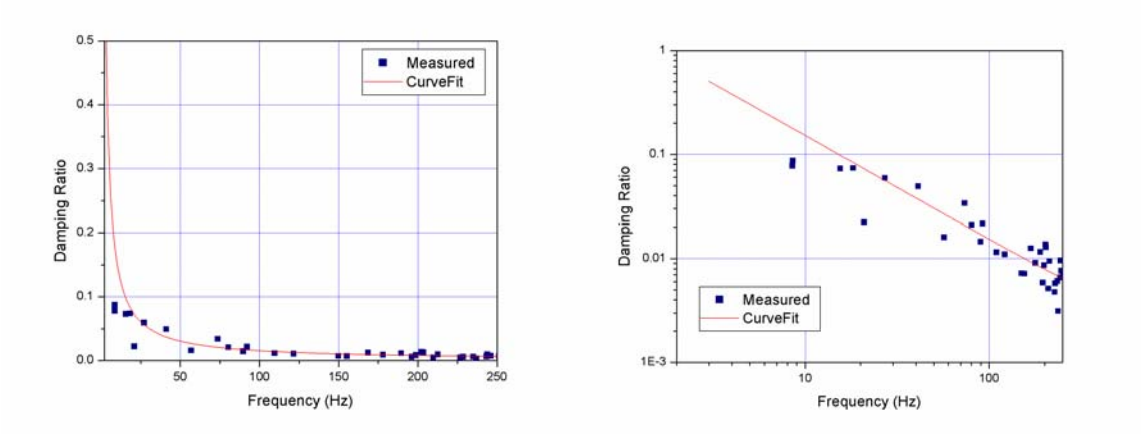

(in Linear Scale) (in Logarithmic Scale)

Figure 8. Modal Damping Ratio at Area 6, Athwartship Direction (Modified)

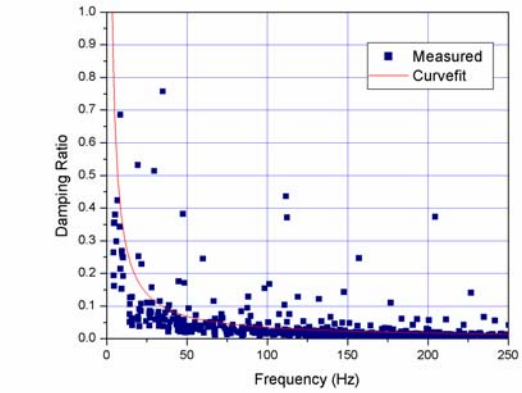

Figure 9. Modal Damping Ratio at Area 6, Vertical Direction (Original)

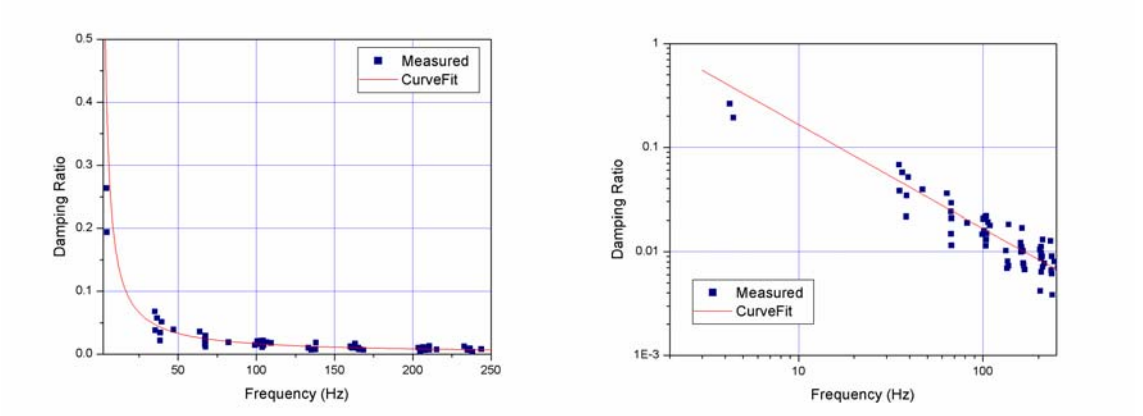

(in Linear Scale) (in Logarithmic Scale)

Figure 10. Modal Damping Ratio at Area 6, Vertical Direction (Modified)

C. CURVE-FITTED RAYLEIGH DAMPING α AND β FOR EACH AREA

The Curve-fitted Rayleigh damping coefficients, α and β, for each categorized area are presented in Table 1 and Table 2, for the athwartship and vertical directions, respectively. Figure 2 is a profile view of the DDG 51 Arleigh Burke Class Destroyer. This drawing shows the major transverse frame positions of the ship.

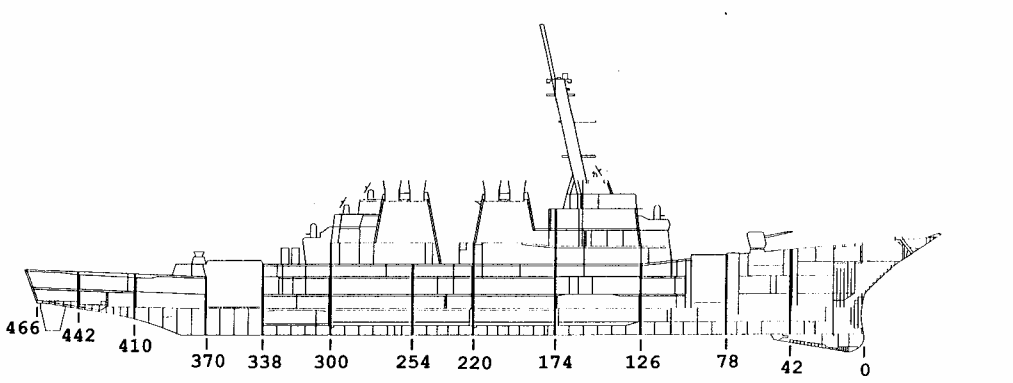

Figure 11. Transverse Frame Locations of the DDG 51 Class Destroyer

Table 1. Rayleigh Damping Results for the Athwartship Direction by Area Group

Area No.	Deck	Frame	Athwartship Position p = port s = starboard	Alpha	Beta	Number of modes used in curvefitting α and β
3	1	56	4'p-2's	2.05E+01	1.22E-06	70
6	1	126.5	CL-5's	2.14E+01	4.69E-06	8
7	1	142	20'p-20's	1.91E+01	5.08E-07	60
8	1	135	17's	1.29E+01	1.11E-05	35
10	1	171.5	CL-15's	2.09E+01	1.90E-06	61
11	1	37.5	5'p-CL	1.79E+01	1.04E-06	37
12	1	258	8'p	1.88E+01	5.74E-06	13
15	1	328	5'p-5's	1.71E+01	4.23E-06	71
16	1	375	25'p-20'p	1.90E+01	3.07E-06	31
18	2	86.5	11'p-11's	1.76E+01	1.34E-06	107
19	2.5	155	31'p-31's	2.04E+01	2.44E-07	60
20	2	137	22'p-CL	1.91E+01	1.72E-06	35
28	2	70	6's-10's	2.03E+01	2.11E-06	31
30	2.5	355.5	10'p-11's	1.95E+01	2.49E-07	55

Area No.	Deck	Frame	Athwartship Position p = port s = starboard	Alpha	Beta	Number of modes used in curvefitting α and β
31	2.5	398	CL-8's	1.67E+01	1.50E-05	11
32	3	192.5	6'p-23's	2.14E+01	2.63E-06	26
33	3	277	20'p-14's	1.98E+01	4.04E-06	53
35	3	129	6'p-CL	2.45E+01	5.90E-06	11
37	3	151	36'p-36's	1.76E+01	2.34E-06	59
40	3	331.5	3's-CL	1.84E+01	2.18E-05	11
41	3	397.5	13'p-CL	1.94E+01	1.39E-06	54
43	3.5	156	8'p-2's	2.00E+01	8.14E-07	125
48	4	174	11'p-11's	1.35E+01	1.91E-06	21
49	4	232.5	6'p-CL	2.23E+01	-1.26E-08	33
53	5	280	CL	1.66E+01	1.16E-05	19
54	5	322.5	17'p-15's	1.90E+01	1.30E-06	75
55	6	150	CL	2.05E+01	3.75E-06	29
56	6	160	CL	1.97E+01	3.11E-06	21
57	7	150	CL	1.77E+01	1.30E-05	8
58	7.5	155.5	8's-CL	1.11E+01	8.42E-06	22
60	8	173.5	32'p-32's	1.40E+01	4.19E-06	63
61	9	168	CL	1.17E+01	2.69E-06	32
62	9	171.5	25'p-25's	1.27E+01	3.82E-06	33
64	10	174	6's-10's	1.93E+01	3.48E-06	17
65	11	181	CL	1.58E+01	7.18E-06	12
67	MD	281.5	4's-5's	2.02E+01	3.14E-06	21

Table 2. Rayleigh Damping Results for the Vertical Direction by Area Group

Area No.	Deck	Frame	Athwartship Position p = port s = starboard	Alpha	Beta	Number of modes used in curvefitting α and β
1	1	60	2'p	2.12E+01	3.54E-06	12
3	1	56	4'p-2's	1.96E+01	4.22E-07	33
4	1	100	15's	1.95E+01	4.08E-06	26
5	1	110	CL	1.97E+01	1.62E-06	55
6	1	126.5	CL-5's	2.16E+01	2.31E-07	12
7	1	142	20'p-20's	2.09E+01	2.11E-07	104
8	1	135	17's	2.05E+01	7.79E-06	26
9	1	159	6'p-4's	2.04E+01	1.07E-06	28
10	1	171.5	CL-15's	2.03E+01	1.16E-06	41

Area No.	Deck	Frame	Athwartship Position p = port s = starboard	Alpha	Beta	Number of modes used in curvefitting α and β
11	1	37.5	5'p-CL	2.04E+01	2.77E-07	16
12	1	258	8'p	2.41E+01	3.18E-05	5
13	1	312.5	6'p-19s	1.67E+01	5.24E-07	79
14	1	324	7'p-6'p	1.96E+01	2.82E-06	21
15	1	328	5'p-5's	2.00E+01	4.19E-07	44
16	1	375	25'p-20'p	1.79E+01	8.38E-07	129
17	1	218	28'p-CL	1.55E+01	1.91E-06	72
18	2	86.5	11'p-11's	1.85E+01	1.82E-06	69
19	2.5	155	31'p-31's	2.03E+01	-7.33E-08	42
20	2	137	22'p-CL	1.92E+01	7.08E-07	77
21	2	134	15's	1.63E+01	2.06E-06	22
22	2	161	12'p-3's	1.67E+01	3.18E-06	115
23	2	162	9's	2.06E+01	1.52E-06	39
24	2	306	4'p-7's	1.87E+01	1.53E-07	19
25	2	35	3'p-11's	2.23E+01	8.53E-07	34
26	2	452	6'p	1.94E+01	3.00E-07	28
27	2	458.5	12's-22's	1.84E+01	2.20E-06	46
28	2	70	6's-10's	1.75E+01	1.48E-06	31
29	2	75	12'p-3'p	2.11E+01	2.17E-06	19
30	2.5	355.5	10'p-11's	1.88E+01	8.61E-07	38
31	2.5	398	CL-8's	2.07E+01	1.51E-06	67
32	3	192.5	6'p-23's	1.70E+01	3.62E-06	55
33	3	277	20'p-14's	2.00E+01	9.57E-07	99
34	3	119.5	4'p-6's	1.90E+01	1.02E-06	19
35	3	129	6'p-CL	1.96E+01	2.51E-06	40
36	3	149	19'p-16'p	2.16E+01	3.84E-06	5
37	3	168	12's	2.22E+01	1.73E-06	19
37	3	151	36'p-36's	1.63E+01	9.65E-07	54
38	3	318 -320	2'p-15's	2.22E+01	2.72E-07	65
40	3	331.5	3's-CL	2.07E+01	1.86E-06	47
41	3	397.5	13'p-CL	1.50E+01	2.77E-06	32
42	3.5	150	19'p-6's	1.81E+01	1.63E-06	49
43	3.5	156	8'p-2's	2.11E+01	1.50E-06	49
44	3.5	147	16'p-15'0	1.80E+01	2.82E-06	59
46	4	150	15's	2.23E+01	1.49E-06	31
47	4	156	3'p-CL	2.12E+01	1.27E-07	14
48	4	174	11'p-11's	1.90E+01	2.65E-07	25
49	4	232.5	6'p-CL	1.84E+01	1.01E-06	30
50	4	292	CL	1.66E+01	2.13E-06	16
51	4	78	2'p	1.77E+01	3.45E-06	7

Area No.	Deck	Frame	Athwartship Position p = port s = starboard	Alpha	Beta	Number of modes used in curvefitting α and β
52	4	96	CL	2.00E+01	2.52E-05	12
53	5	280	CL	2.04E+01	-5.41E-08	42
54	5	322.5	17'p-15's	1.91E+01	3.35E-06	26
55	6	150	CL	2.25E+01	3.10E-07	17
56	6	160	CL	2.03E+01	5.66E-05	12
57	7	150	CL	2.35E+01	5.21E-06	7
60	8	173.5	32'p-32's	1.01E+01	6.16E-06	10
61	9	168	CL	1.90E+01	9.63E-06	10
62	9	171.5	25'p-25's	2.09E+01	4.86E-07	89
63	10	174	3's-CL	2.29E+01	-1.24E-07	16
65	11	181	CL	2.01E+01	4.57E-06	15
66	HOLD	433	2'p	1.29E+01	1.24E-05	10
67	MD	281.5	4's-5's	2.02E+01	2.84E-05	4

Table 3 shows the weighted mean value of α for each of the directions of motion. The weighting factor, shown in the rightmost column of Table 1, is defined as the number of modes used in the curve-fitting α and β. Thus, it can be concluded that weighted mean values of α are similar in both directions.

Table 4 shows the weighted mean value of β for each direction of motion, the weighting factor is the rightmost column of Table 2, the number of modes used in curve-fitting α and β. It can be concluded that weighted mean values in athwartship direction are slightly larger than those of the vertical direction. Equation 68 is used to calculate the mean α coefficient,

$$\alpha_{mean} = \frac{\sum_{i=1}^{M} \alpha_i N_i}{\sum_{i=1}^{M} N_i} \tag{68}$$

where the variable M stand for the of areas to be considered .

Table 3. Weighted Mean of α

Athwartship Direction	Vertical Direction
18.4	19.2

Table 4. Weighted Mean of β

Athwartship Direction	Vertical Direction
2.82E-06	2.09E-06

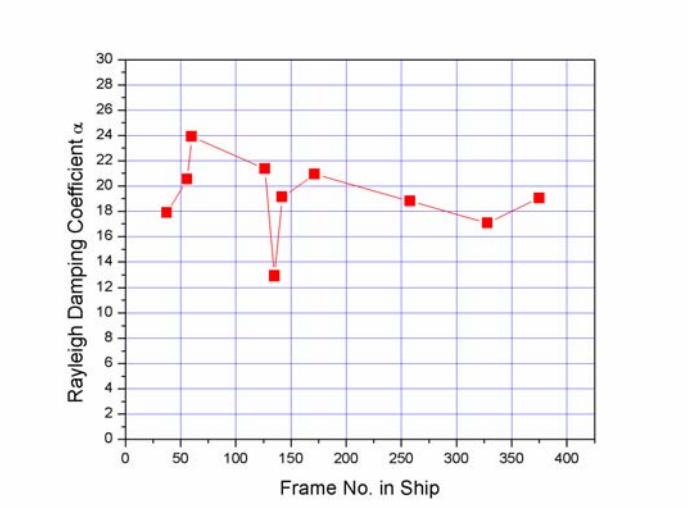

Figure 12. Rayleigh Damping Coefficient α for Athwartship Direction on Deck 1

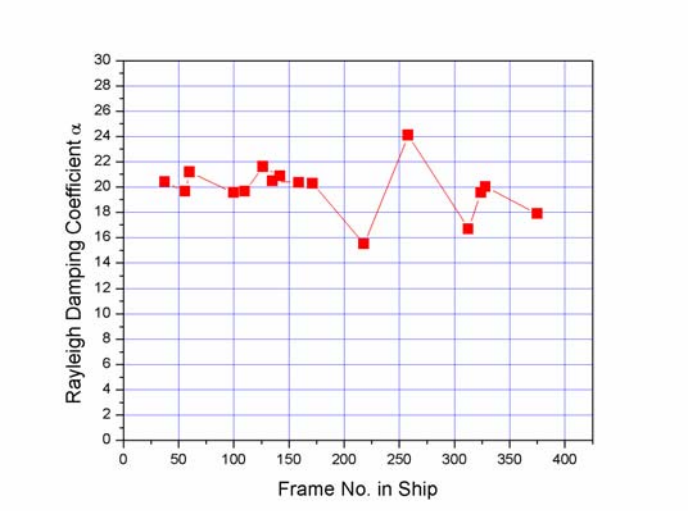

Figure 13. Rayleigh Damping Coefficient α for Vertical Direction on Deck 1

V. EFFECTS OF DAMPING TO SHIP SHOCK RESPONSES

In the 1994, the USS JOHN PAUL JONES (DDG 53) was chosen as the representative ship of the DDG 51 Arleigh Burke Class Destroyer and subsequently subjected to a series of shock trials. Some seven years later in the summer of 2001, similar ship shock trials were conducted on the USS WINSTON S. CHURCHILL (DDG 81). This latter series of live fire tests was performed on the 31st ship in the same class due to the significant design changes incorporated into the Flight IIA version of this ship. Some of the significant changes that were found in DDG 81 included an extension in the ship's overall length and the additional of two helicopter hangers.

Starting with a highly complex finite element model of the ship and the surrounding fluid mesh, shown in Figure 14, the shock response velocity was calculated for various locations throughout the ship using the modeling and simulation process outlined in Figure 15 [4].

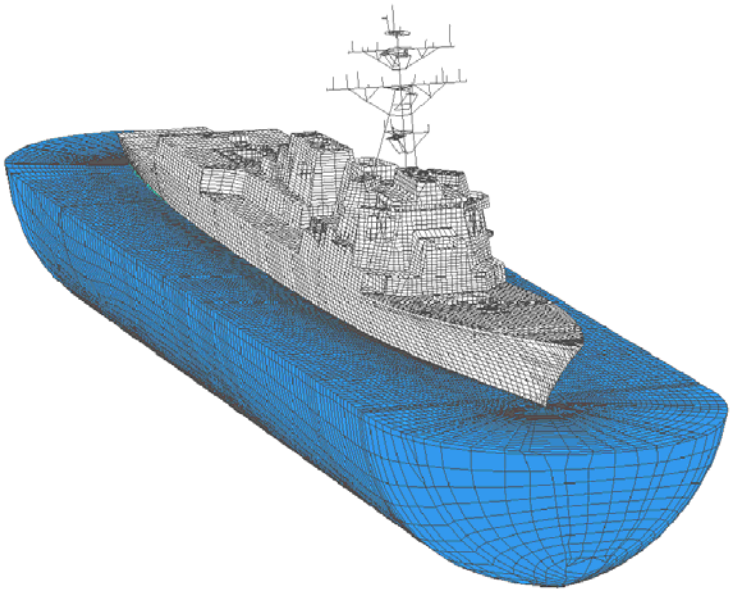

Figure 14. DDG 81 Coupled Fluid-Structure Model

The results of this process were compared with the actual ship shock trial sensor data obtained during the 2001 Live Fire Testing and Evaluation.

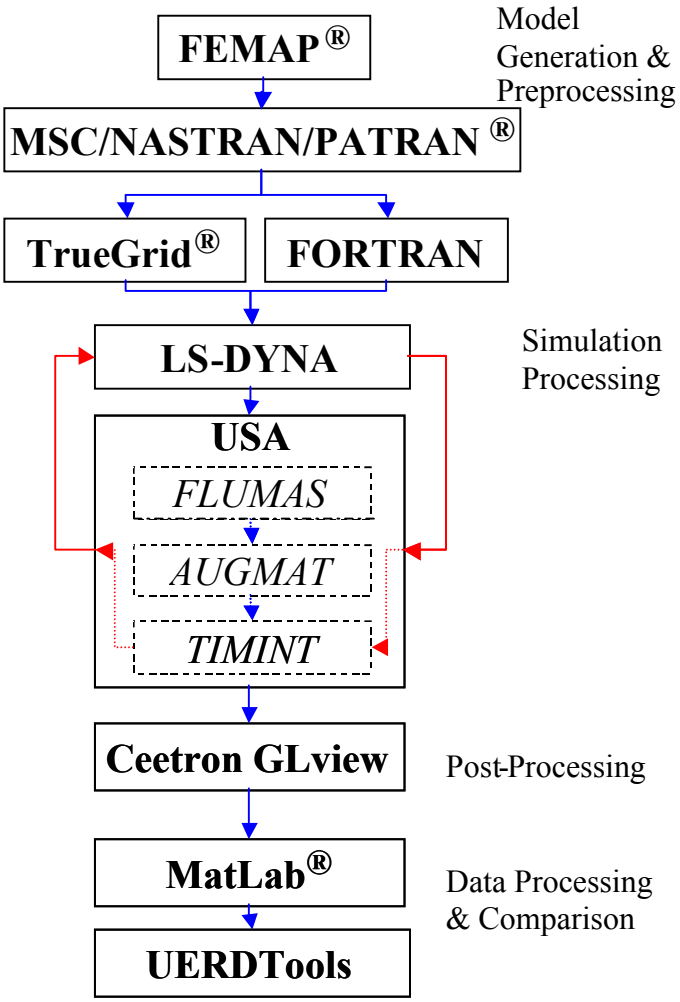

Figure 15. Model Generation and Simulation Flow Chart

Additionally the shock velocity response plots obtained from the aforementioned process were compared against the earlier conducted simulations that used the Rayleigh Damping Coefficients previously used in the DDG 53 modeling and simulation effort, which occurred during the mid 1990's at the Naval Postgraduate School. The values for these coefficients are listed in Table 5.

Table 5. Rayleigh Damping Coefficient for 4% & 8% Proportional Damping

Damping Value	α	β
4%	2.64	4.99E-5
8%	4.93	9.89E-5

In this case the Rayleigh parameters (α, β) were based on evaluation of the damping values at two given points, 5 Hz and 250 Hz, which cover the range of data which was required for subsequent comparisons.

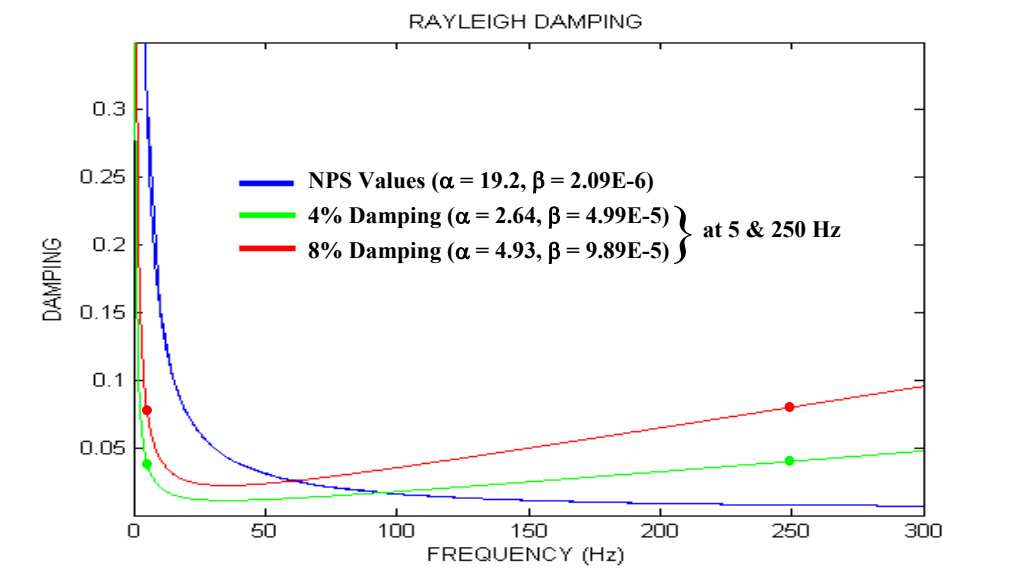

Figure 16. Rayleigh Damping Values (in Linear Scale)

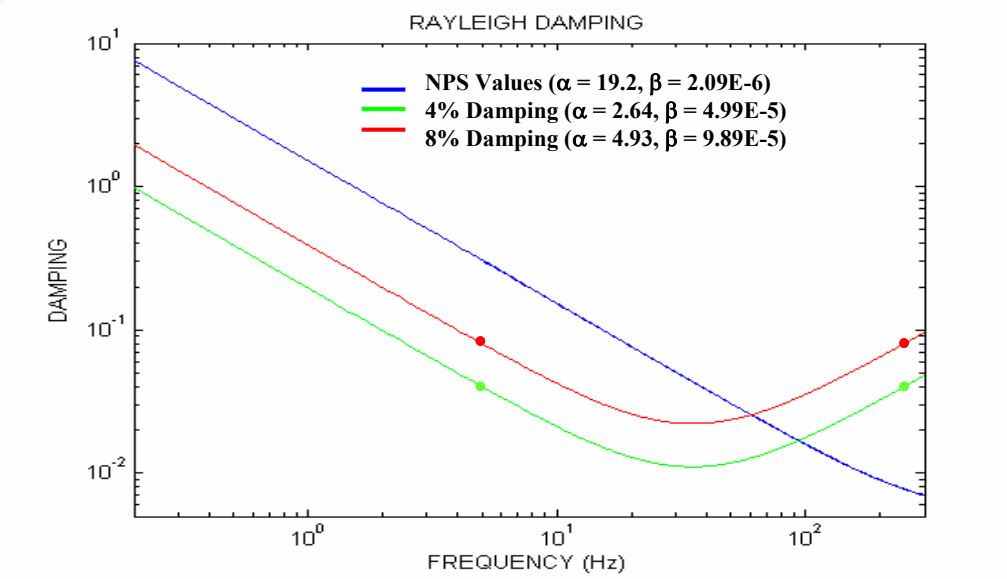

Figure 17. Rayleigh Damping Values (in Logarithmic Scale)

The following series of velocity response plots compares the Rayleigh damping coefficients, α and β, presented in Tables 3 and 4 with coefficients that were used in previous studies conducted on the DDG 53 and DDG 81, which appear in Table 5.

Russell's Error Factor [5-7] was chosen as a means of comparing the velocity response data against the actual ship shock trial data. For the purpose of this study, an established set of acceptance criteria was taken from the work accomplished in 2003 on the DDG 81 Ship Shock Simulation [4]. These values are presented in Table 6.

Table 6. Russell's Correlation Acceptance Criteria

$RC \leq 0.15$	Excellent
$0.15 < RC < 0.28$	Good
$RC \geq 0.28$	Poor

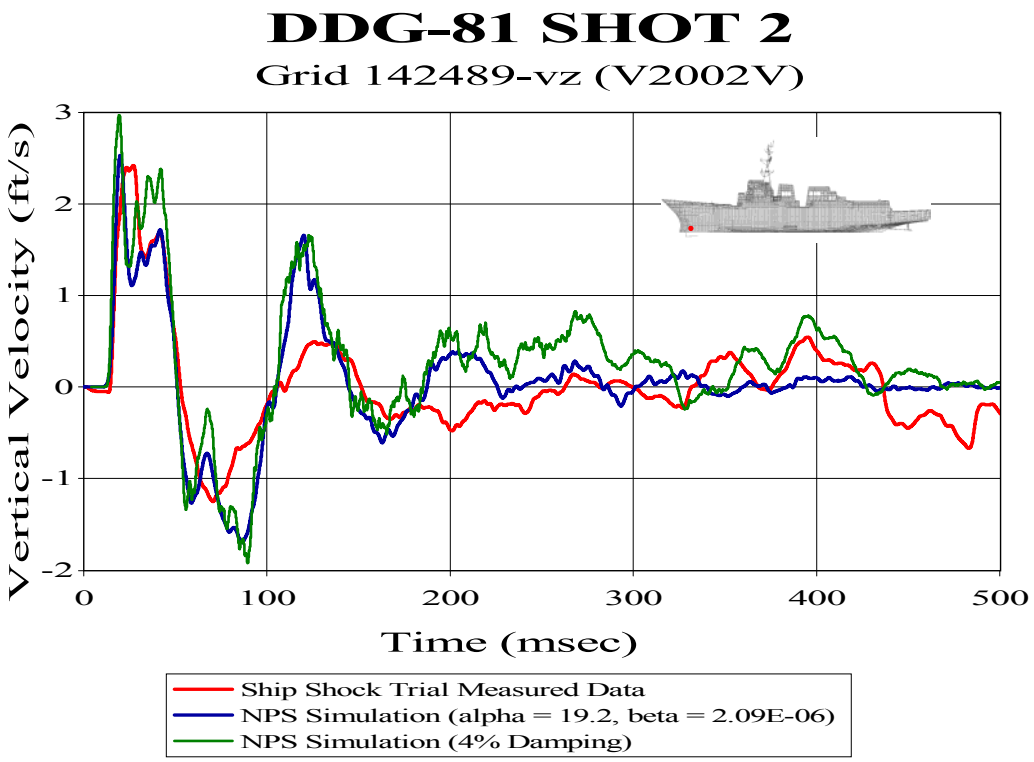

Figure 18. Sample Vertical Velocity Response: Deck Sensor

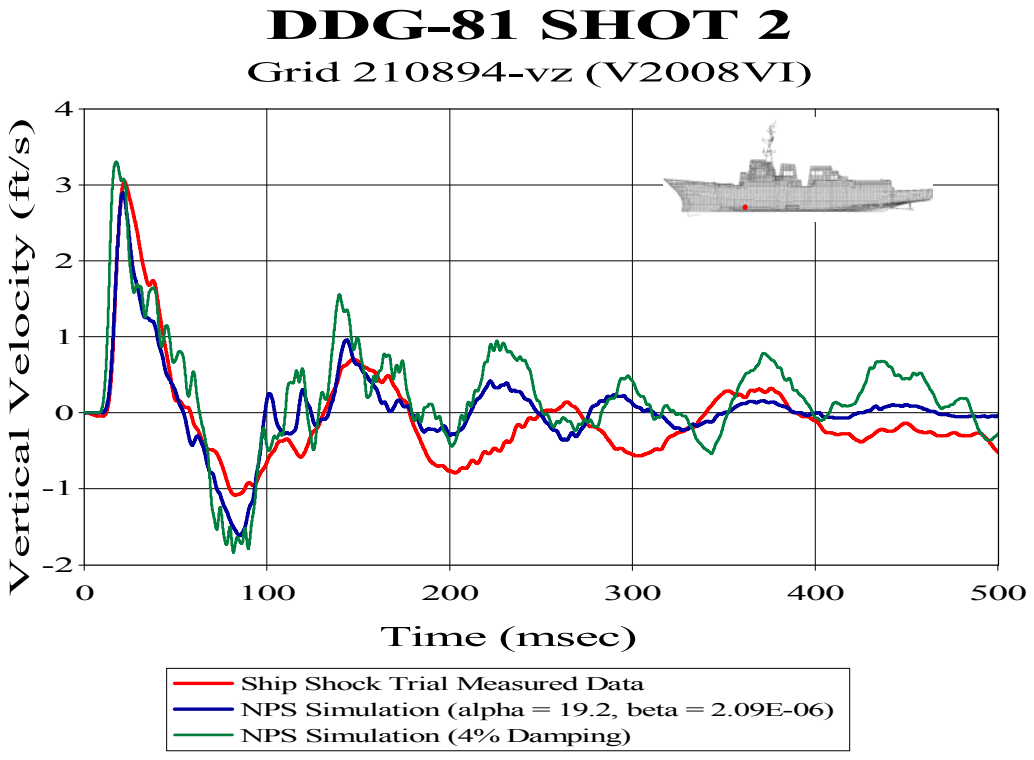

Figure 19. Sample Vertical Velocity Response: Deck Sensor

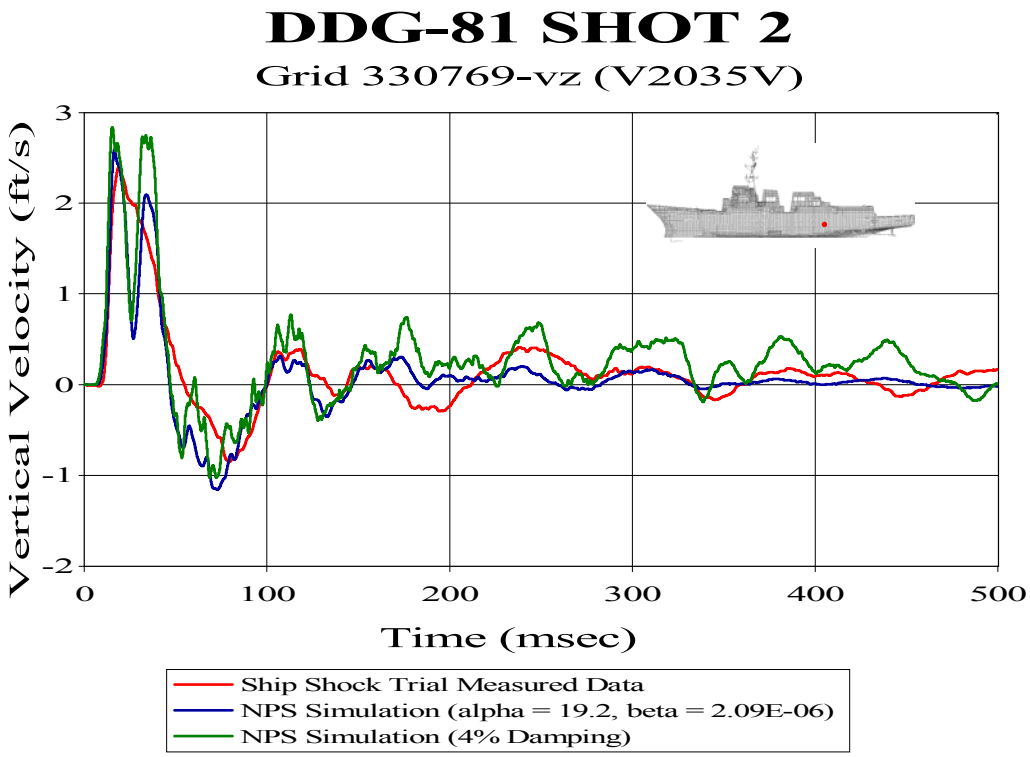

Figure 20. Sample Vertical Velocity Response: Keel Sensor

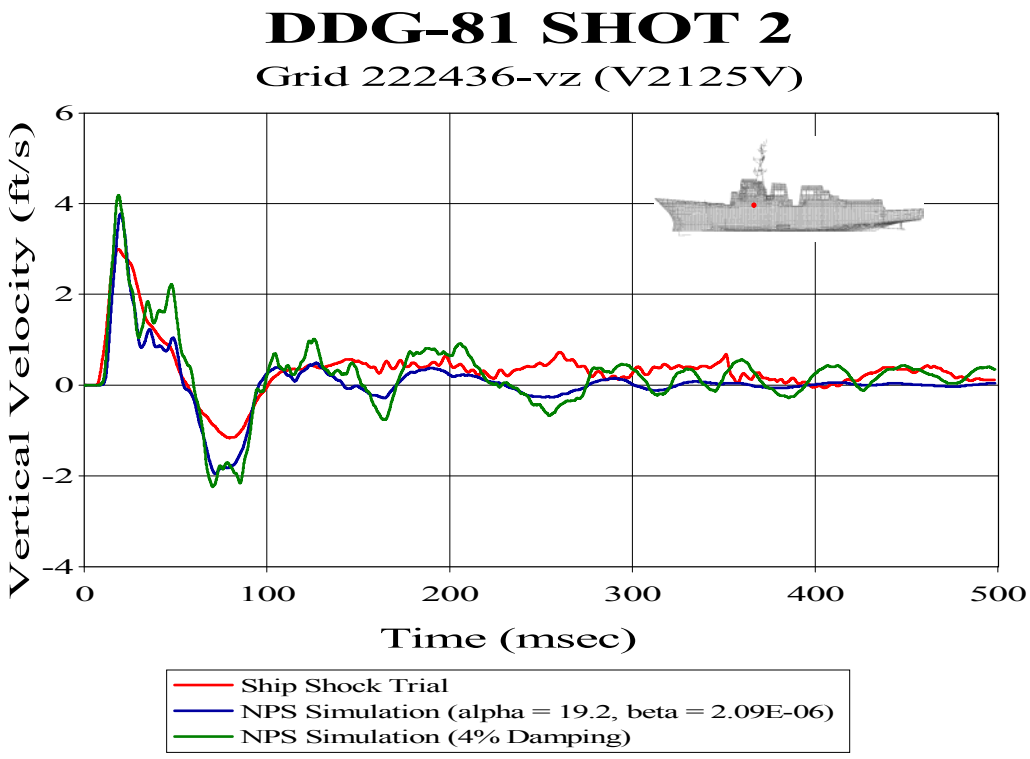

Figure 21. Sample Vertical Velocity Response: Bulkhead Sensor

As the velocity response plot comparisons in Figure 18 through Figure 21 show, there is a much better correlation between the NPS damping values and the ship shock trial data, than with the fixed 4% damping. For the sensors examined of which the approximate location of each is indicated on the time history plots by a red dot, a Russell's Comprehensive (RC) error correlation factor was computed. The mean RC for the 4% Damping cases was 0.25 while in comparison when the new NPS damping values from Table 3 and Table 4 were used, the mean RC value was only 0.18. Recalling that by Russell's correlation criteria, a value below 0.15 is considered an excellent correlation, the simulations using the new NPS damping values consistently show better overall correlation and an average reduction of approximately 25% in deviation from the recorded ship shock trial data versus those using the fixed 4% damping. Table 7 illustrates a sampling of the supporting data.

Table 7. Comparison of Russell's Error Factor for DDG 81Shot 2 (vertical direction)

Ship Shock Simulation with Shot 2 Geometry, Dense Mesh and 738 in Cavitation Depth												
Sensor	Node	Mounting Type	Location (in)*			Shock Trial Data vs. 4% Damping			Shock Trial Data vs. NPS Damping		
						SHIP SHOCK TRIAL DATA (<250HZ)			SHIP SHOCK TRIAL DATA (<250HZ)		
						LS-DYNA/USA DATA (<250HZ)			LS-DYNA/USA DATA (<250HZ)		
			x	y	z	RM	RP	RC	RM	RP	RC
V2002V	142489	Deck	4656	24	85	0.1974	0.2715	0.2975	0.0679	0.2175	0.2019
V2008VI	210894	Deck	4064	176	171	0.1207	0.2689	0.258	0.1200	0.1932	0.2016
V2035V	330769	Keel	1152	135	193	0.1643	0.1849	0.2192	0.0009	0.1692	0.15
V2125V	222436	Bulkhead	3504	375	390	0.1651	0.1936	0.2255	0.0214	0.1914	0.1707
Russell Error Correlation					Sum(E(X))	0.64750	0.91890	1.00020	0.21020	0.77130	0.72420
	> 0.28	Poor			Sum(E(X^2))	0.10779	0.21769	0.25397	0.01947	0.14990	0.13304
	< 0.15	Excellent			**Mean**	**0.16188**	**0.22973**	**0.25005**	**0.05255**	**0.19283**	**0.18105**
					Standard Deviation	0.03148	0.04688	0.03591	0.05299	0.01974	0.02535

* Referenced to the G&C NASTRAN Model coordinate origin located at the stern. In the Y-direction, port is postive from the centerline.

Figure 22 is a graphical representation of the data presented in Table 7. Notice that the Russell's Comprehensive correlation factor for the simulations using the NPS damping values are all in the excellent or highly acceptable range, while the results from the simulations performed using the fixed 4% damping values are only marginally acceptable or fall outside of the acceptable range all together. Note as well that there is considerable improvement in the accuracy of the magnitude component of the Russell's correlation in the simulations using the NPS damping values, as demonstrated by the grouping of points nearer the ordinate.

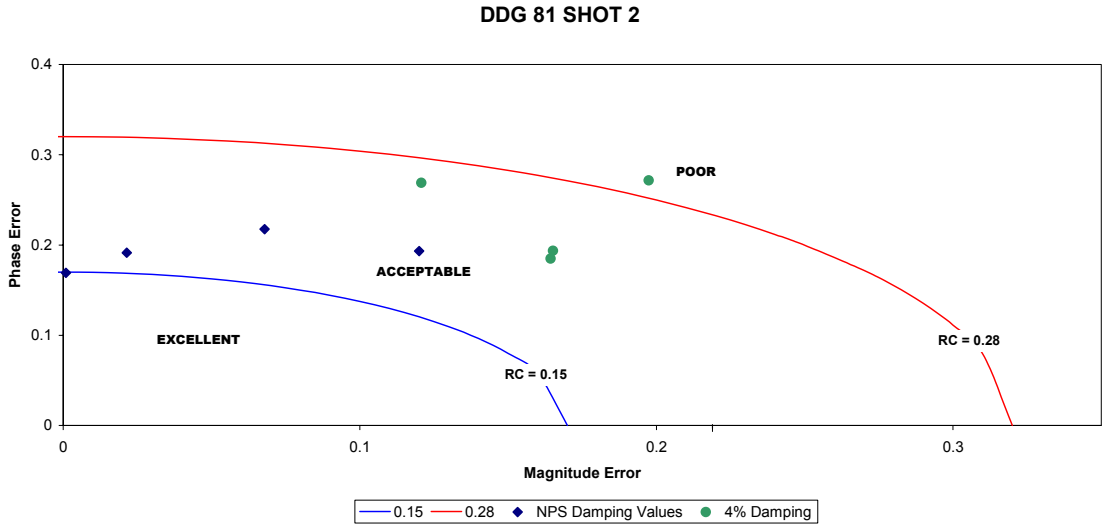

Figure 22. Russell's Error Factor for Selected Sensors of DDG 81 Shot 2

In this small but representative sampling of data points from various locations throughout the ship, comparison of the Russell's error correlation shows that using the NPS damping values tends to improve the accuracy of the simulation from 20% to 30%. These results are presented in Table 8.

Table 8. Relative % Change in RC for NPS Damping versus 4% Damping Case

Sensor	Node	Ship Compartment Location	Percent Relavtive Change
V2008VI	210894	4th Deck	32.13%
V2002V	142489	4th Deck	21.86%
V2035V	330769	3rd Deck	31.57%
V2125V	222436	1st Deck	24.30%
Average Improvement in Correlation			27.47%

VI. CONCLUSIONS

Rayleigh damping representation for modeling ship system damping has been investigated based on the ship shock trial data. Based on the results of studies, a set of Rayleigh damping parameters (α and β) are recommended for ship shock response predictions. The results of investigation also indicate that (i) the system damping is largely affected by mass driven (α[M]), and (ii) the damping decreases as frequency increases as we commonly understood.

THIS PAGE INTENTIONALLY LEFT BLANK

LIST OF REFERENCES

1. Ewins, D. J., "Modal Testing : Theory and Practice", Research Studies Press, 1984
2. Bendat, Julius S. and Piersol, Allan G., "Random Data", 2nd edition, Willey-Interscience 1986
3. Engeln-Mullges, Gisela and Uhlig, Frank, "Numerical Algorithms with Fortran", Springer, 1996
4. Schneider, N.A. and Shin, Y.S. "Ship Shock Trial Modeling and Simulation for USS Winston S. Churchill (DDG81)," Tech Report NPS-ME-03-004, Naval Postgraduate School, December 2003.
5. Russel, D.D., "Error Measures for Comparing Transient Data: Part I: Development of a Comprehensive Error Measure", 68th Shock and Vibration Symposium Proceedings, Vol. I, November 1997.
6. Russell, D.D., "DDG53 Shock Trial Simulation Acceptance Criteria", 69th Shock and Vibration Symposium, October 1998.
7. Russel, D.D., "Error Measures for Comparing Transient Data: Part II: Error Measure Case Study", 68th Shock and Vibration Symposium Proceedings, Vol. I, November 1997.

APPENDIX A. FIGURES OF THE RESULTS OF RAYLEIGH DAMPING CURVE-FITTING

A. Results in the Athwartship Direction

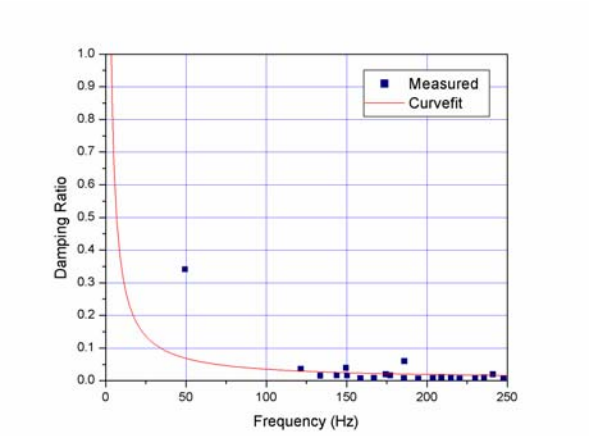

Figure 23. Modal Damping Ratio at Area 1, Athwartship Direction (Original)

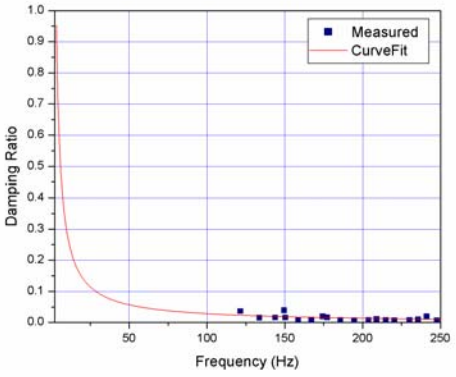

(in Linear Scale)

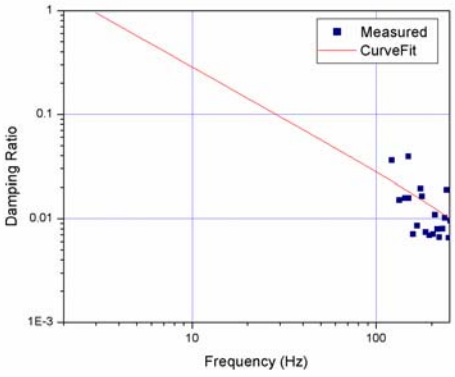

(in Logarithmic Scale)

Figure 24. Modal Damping Ratio at Area 1, Athwartship Direction (Modified)

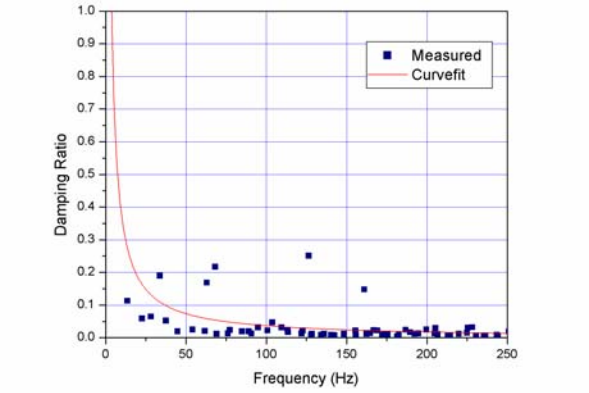

Figure 25. Modal Damping Ratio at Area 3, Athwartship Direction (Original)

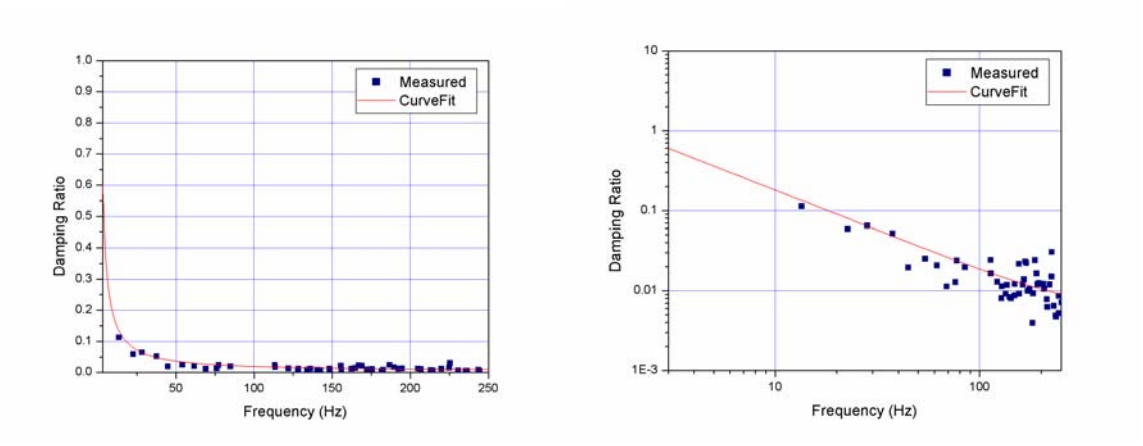

(in Linear Scale) (in Logarithmic Scale)

Figure 26. Modal Damping Ratio at Area 3, Athwartship Direction (Modified)

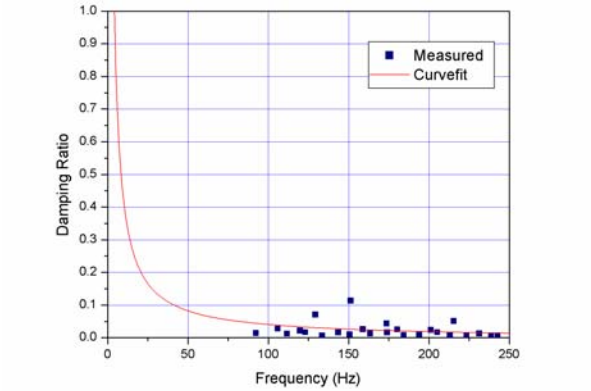

Figure 27. Modal Damping Ratio at Area 6, Athwartship Direction (Original)

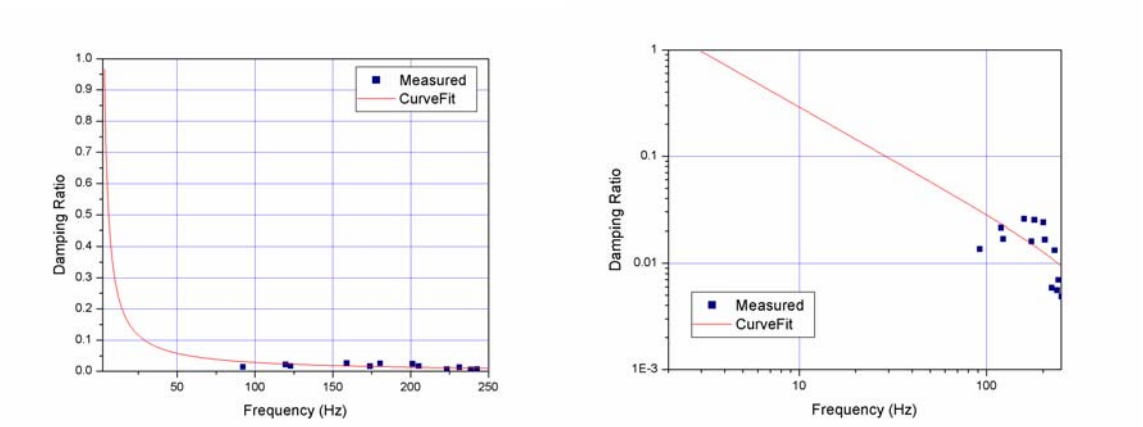

(in Linear Scale) (in Logarithmic Scale)

Figure 28. Modal Damping Ratio at Area 6, Athwartship Direction (Modified)

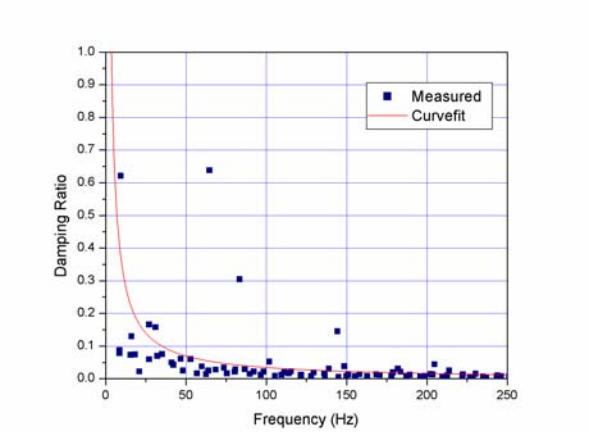

Figure 29. Modal Damping Ratio at Area 7, Athwartship Direction (Original)

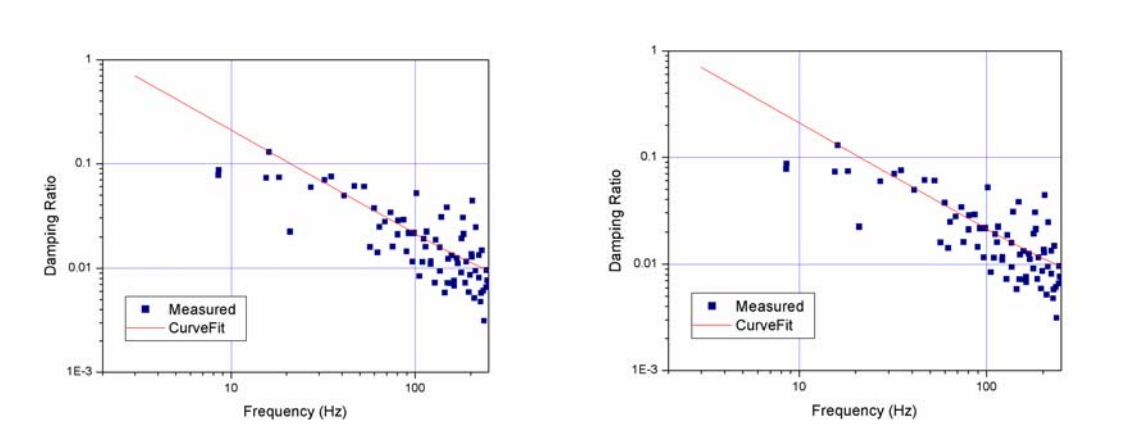

(in Linear Scale) (in Logarithmic Scale)

Figure 30. Modal Damping Ratio at Area 7, Athwartship Direction (Modified)

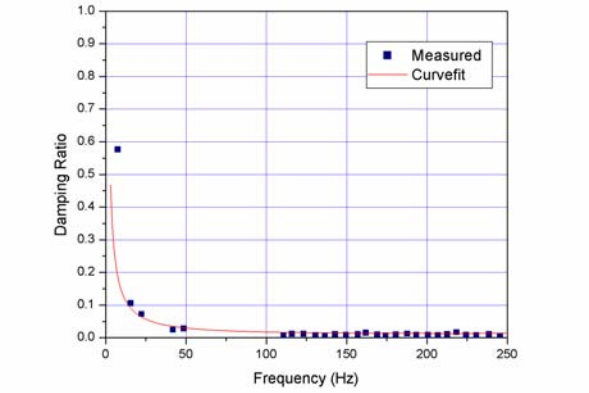

Figure 31. Modal Damping Ratio at Area 8, Athwartship Direction (Original)

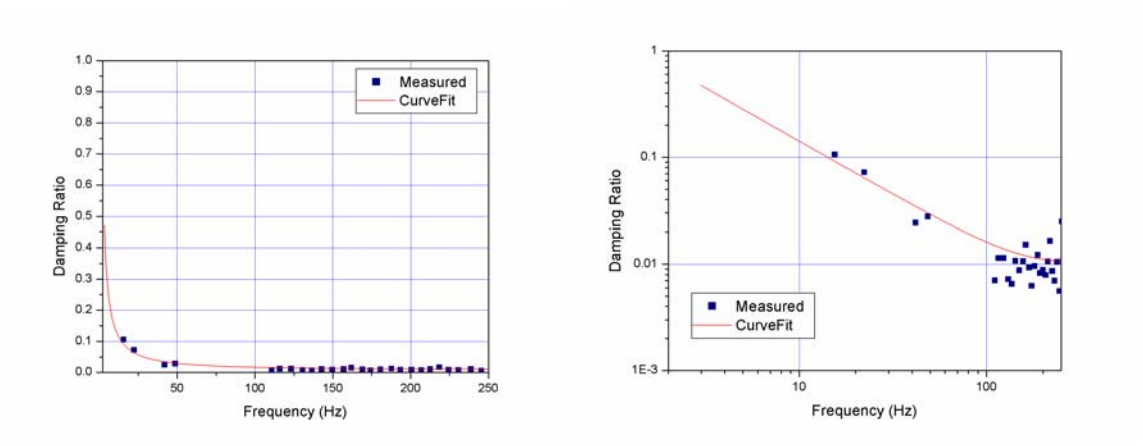

(in Linear Scale) (in Logarithmic Scale)

Figure 32. Modal Damping Ratio at Area 8, Athwartship Direction (Modified)

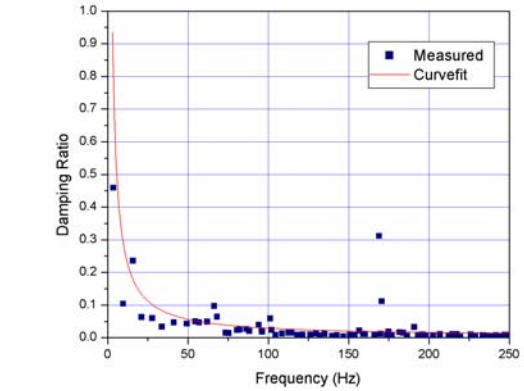

Figure 33. Modal Damping Ratio at Area 10, Athwartship Direction (Original)

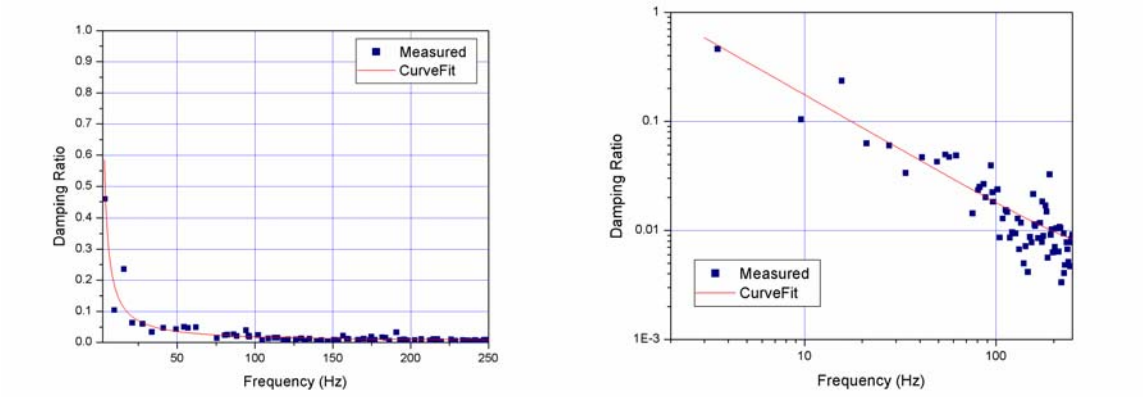

(in Linear Scale) (in Logarithmic Scale)

Figure 34. Modal Damping Ratio at Area 10, Athwartship Direction (Modified)

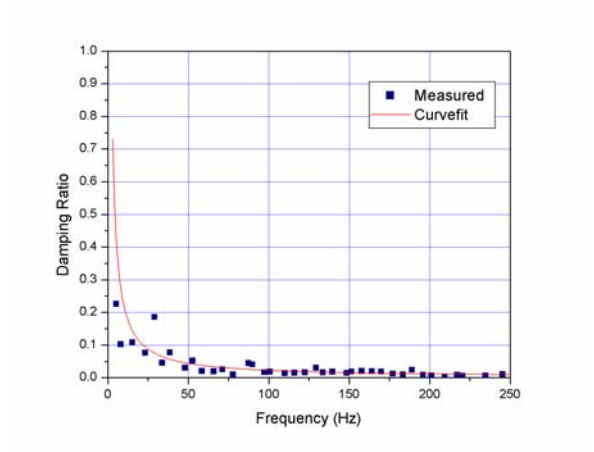

Figure 35. Modal Damping Ratio at Area 11, Athwartship Direction (Original)

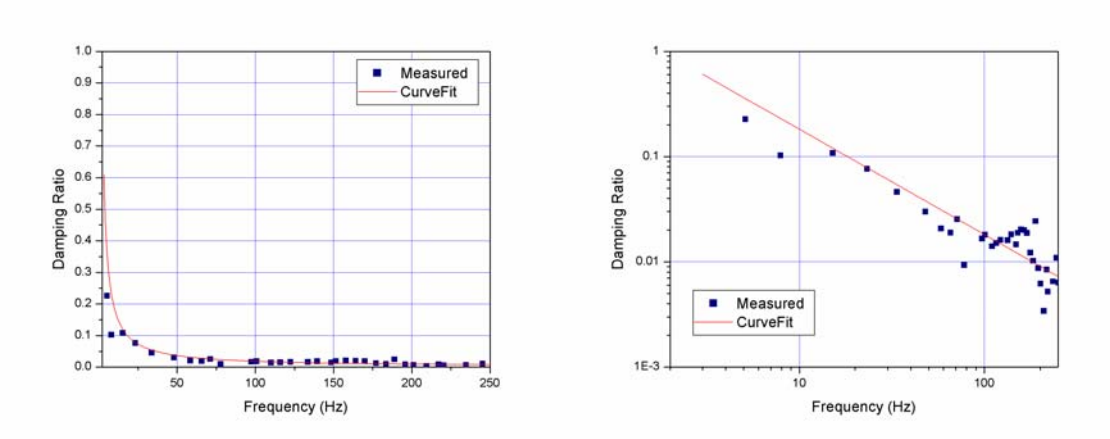

(in Linear Scale) (in Logarithmic Scale)

Figure 36. Modal Damping Ratio at Area 11, Athwartship Direction (Modified)

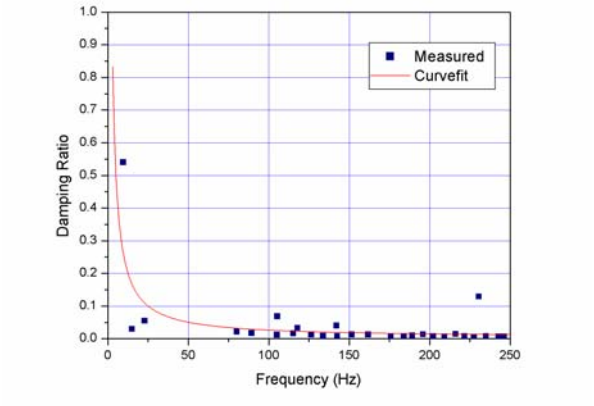

Figure 37. Modal Damping Ratio at Area 12, Athwartship Direction (Original)

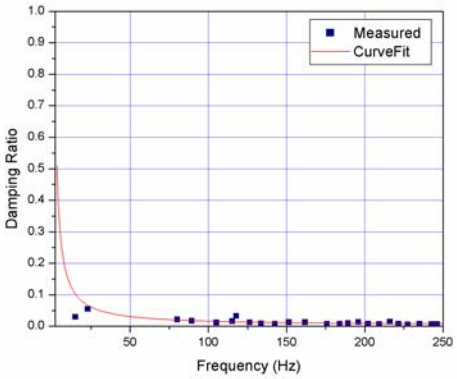

(in Linear Scale)

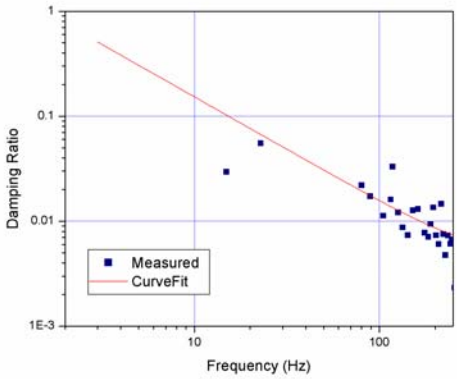

(in Logarithmic Scale)

Figure 38. Modal Damping Ratio at Area 12, Athwartship Direction (Modified)

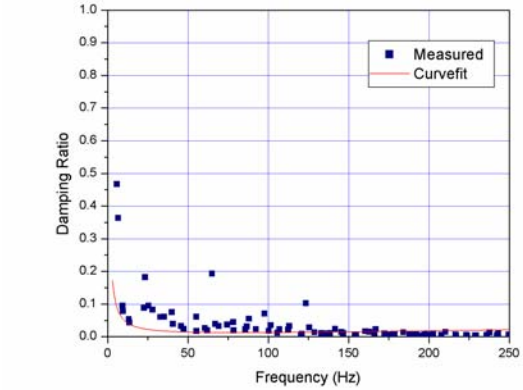

Figure 39. Modal Damping Ratio at Area 15, Athwartship Direction (Original)

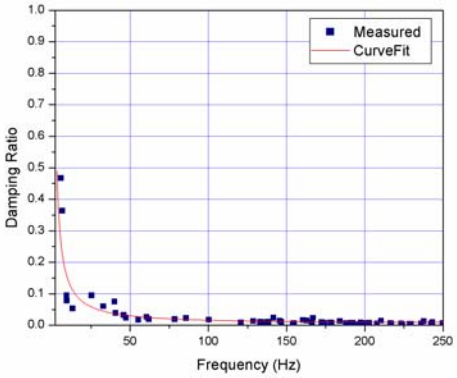

(in Linear Scale)

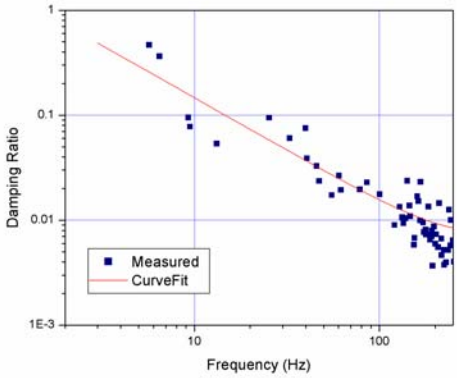

(in Logarithmic Scale)

Figure 40. Modal Damping Ratio at Area 15, Athwartship Direction (Modified)

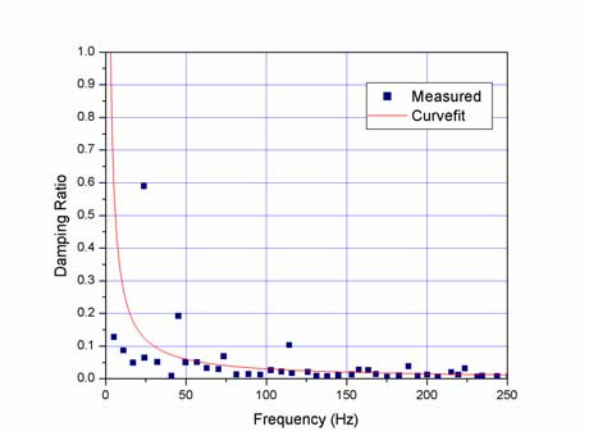

Figure 41. Modal Damping Ratio at Area 16, Athwartship Direction (Original)

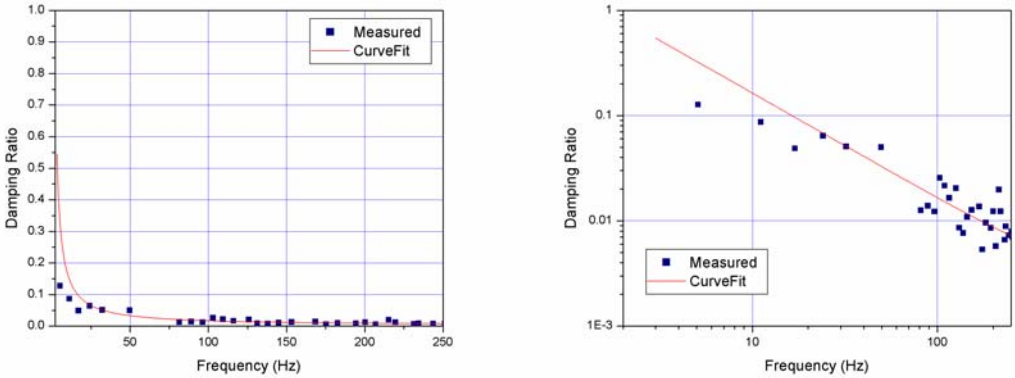

(in Linear Scale) (in Logarithmic Scale)

Figure 42. Modal Damping Ratio at Area 16, Athwartship Direction (Modified)

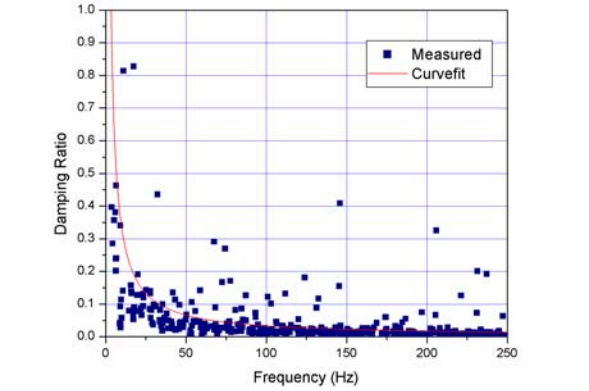

Figure 43. Modal Damping Ratio at Area 18, Athwartship Direction (Original)

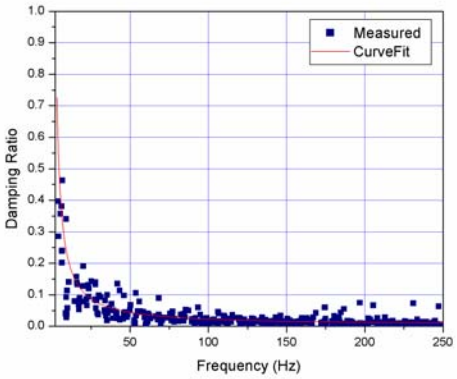

(in Linear Scale)

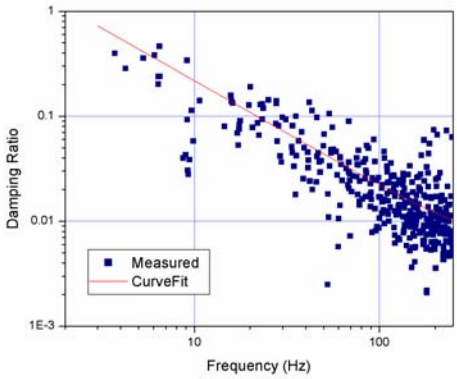

(in Logarithmic Scale)

Figure 44. Modal Damping Ratio at Area 18, Athwartship Direction (Modified)

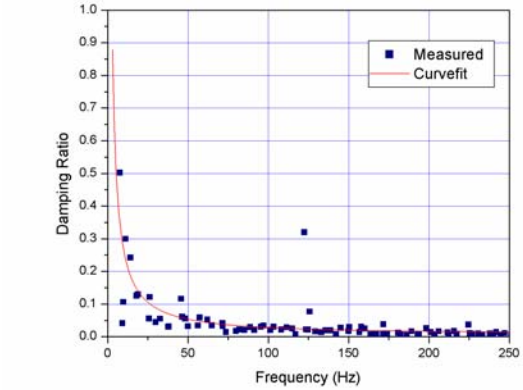

Figure 45. Modal Damping Ratio at Area 19, Athwartship Direction (Original)

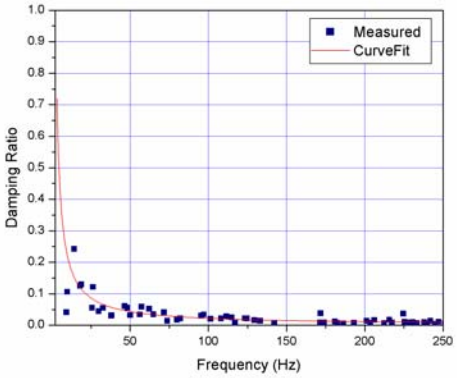

(in Linear Scale)

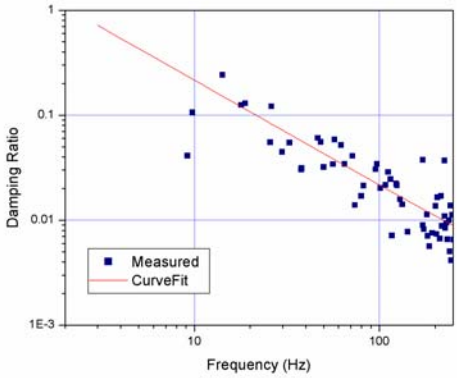

(in Logarithmic Scale)

Figure 46. Modal Damping Ratio at Area 19, Athwartship Direction (Modified)

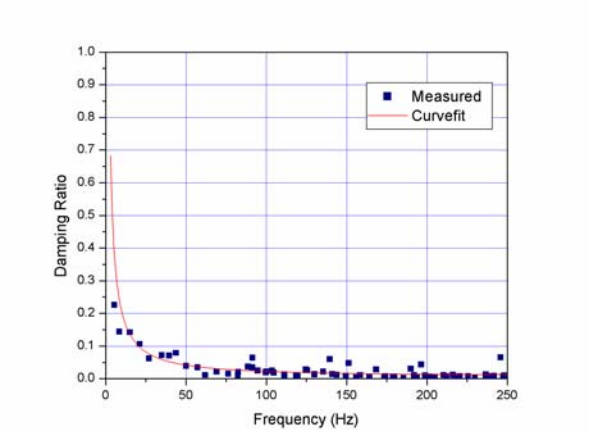

Figure 47. Modal Damping Ratio at Area 20, Athwartship Direction (Original)

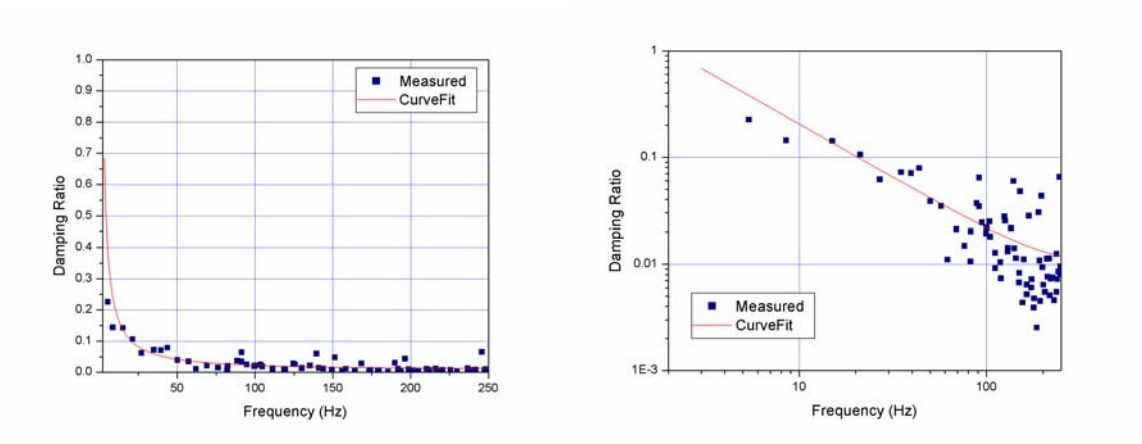

(in Linear Scale) (in Logarithmic Scale)

Figure 48. Modal Damping Ratio at Area 20, Athwartship Direction (Modified)

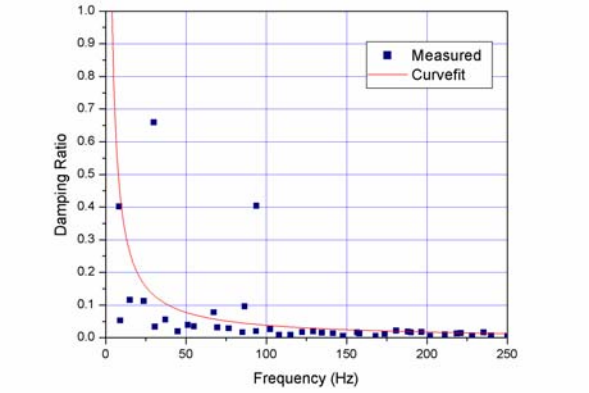

Figure 49. Modal Damping Ratio at Area 28, Athwartship Direction (Original)

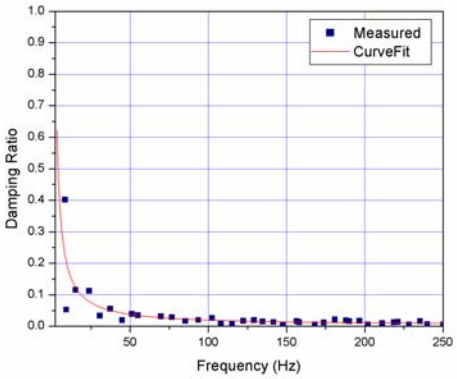

(in Linear Scale)

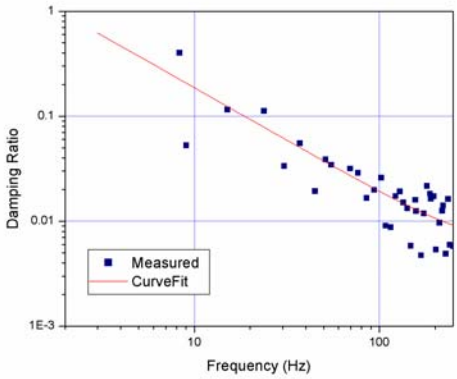

(in Logarithmic Scale)

Figure 50. Modal Damping Ratio at Area 28, Athwartship Direction (Modified)

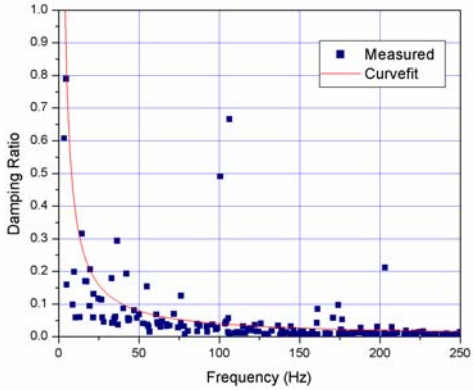

Figure 51. Modal Damping Ratio at Area 30, Athwartship Direction (Original)

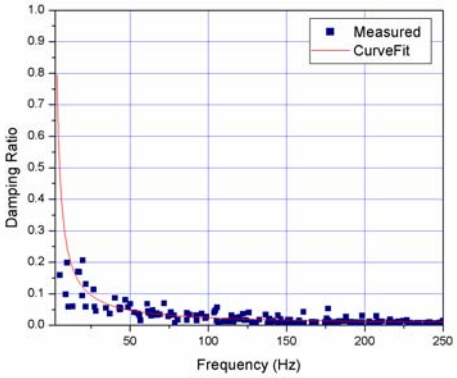

(in Linear Scale)

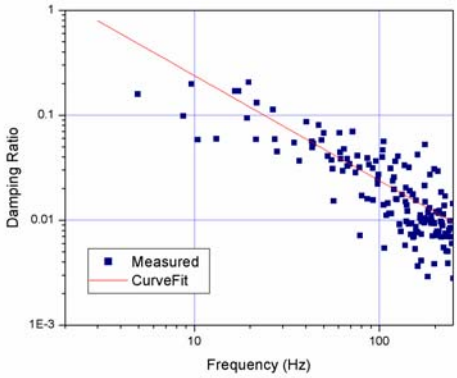

(in Logarithmic Scale)

Figure 52. Modal Damping Ratio at Area 30, Athwartship Direction (Modified)

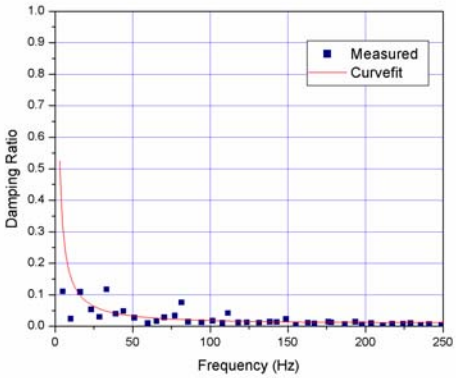

Figure 53. Modal Damping Ratio at Area 31, Athwartship Direction (Original)

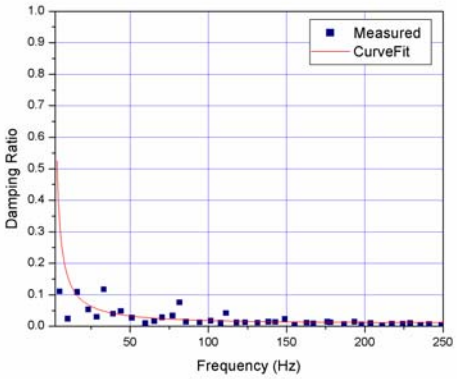

(in Linear Scale)

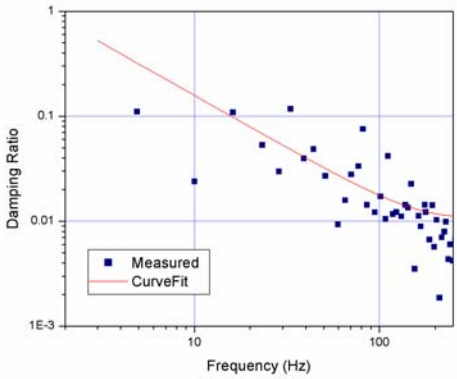

(in Logarithmic Scale)

Figure 54. Modal Damping Ratio at Area 31, Athwartship Direction (Modified)

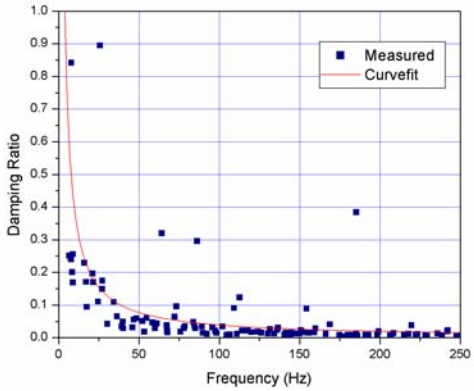

Figure 55. Modal Damping Ratio at Area 32, Athwartship Direction (Original)

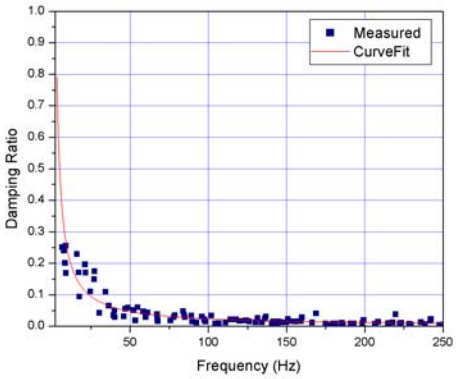

(in Linear Scale)

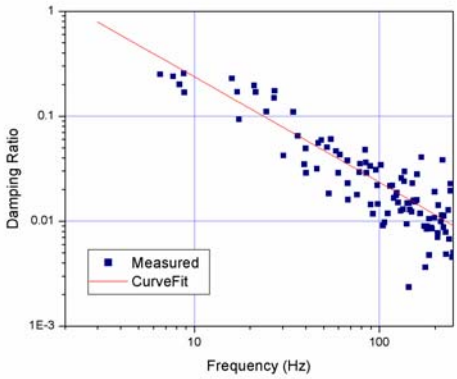

(in Logarithmic Scale)

Figure 56. Modal Damping Ratio at Area 32, Athwartship Direction (Modified)

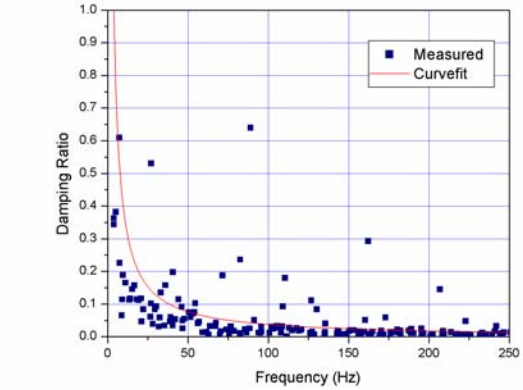

Figure 57. Modal Damping Ratio at Area 33, Athwartship Direction (Original)

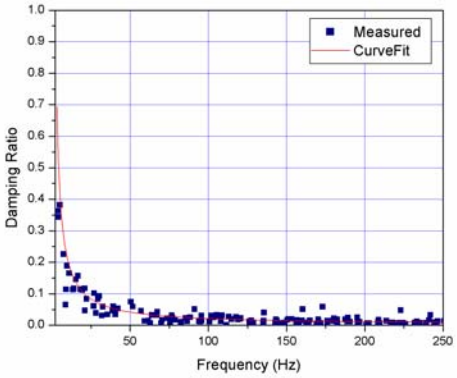

(in Linear Scale)

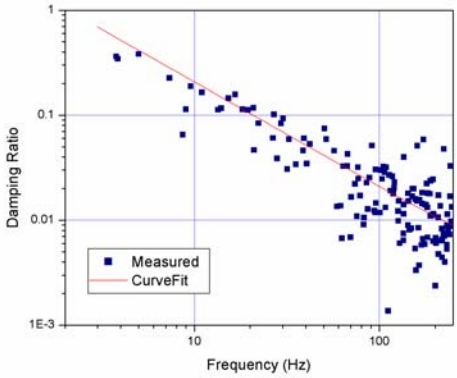

(in Logarithmic Scale)

Figure 58. Modal Damping Ratio at Area 33, Athwartship Direction (Modified)

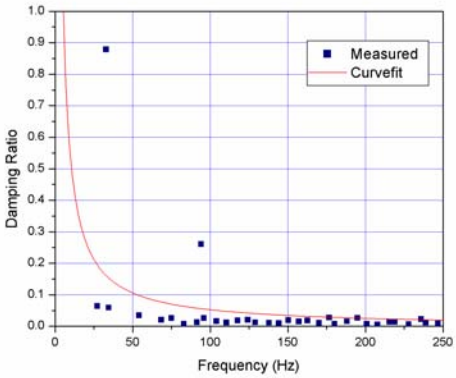

Figure 59. Modal Damping Ratio at Area 35, Athwartship Direction (Original)

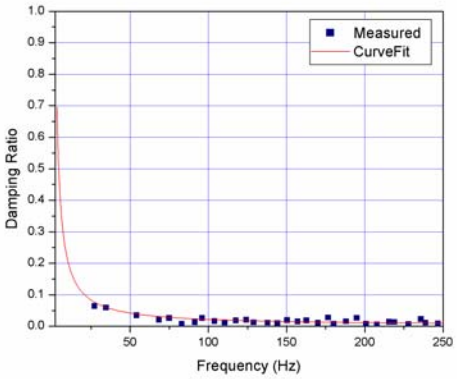

(in Linear Scale)

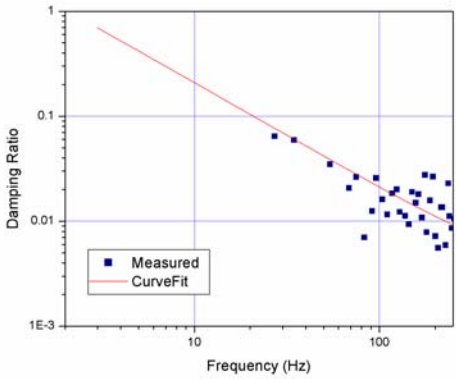

(in Logarithmic Scale)

Figure 60. Modal Damping Ratio at Area 35, Athwartship Direction (Modified)

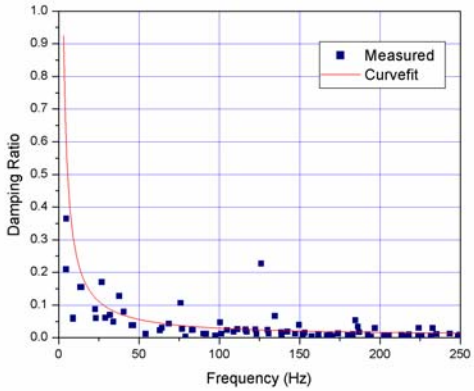

Figure 61. Modal Damping Ratio at Area 37, Athwartship Direction (Original)

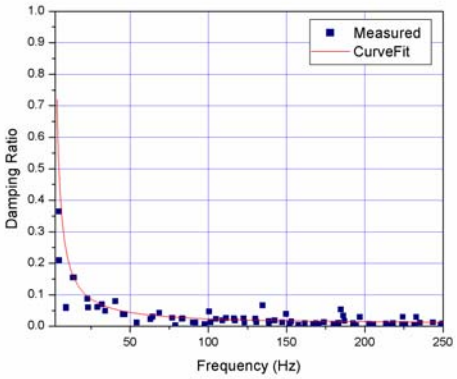

(in Linear Scale)

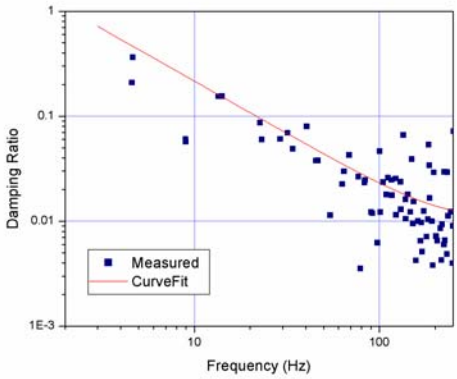

(in Logarithmic Scale)

Figure 62. Modal Damping Ratio at Area 37, Athwartship Direction (Modified)

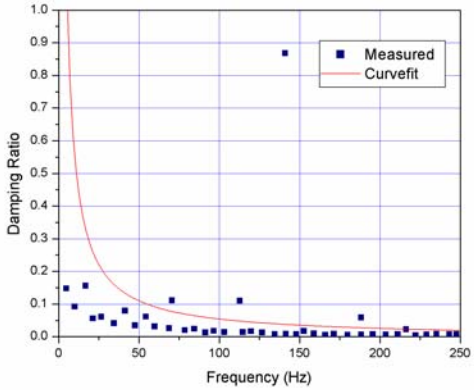

Figure 63. Modal Damping Ratio at Area 40, Athwartship Direction (Original)

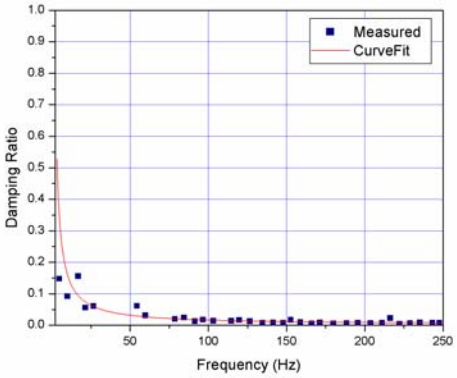

(in Linear Scale)

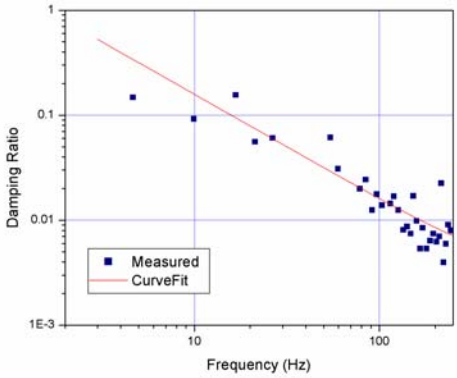

(in Logarithmic Scale)

Figure 64. Modal Damping Ratio at Area 40, Athwartship Direction (Modified)

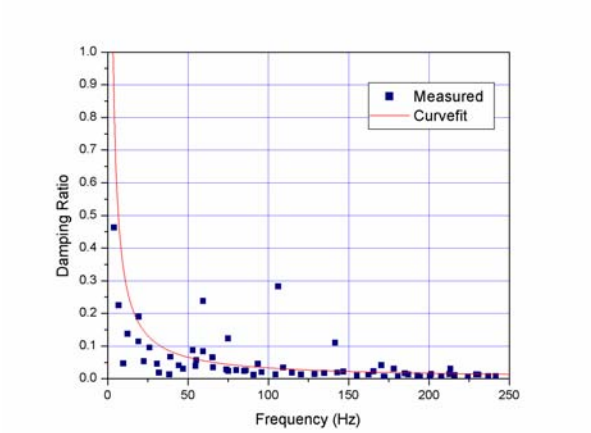

Figure 65. Modal Damping Ratio at Area 41, Athwartship Direction (Original)

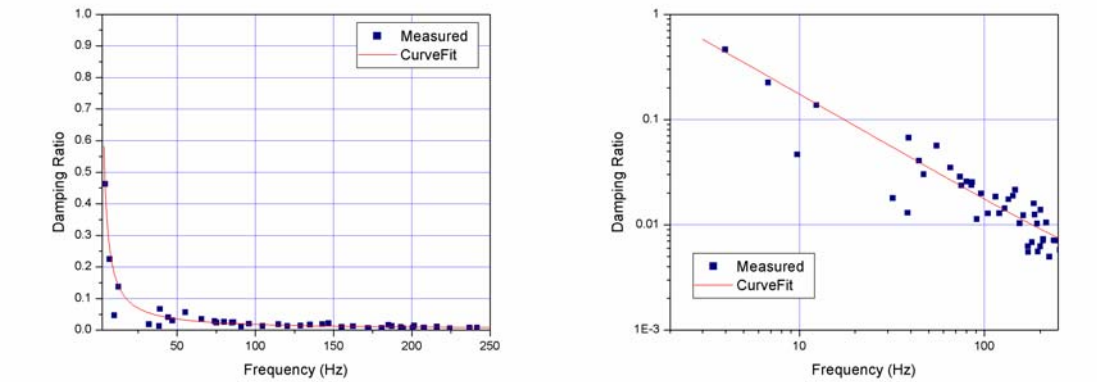

(in Linear Scale) (in Logarithmic Scale)

Figure 66. Modal Damping Ratio at Area 41, Athwartship Direction (Modified)

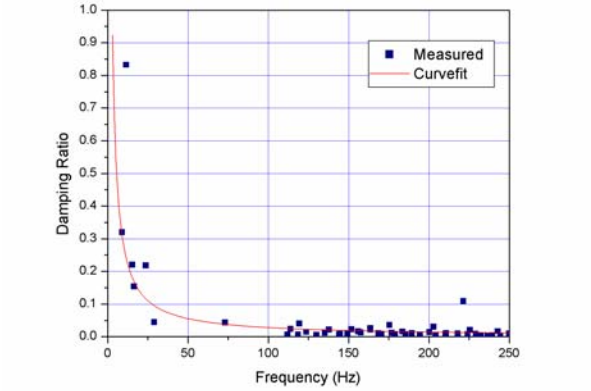

Figure 67. Modal Damping Ratio at Area 42, Athwartship Direction (Original)

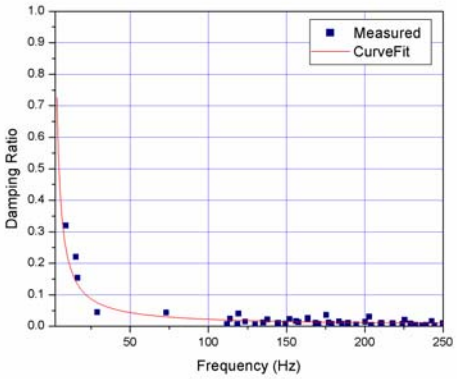

(in Linear Scale)

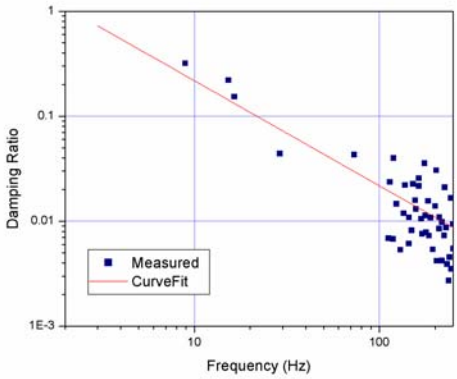

(in Logarithmic Scale)

Figure 68. Modal Damping Ratio at Area 42, Athwartship Direction (Modified)

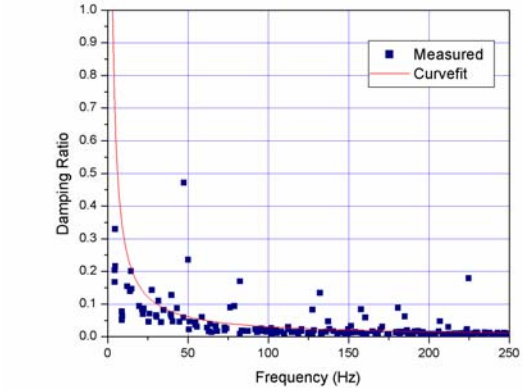

Figure 69. Modal Damping Ratio at Area 43, Athwartship Direction (Original)

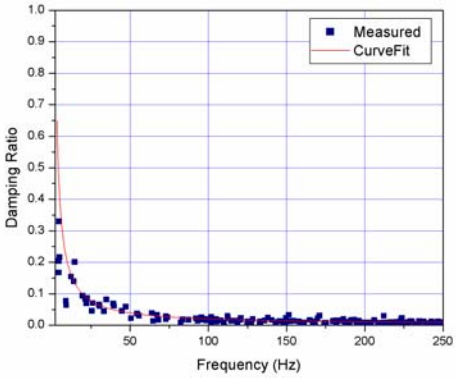

(in Linear Scale)

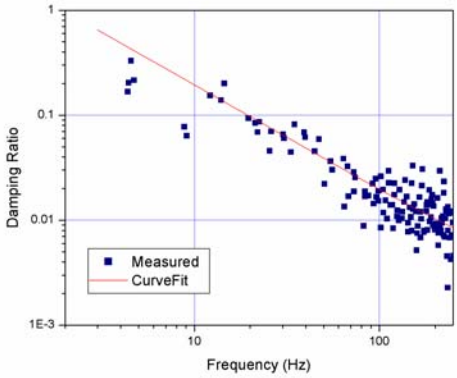

(in Logarithmic Scale)

Figure 70. Modal Damping Ratio at Area 43, Athwartship Direction (Modified)

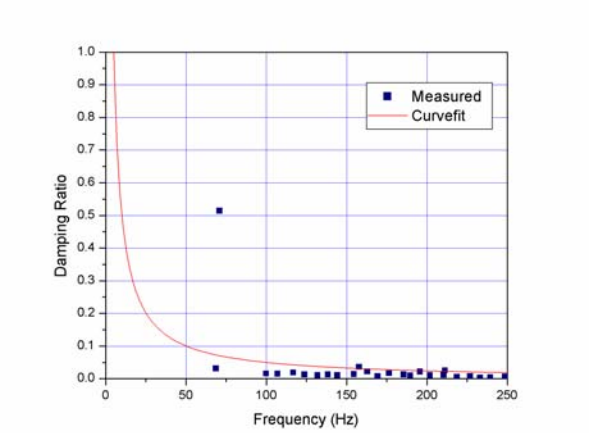

Figure 71. Modal Damping Ratio at Area 47, Athwartship Direction (Original)

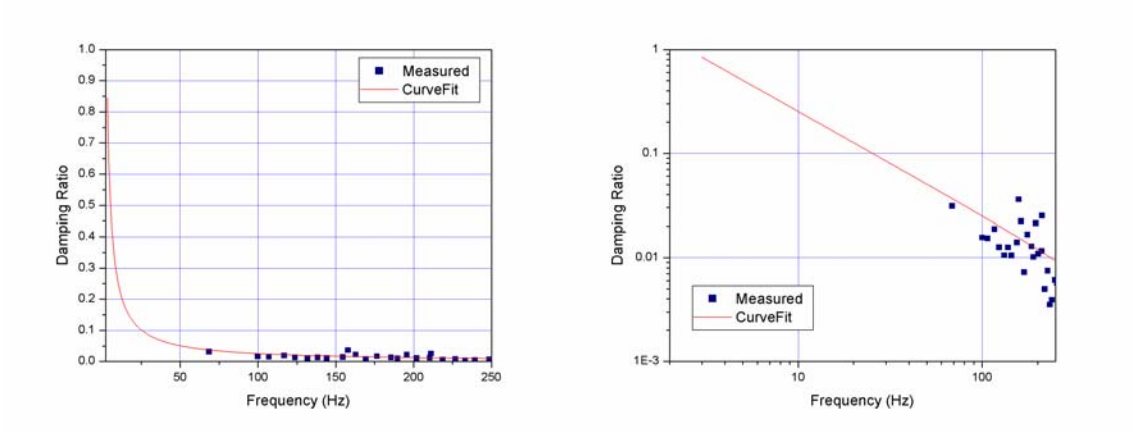

(in Linear Scale) (in Logarithmic Scale)

Figure 72. Modal Damping Ratio at Area 47, Athwartship Direction (Modified)

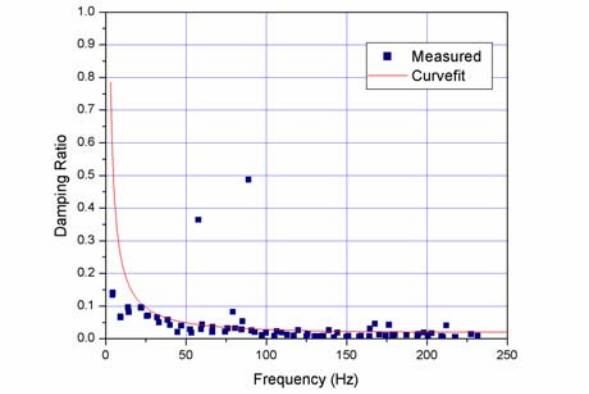

Figure 73. Modal Damping Ratio at Area 48, Athwartship Direction (Original)

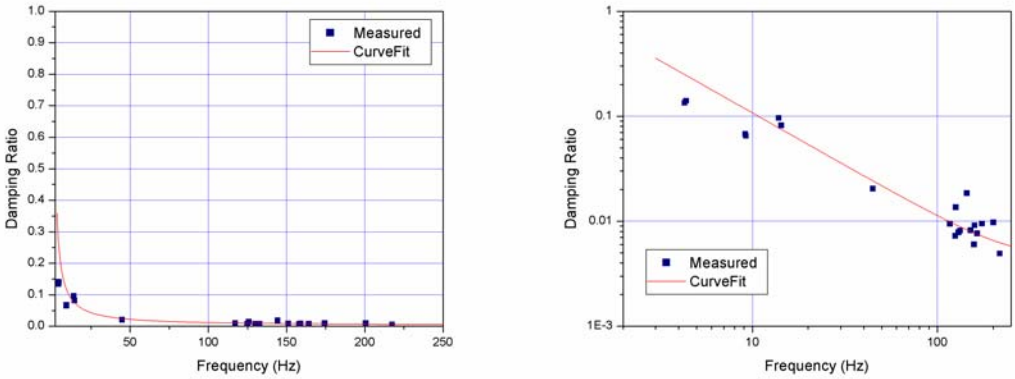

(in Linear Scale) (in Logarithmic Scale)

Figure 74. Modal Damping Ratio at Area 48, Athwartship Direction (Modified)

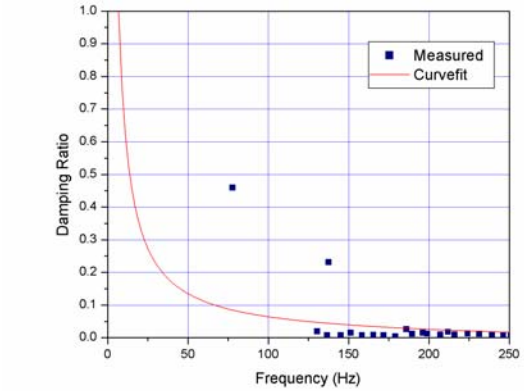

Figure 75. Modal Damping Ratio at Area 49, Athwartship Direction (Original)

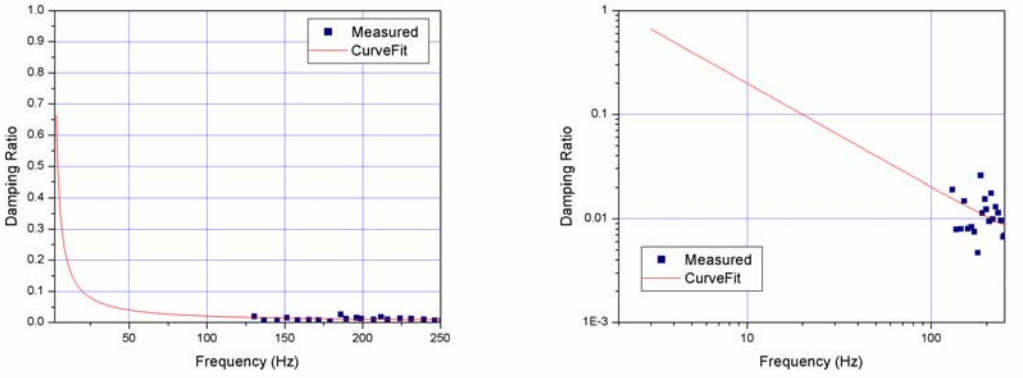

(in Linear Scale) (in Logarithmic Scale)

Figure 76. Modal Damping Ratio at Area 49, Athwartship Direction (Modified)

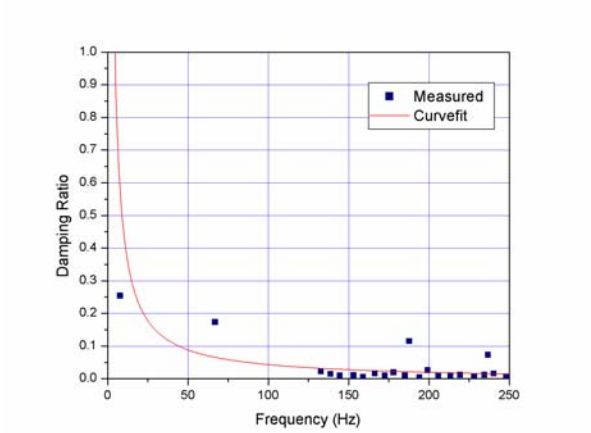

Figure 77. Modal Damping Ratio at Area 50, Athwartship Direction (Original)

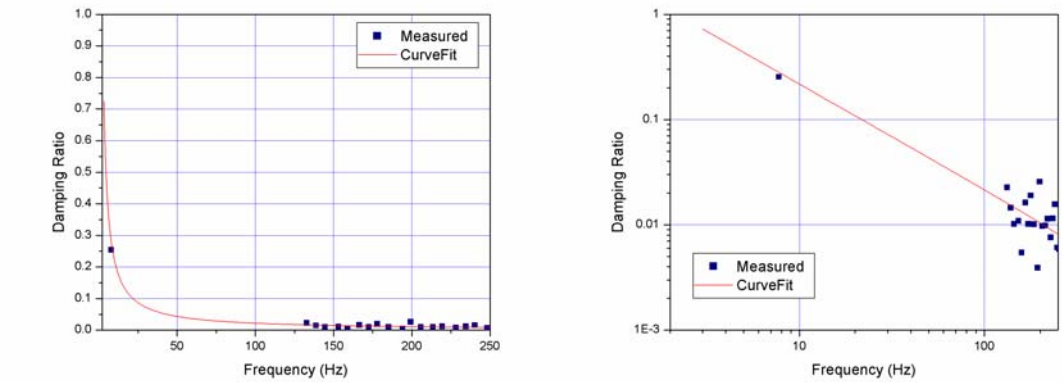

(in Linear Scale) (in Logarithmic Scale)

Figure 78. Modal Damping Ratio at Area 50, Athwartship Direction (Modified)

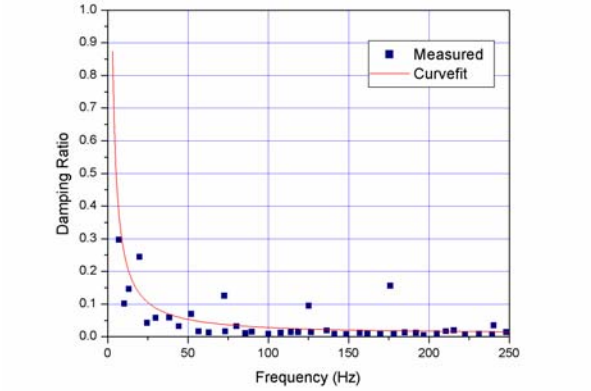

Figure 79. Modal Damping Ratio at Area 53, Athwartship Direction (Original)

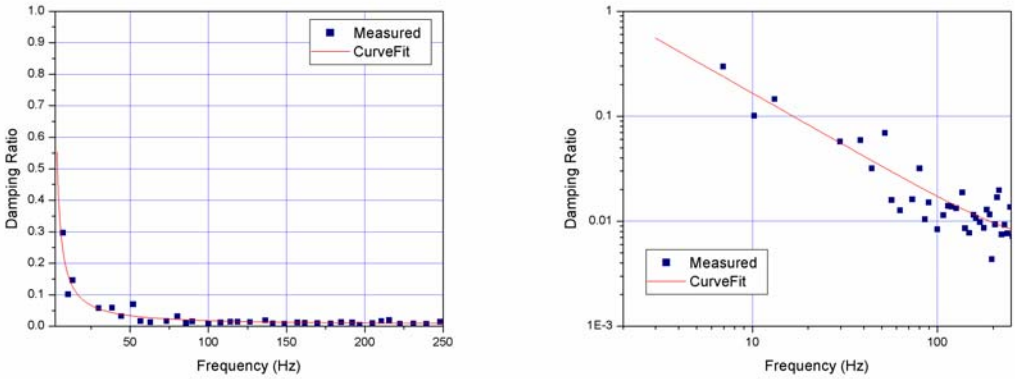

(in Linear Scale) (in Logarithmic Scale)

Figure 80. Modal Damping Ratio at Area 53, Athwartship Direction (Modified)

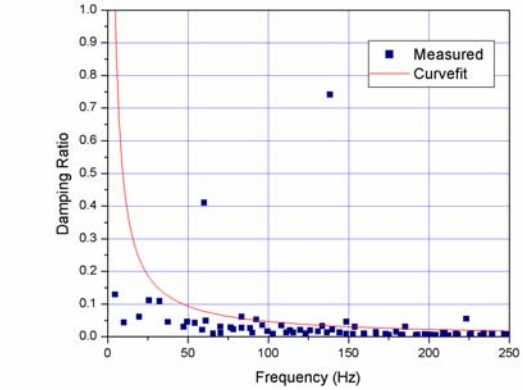

Figure 81. Modal Damping Ratio at Area 54, Athwartship Direction (Original)

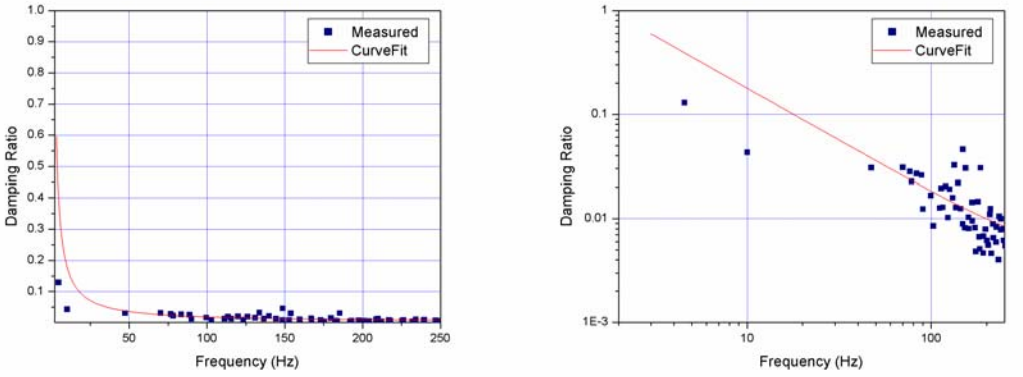

(in Linear Scale) (in Logarithmic Scale)

Figure 82. Modal Damping Ratio at Area 54, Athwartship Direction (Modified)

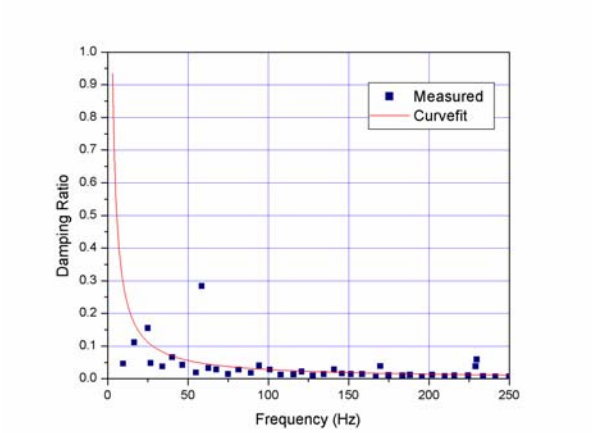

Figure 83. Modal Damping Ratio at Area 55, Athwartship Direction (Original)

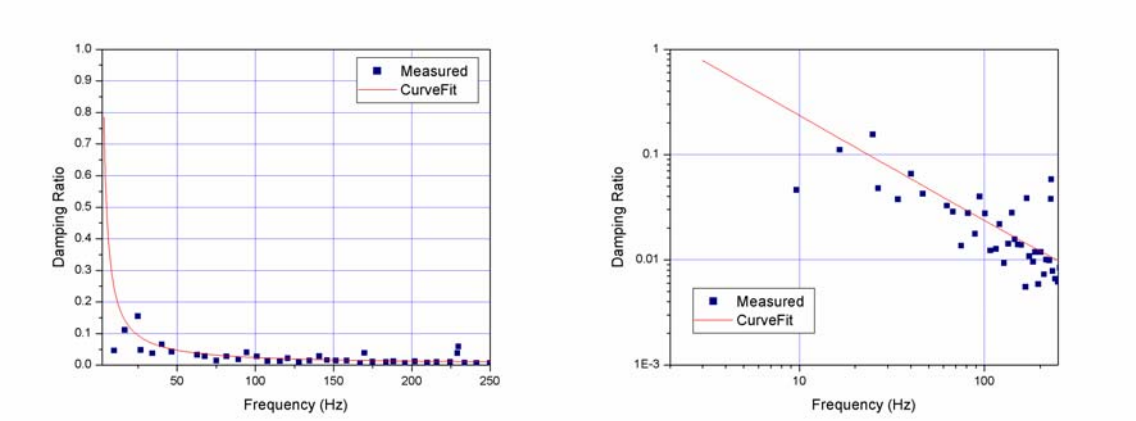

(in Linear Scale) (in Logarithmic Scale)

Figure 84. Modal Damping Ratio at Area 55, Athwartship Direction (Modified)

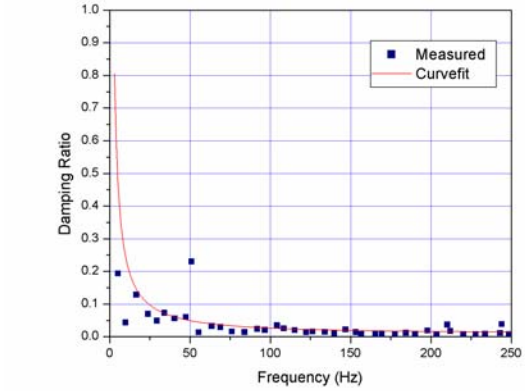

Figure 85. Modal Damping Ratio at Area 56, Athwartship Direction (Original)

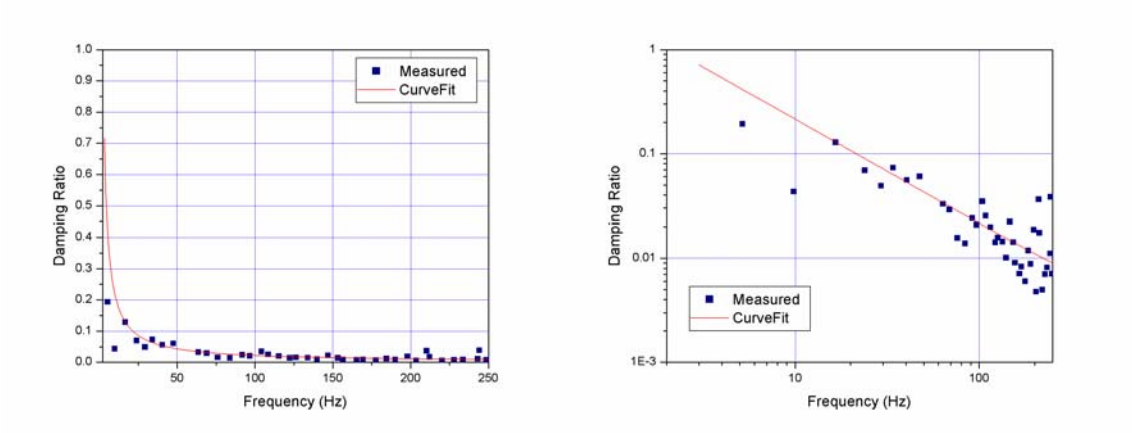

(in Linear Scale) (in Logarithmic Scale)

Figure 86. Modal Damping Ratio at Area 56, Athwartship Direction (Modified)

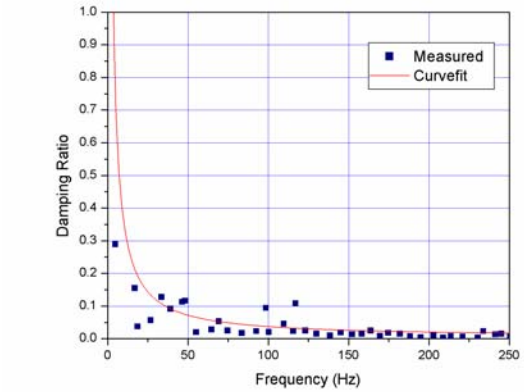

Figure 87. Modal Damping Ratio at Area 57, Athwartship Direction (Original)

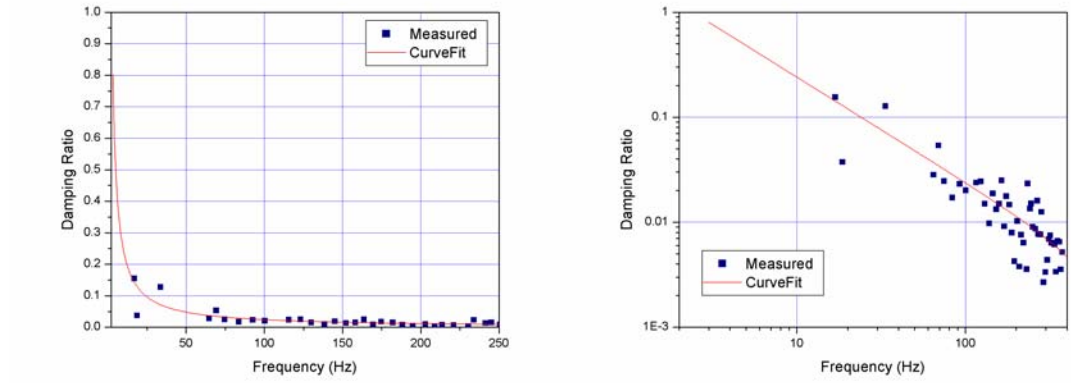

(in Linear Scale) (in Logarithmic Scale)

Figure 88. Modal Damping Ratio at Area 57, Athwartship Direction (Modified)

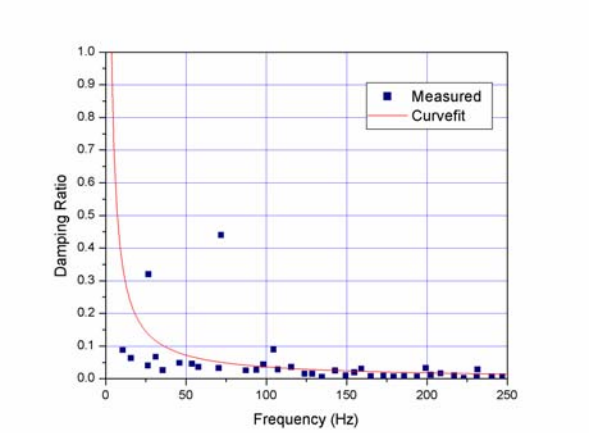

Figure 89. Modal Damping Ratio at Area 58, Athwartship Direction (Original)

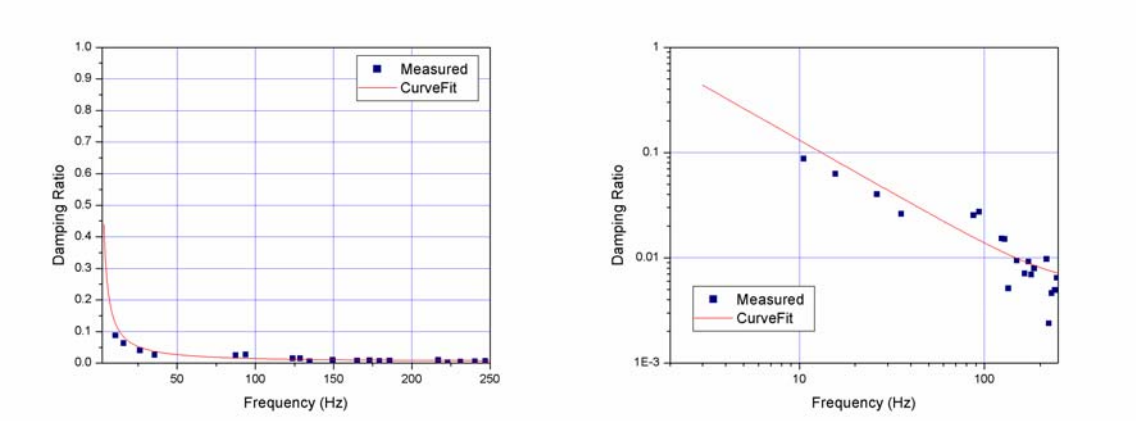

(in Linear Scale) (in Logarithmic Scale)

Figure 90. Modal Damping Ratio at Area 58, Athwartship Direction (Modified)

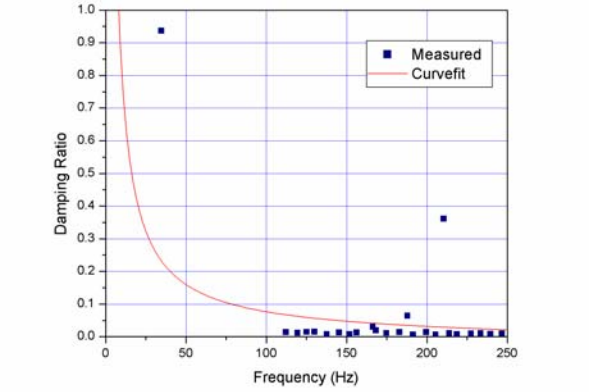

Figure 91. Modal Damping Ratio at Area 59, Athwartship Direction (Original)

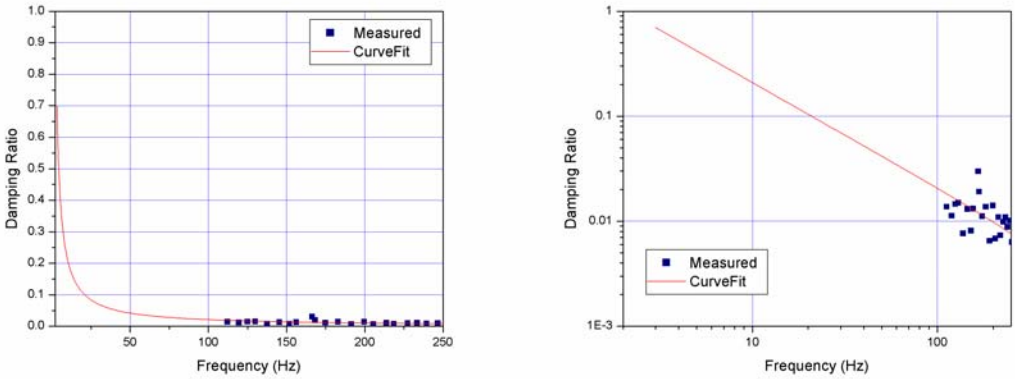

(in Linear Scale) (in Logarithmic Scale)

Figure 92. Modal Damping Ratio at Area 59, Athwartship Direction (Modified)

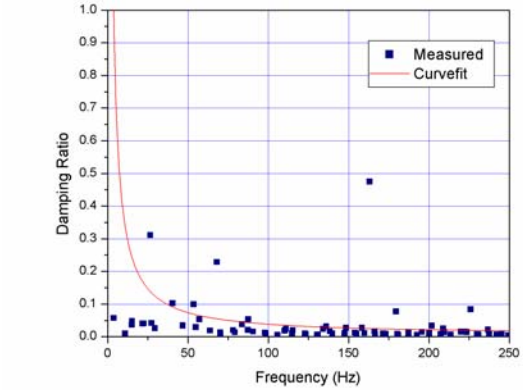

Figure 93. Modal Damping Ratio at Area 60, Athwartship Direction (Original)

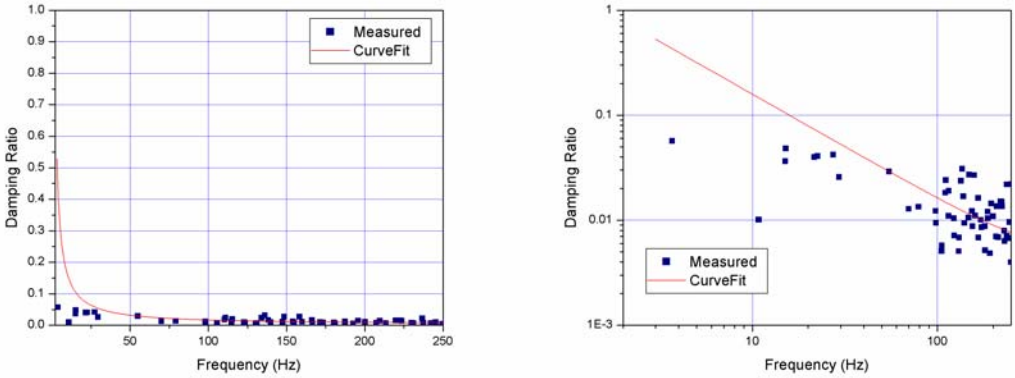

(in Linear Scale) (in Logarithmic Scale)

Figure 94. Modal Damping Ratio at Area 60, Athwartship Direction (Modified)

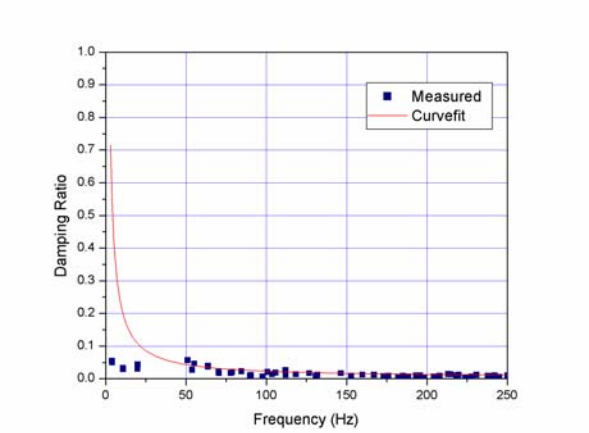

Figure 95. Modal Damping Ratio at Area 61, Athwartship Direction (Original)

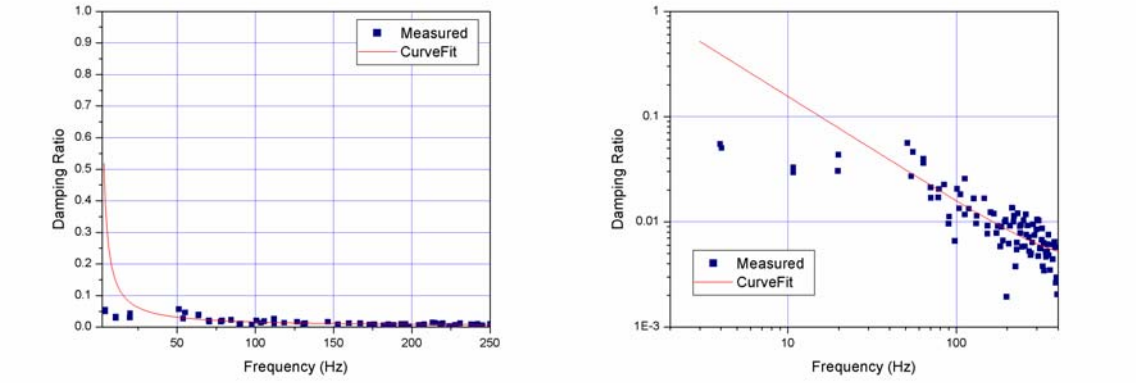

(in Linear Scale) (in Logarithmic Scale)

Figure 96. Modal Damping Ratio at Area 61, Athwartship Direction (Modified)

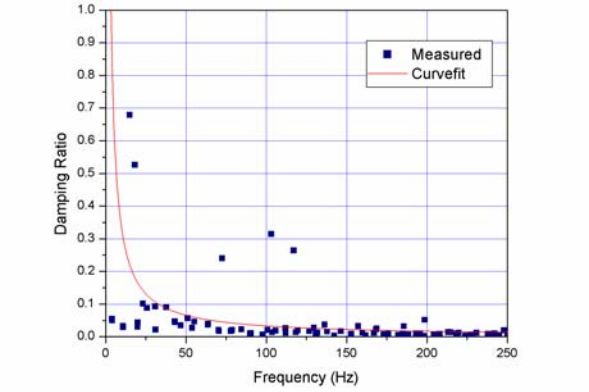

Figure 97. Modal Damping Ratio at Area 62, Athwartship Direction (Original)

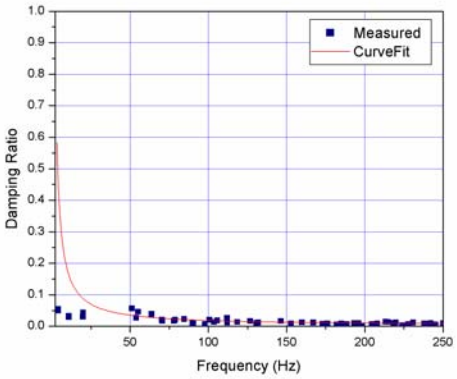

(in Linear Scale)

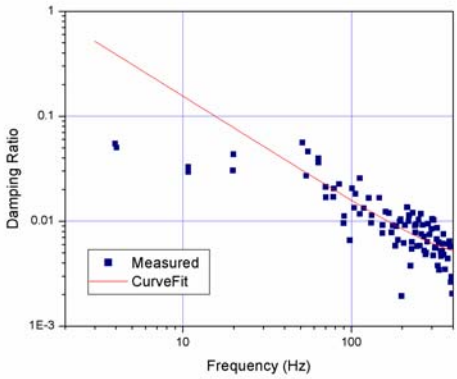

(in Logarithmic Scale)

Figure 98. Modal Damping Ratio at Area 62, Athwartship Direction (Modified)

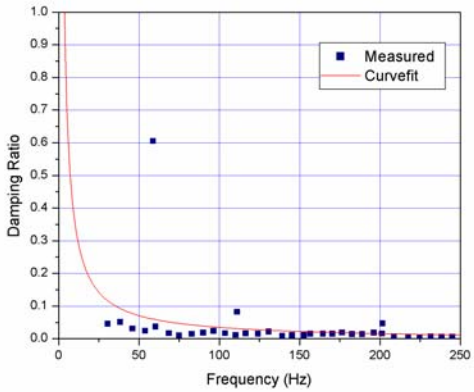

Figure 99. Modal Damping Ratio at Area 64, Athwartship Direction (Original)

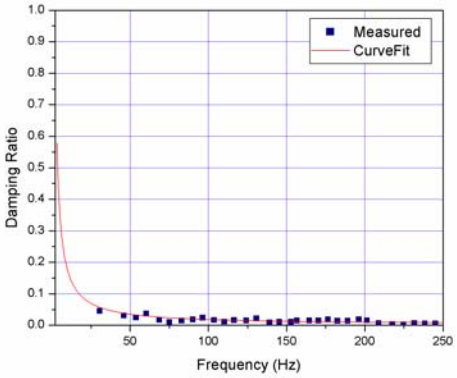

(in Linear Scale)

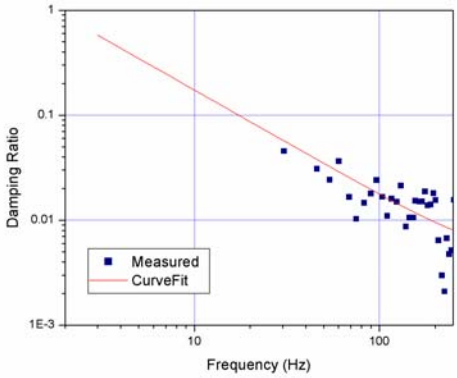

(in Logarithmic Scale)

Figure 100. Modal Damping Ratio at Area 64, Athwartship Direction (Modified)

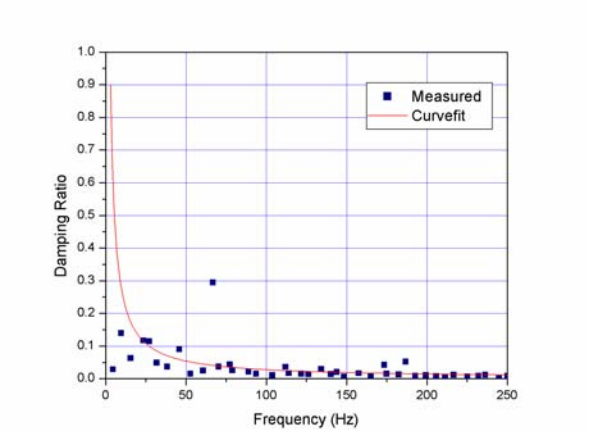

Figure 101. Modal Damping Ratio at Area 65, Athwartship Direction (Original)

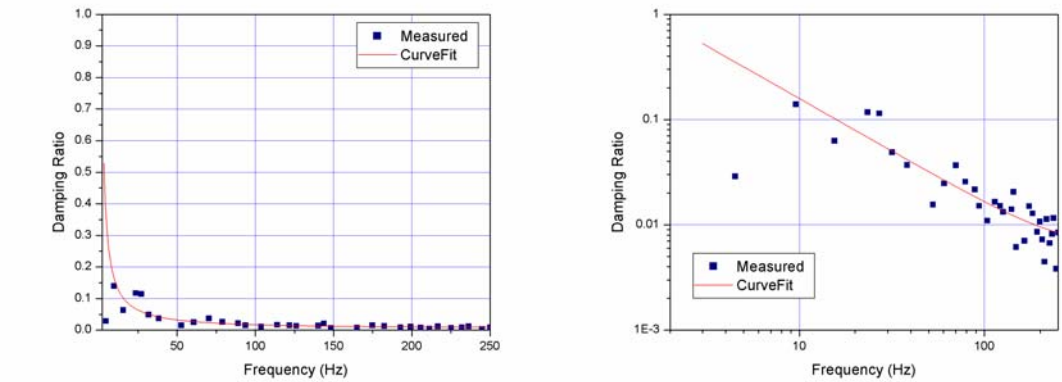

(in Linear Scale) (in Logarithmic Scale)

Figure 102. Modal Damping Ratio at Area 65, Athwartship Direction (Modified)

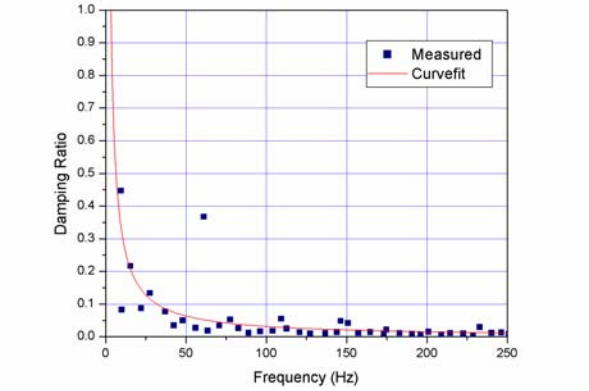

Figure 103. Modal Damping Ratio at Area 67, Athwartship Direction (Original)

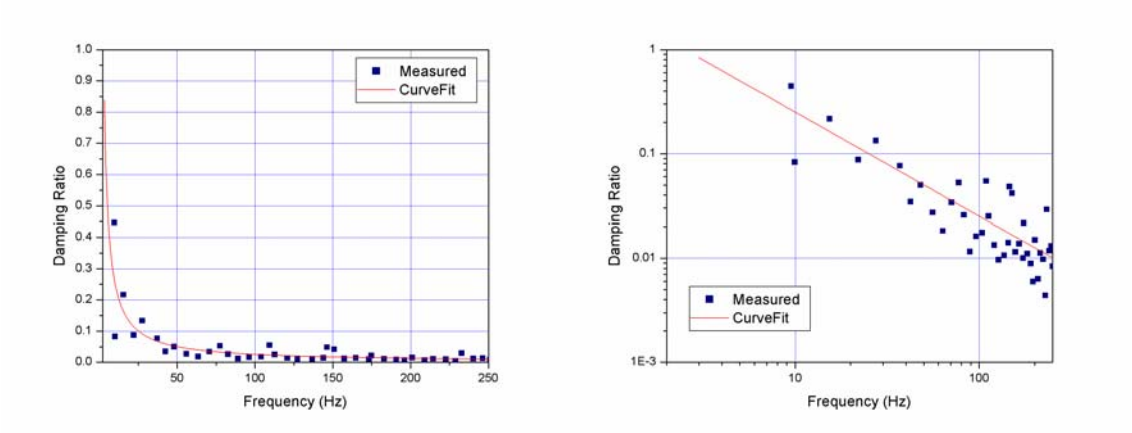

(in Linear Scale) (in Logarithmic Scale)

Figure 104. Modal Damping Ratio at Area 67, Athwartship Direction (Modified)

B. Results in the Vertical Direction

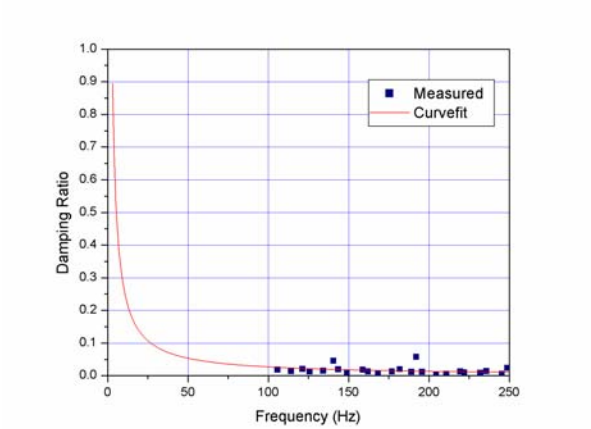

Figure 105. Modal Damping Ratio at Area 1, Vertical Direction (Original)

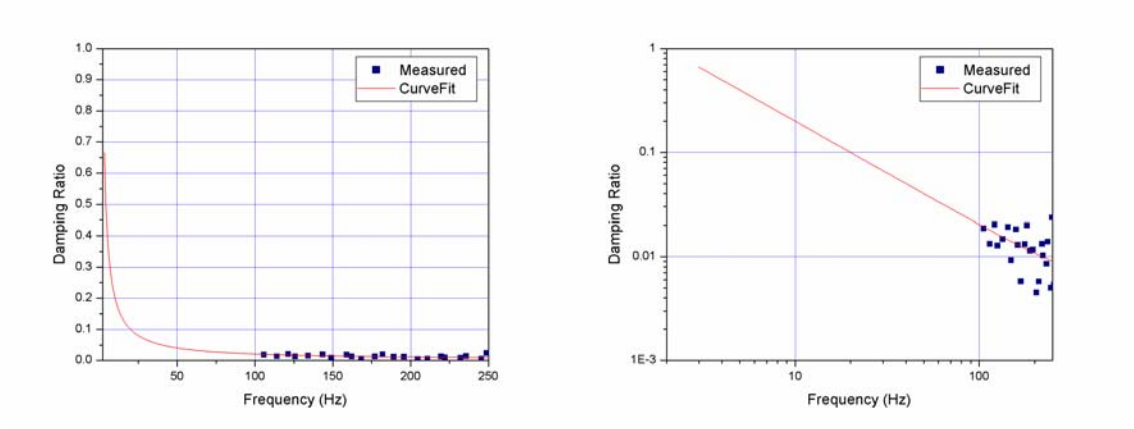

(in Linear Scale) (in Logarithmic Scale)

Figure 106. Modal Damping Ratio at Area 1, Vertical Direction (Modified)

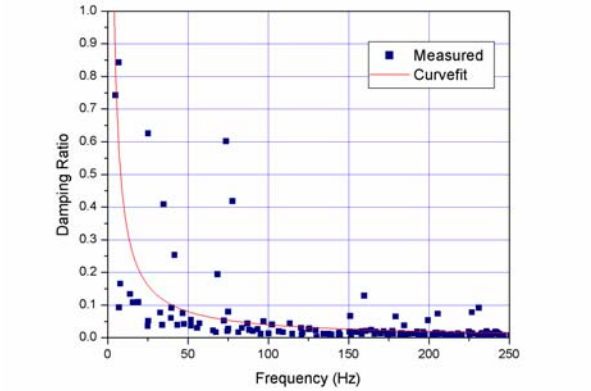

Figure 107. Modal Damping Ratio at Area 3, Vertical Direction (Original)

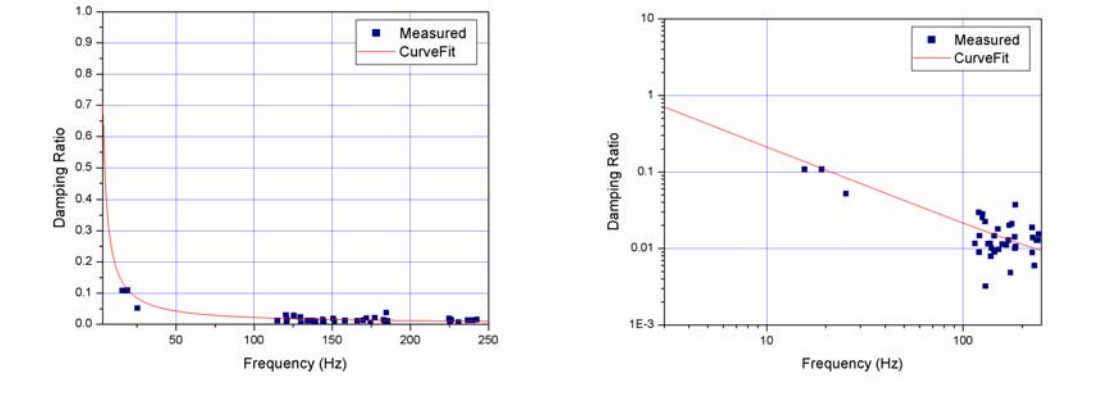

(in Linear Scale) (in Logarithmic Scale)

Figure 108. Modal Damping Ratio at Area 3, Vertical Direction (Modified)

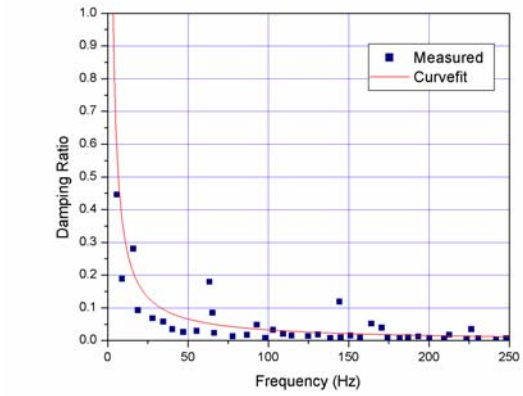

Figure 109. Modal Damping Ratio at Area 4, Vertical Direction (Original)

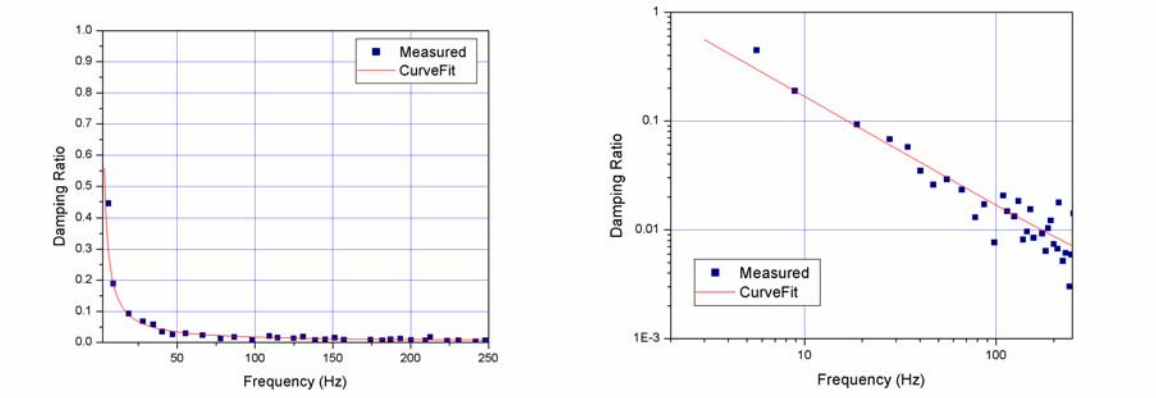

(in Linear Scale) (in Logarithmic Scale)

Figure 110. Modal Damping Ratio at Area 4, Vertical Direction (Modified)

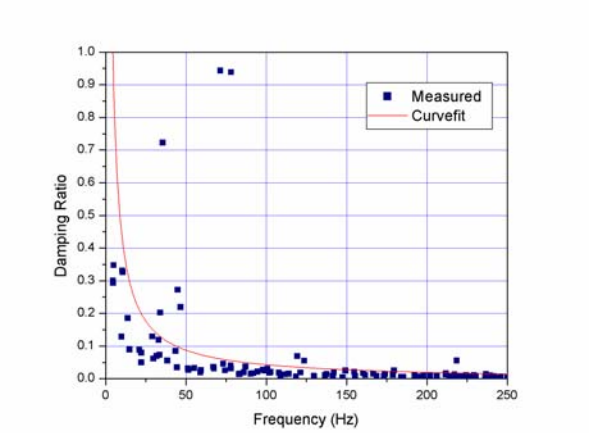

Figure 111. Modal Damping Ratio at Area 5, Vertical Direction (Original)

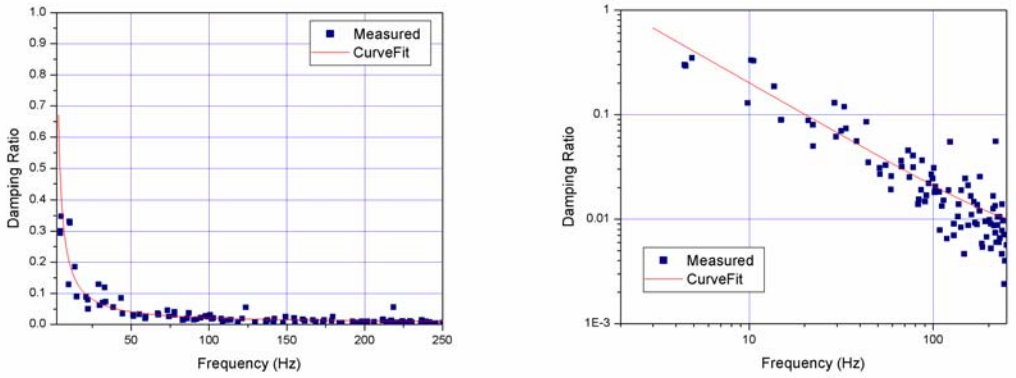

(in Linear Scale) (in Logarithmic Scale)

Figure 112. Modal Damping Ratio at Area 5, Vertical Direction (Modified)

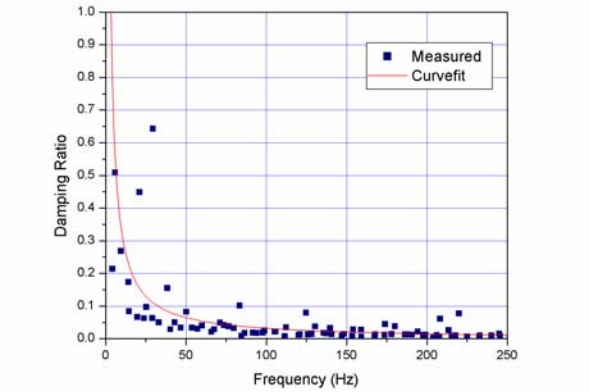

Figure 113. Modal Damping Ratio at Area 6, Vertical Direction (Original)

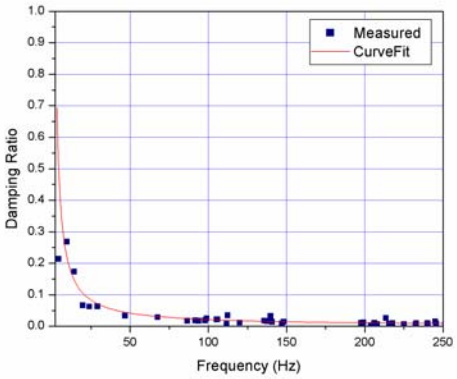

(in Linear Scale)

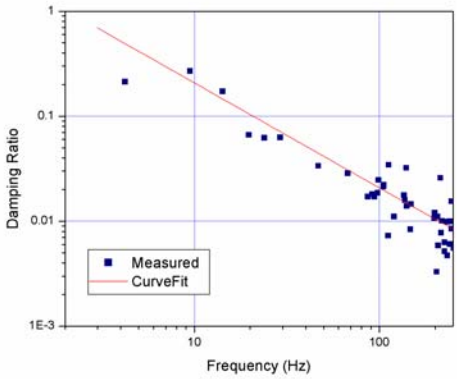

(in Logarithmic Scale)

Figure 114. Modal Damping Ratio at Area 6, Vertical Direction (Modified)

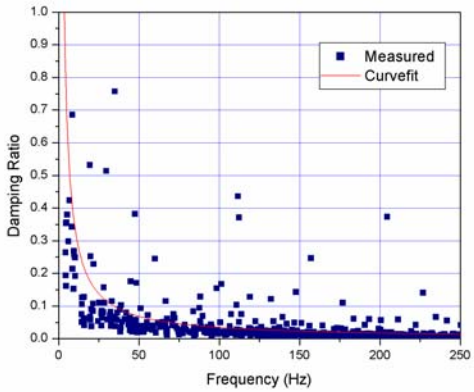

Figure 115. Modal Damping Ratio at Area 7, Vertical Direction (Original)

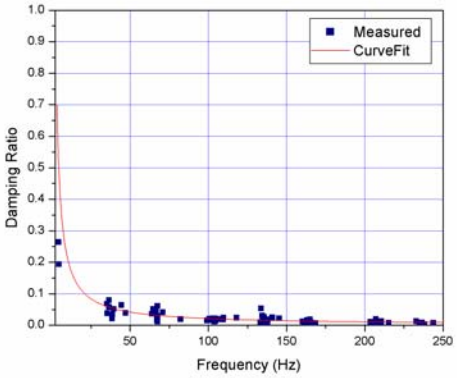

(in Linear Scale)

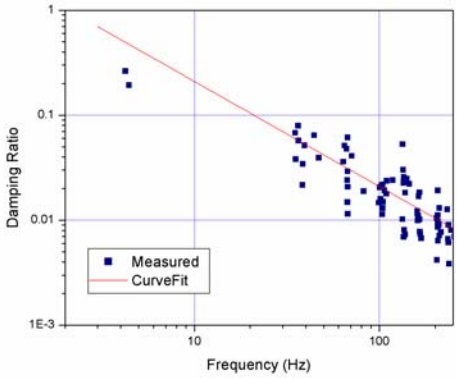

(in Logarithmic Scale)

Figure 116. Modal Damping Ratio at Area 7, Vertical Direction (Modified)

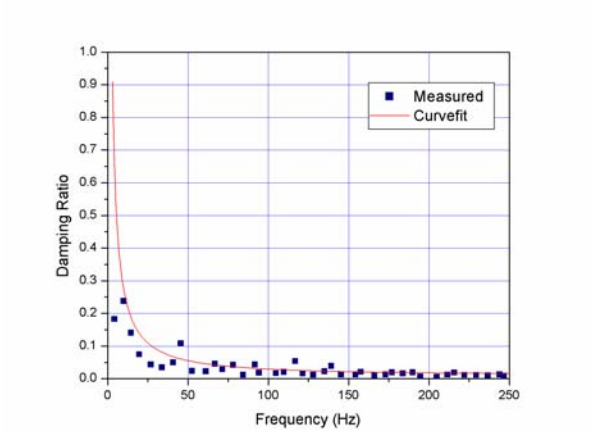

Figure 117. Modal Damping Ratio at Area 8, Vertical Direction (Original)

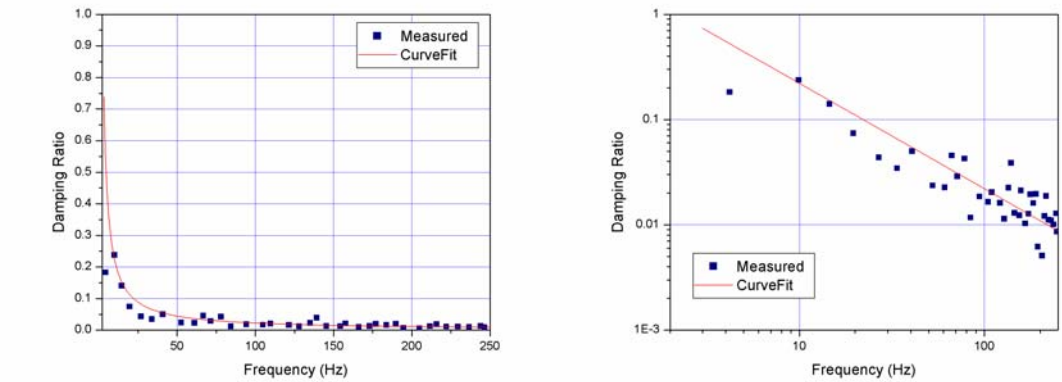

(in Linear Scale) (in Logarithmic Scale)

Figure 118. Modal Damping Ratio at Area 8, Vertical Direction (Modified)

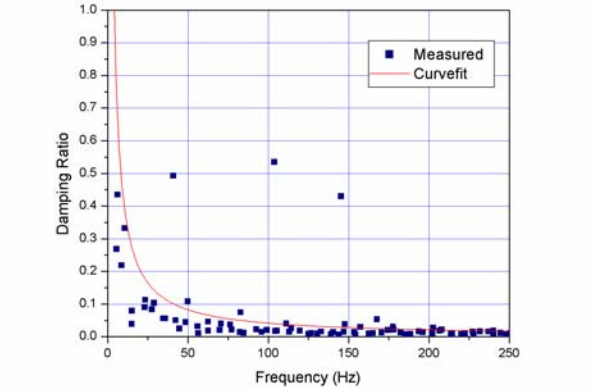

Figure 119. Modal Damping Ratio at Area 9, Vertical Direction (Original)

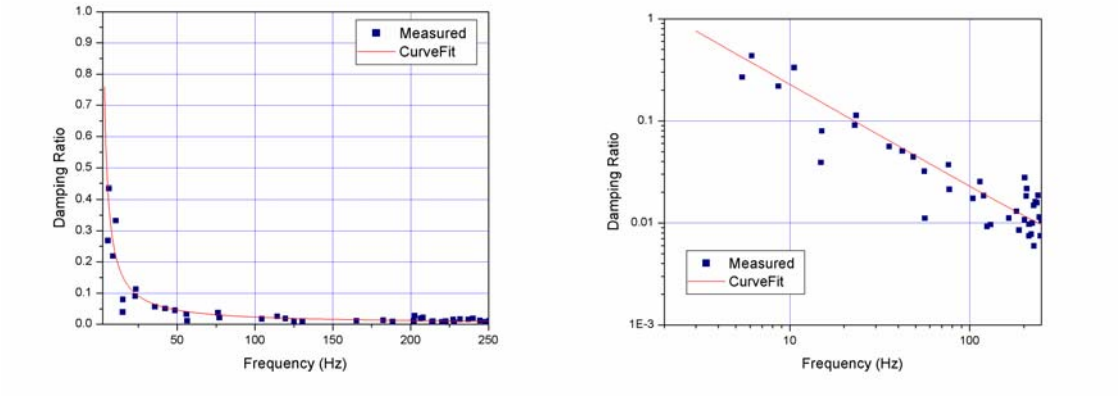

(in Linear Scale) (in Logarithmic Scale)

Figure 120. Modal Damping Ratio at Area 9, Vertical Direction (Modified)

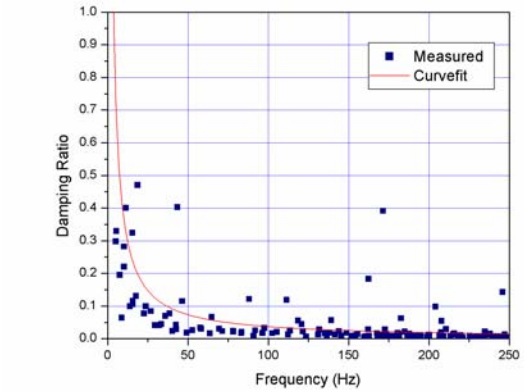

Figure 121. Modal Damping Ratio at Area 10, Vertical Direction (Original)

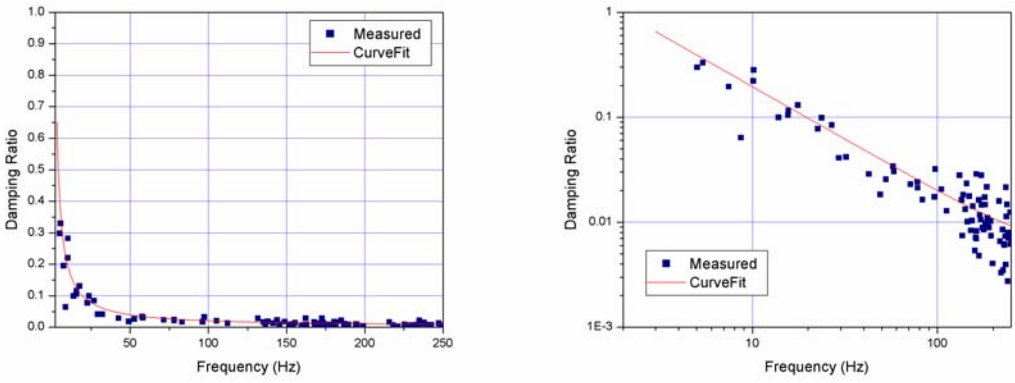

(in Linear Scale) (in Logarithmic Scale)

Figure 122. Modal Damping Ratio at Area 10, Vertical Direction (Modified)

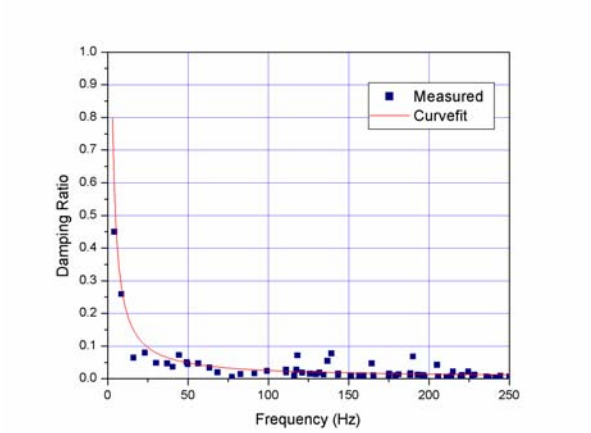

Figure 123. Modal Damping Ratio at Area 11, Vertical Direction (Original)

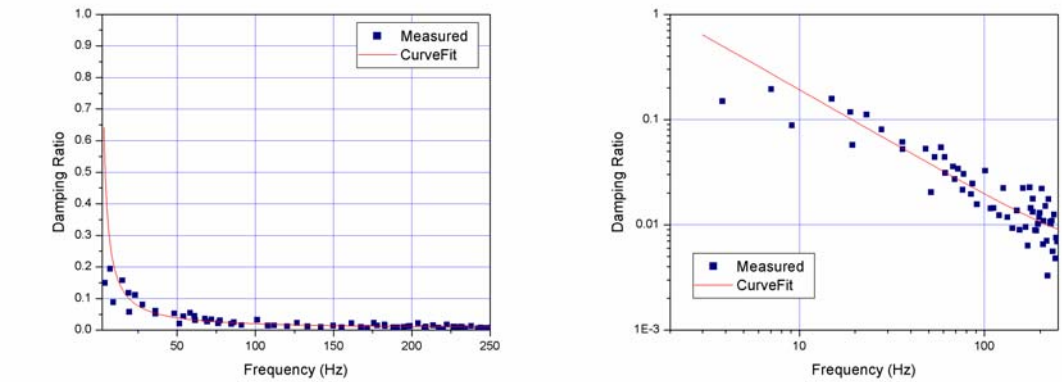

(in Linear Scale) (in Logarithmic Scale)

Figure 124. Modal Damping Ratio at Area 11, Vertical Direction (Modified)

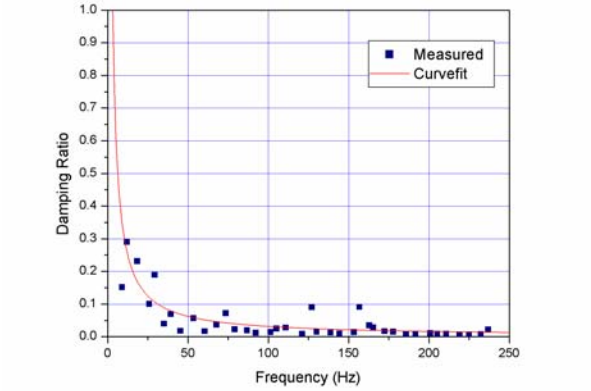

Figure 125. Modal Damping Ratio at Area 12, Vertical Direction (Original)

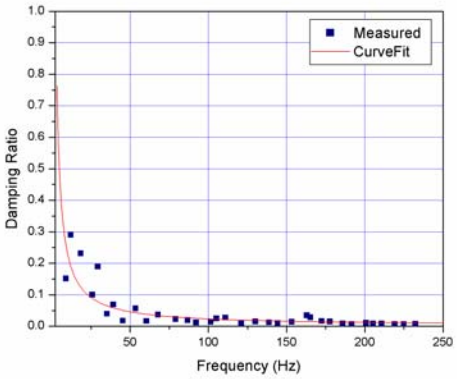

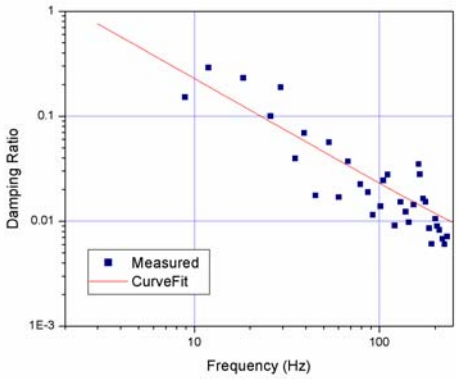

(in Linear Scale) (in Logarithmic Scale)

Figure 126. Modal Damping Ratio at Area 12, Vertical Direction (Modified)

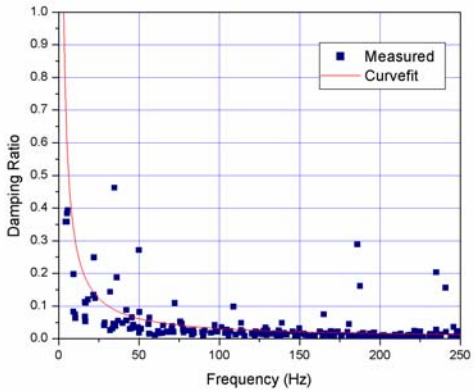

Figure 127. Modal Damping Ratio at Area 13, Vertical Direction (Original)

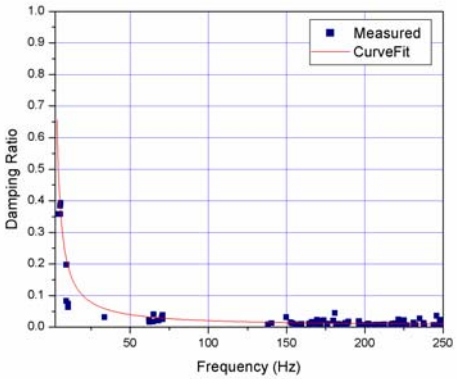

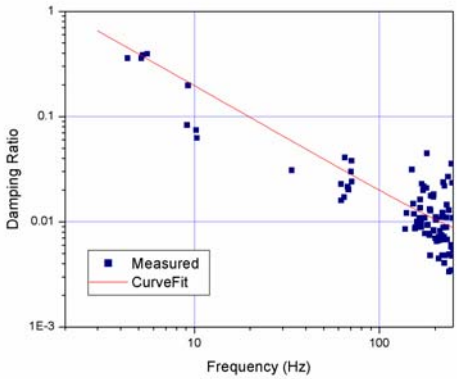

(in Linear Scale) (in Logarithmic Scale)

Figure 128. Modal Damping Ratio at Area 13, Vertical Direction (Modified)

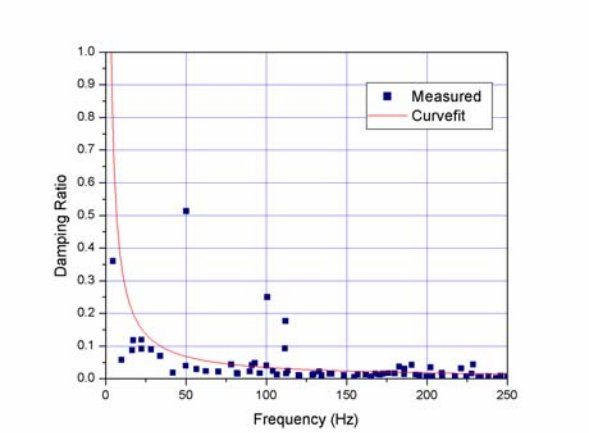

Figure 129. Modal Damping Ratio at Area 14, Vertical Direction (Original)

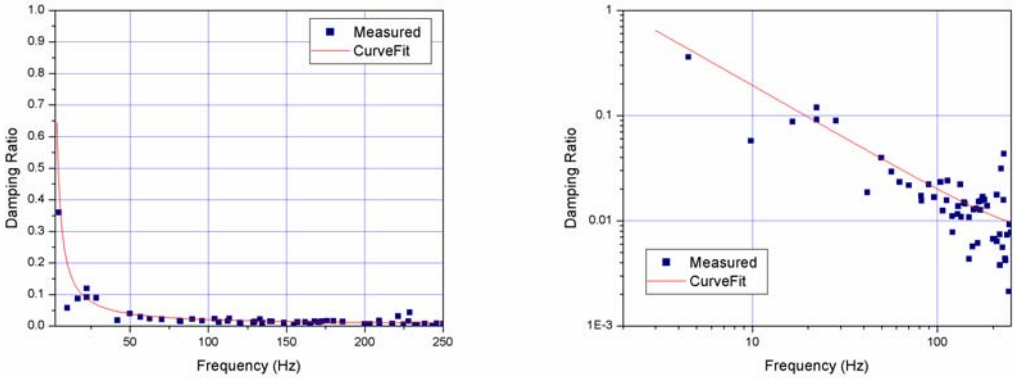

(in Linear Scale) (in Logarithmic Scale)

Figure 130. Modal Damping Ratio at Area 14, Vertical Direction (Modified)

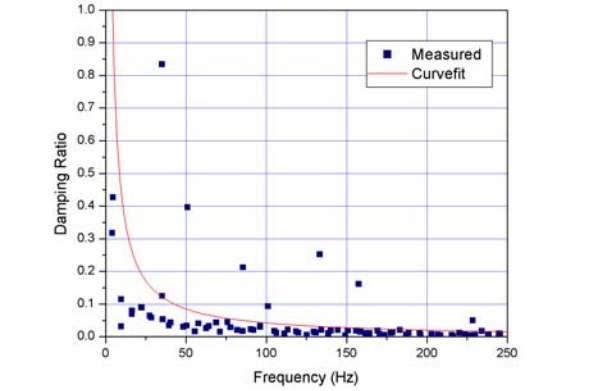

Figure 131. Modal Damping Ratio at Area 15, Vertical Direction (Original)

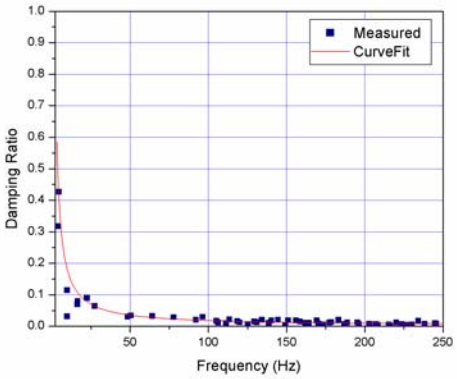

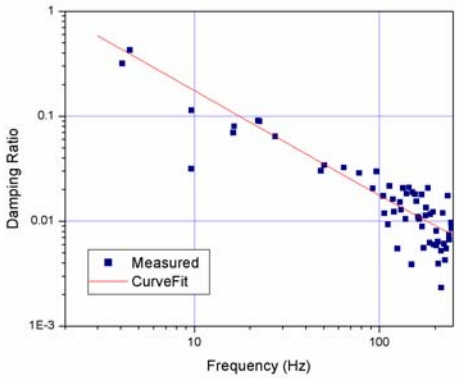

(in Linear Scale) (in Logarithmic Scale)

Figure 132. Modal Damping Ratio at Area 15, Vertical Direction (Modified)

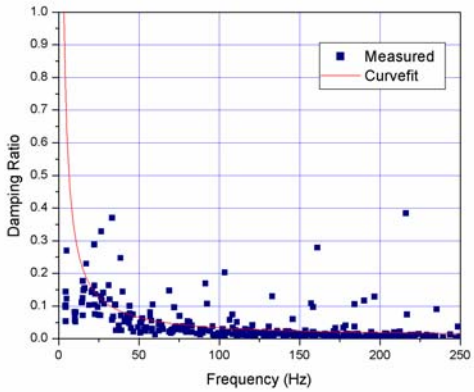

Figure 133. Modal Damping Ratio at Area 16, Vertical Direction (Original)

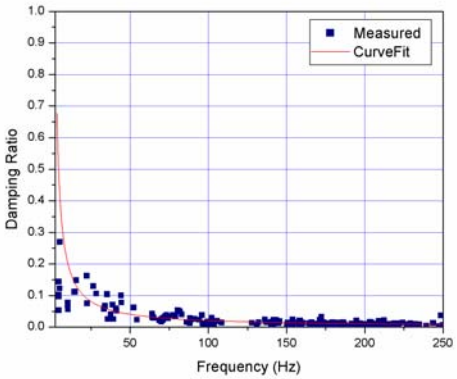

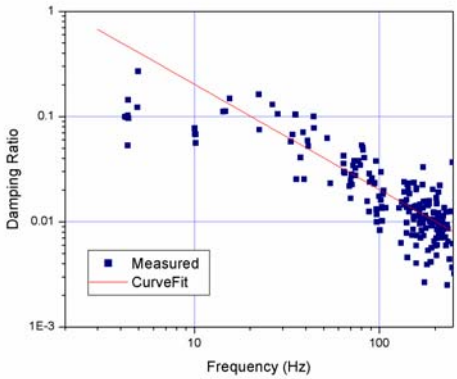

(in Linear Scale) (in Logarithmic Scale)

Figure 134. Modal Damping Ratio at Area 16, Vertical Direction (Modified)

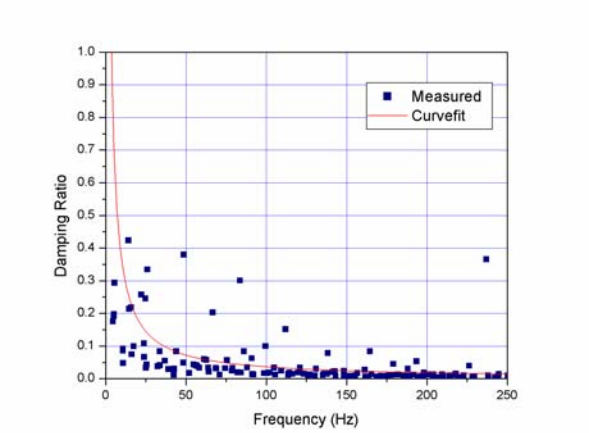

Figure 135. Modal Damping Ratio at Area 17, Vertical Direction (Original)

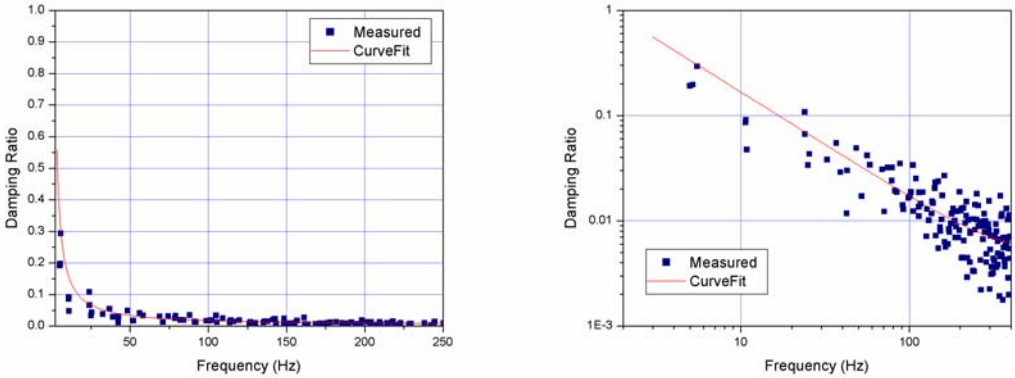

(in Linear Scale) (in Logarithmic Scale)

Figure 136. Modal Damping Ratio at Area 17, Vertical Direction (Modified)

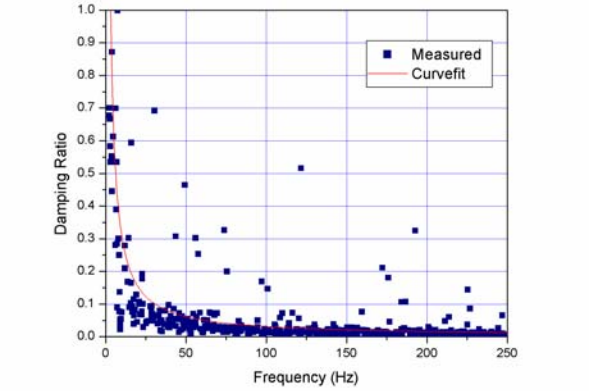

Figure 137. Modal Damping Ratio at Area 18, Vertical Direction (Original)

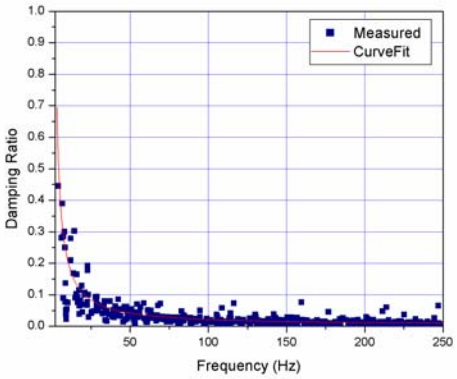

(in Linear Scale)

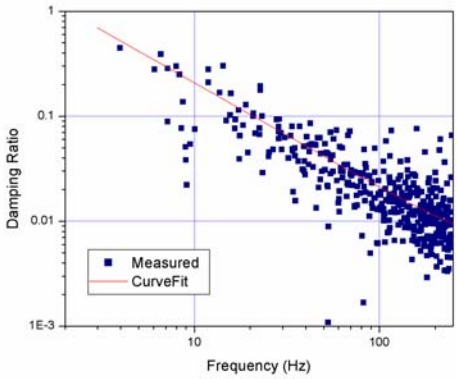

(in Logarithmic Scale)

Figure 138. Modal Damping Ratio at Area 18, Vertical Direction (Modified)

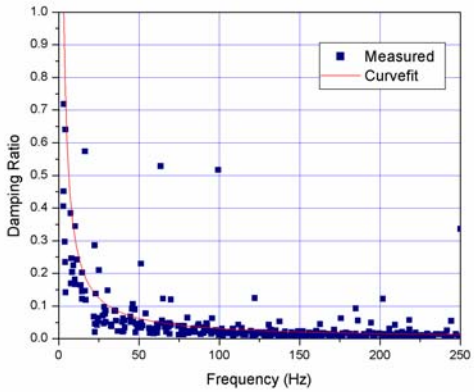

Figure 139. Modal Damping Ratio at Area 19, Vertical Direction (Original)

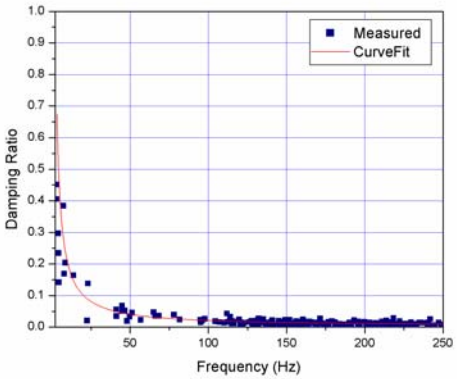

(in Linear Scale)

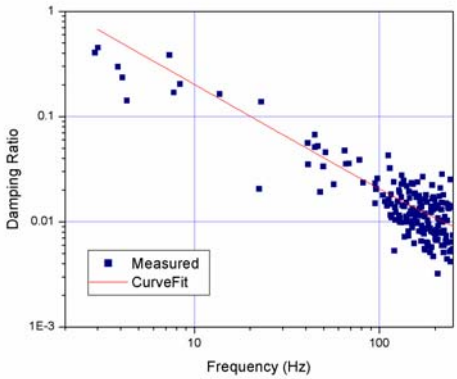

(in Logarithmic Scale)

Figure 140. Modal Damping Ratio at Area 19, Vertical Direction (Modified)

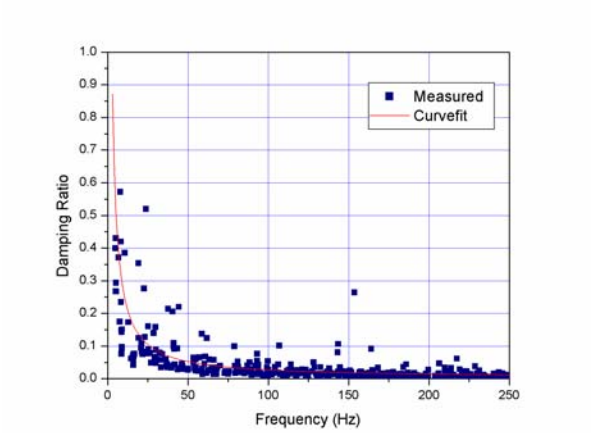

Figure 141. Modal Damping Ratio at Area 20, Vertical Direction (Original)

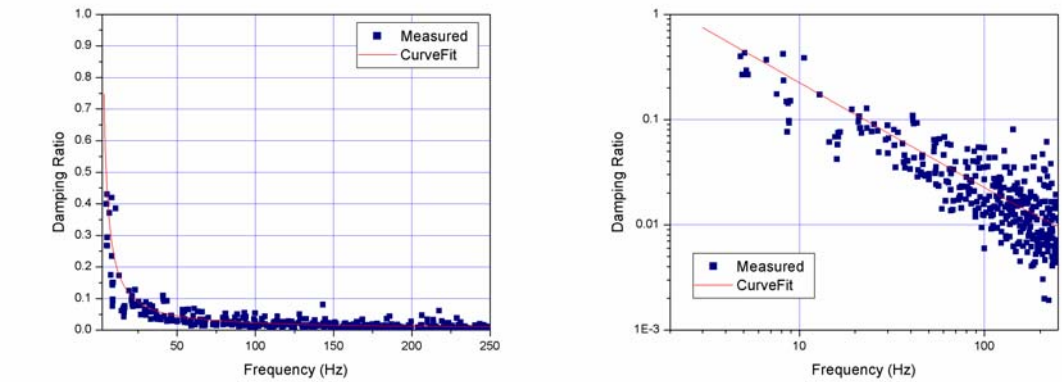

(in Linear Scale) (in Logarithmic Scale)

Figure 142. Modal Damping Ratio at Area 20, Vertical Direction (Modified)

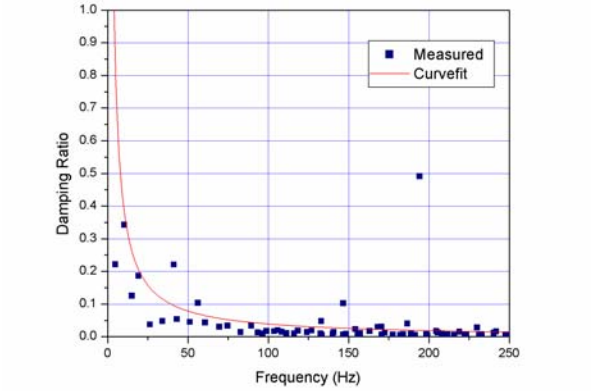

Figure 143. Modal Damping Ratio at Area 21, Vertical Direction (Original)

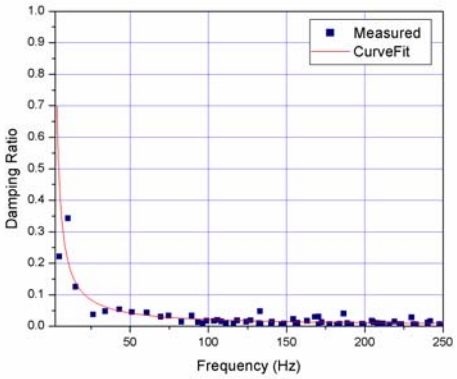

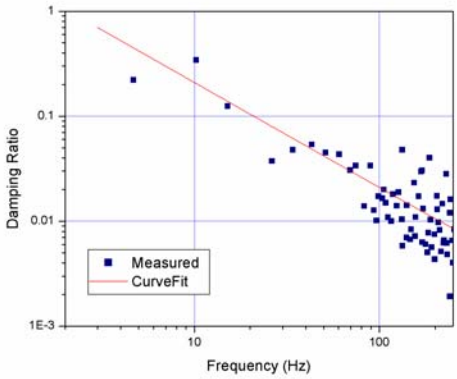

(in Linear Scale) (in Logarithmic Scale)

Figure 144. Modal Damping Ratio at Area 21, Vertical Direction (Modified)

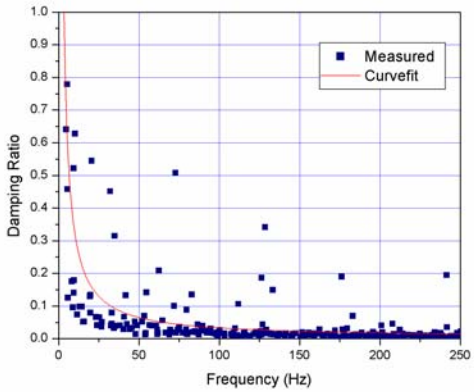

Figure 145. Modal Damping Ratio at Area 22, Vertical Direction (Original)

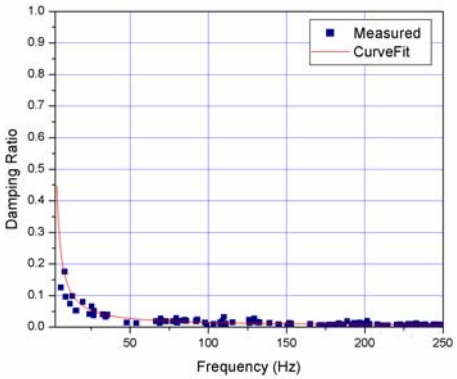

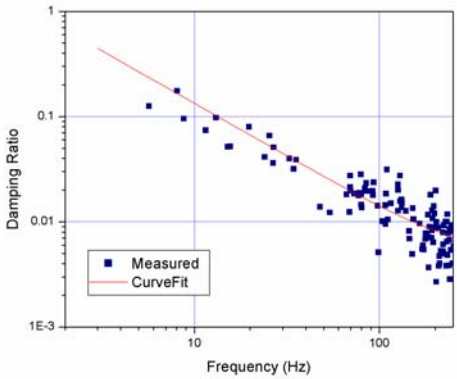

(in Linear Scale) (in Logarithmic Scale)

Figure 146. Modal Damping Ratio at Area 22, Vertical Direction (Modified)

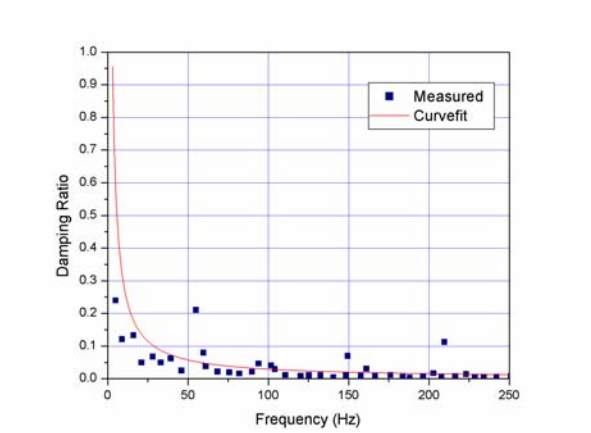

Figure 147. Modal Damping Ratio at Area 23, Vertical Direction (Original)

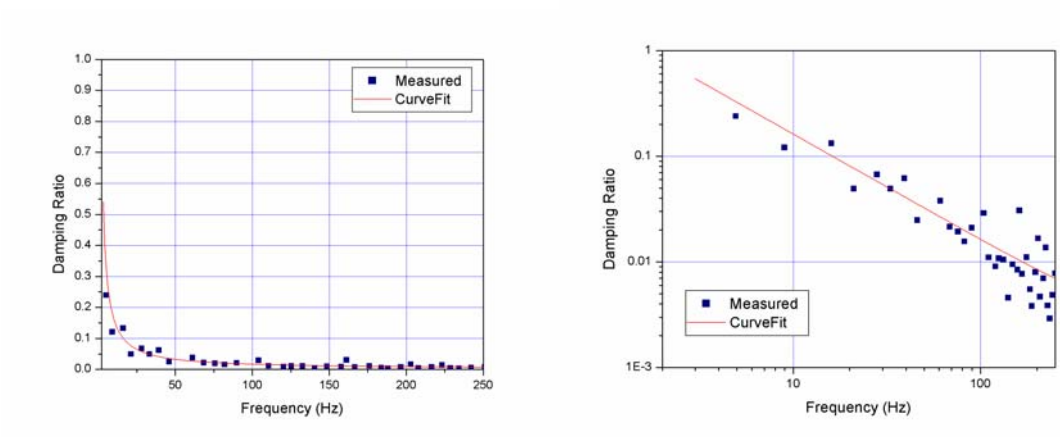

(in Linear Scale) (in Logarithmic Scale)

Figure 148. Modal Damping Ratio at Area 23, Vertical Direction (Modified)

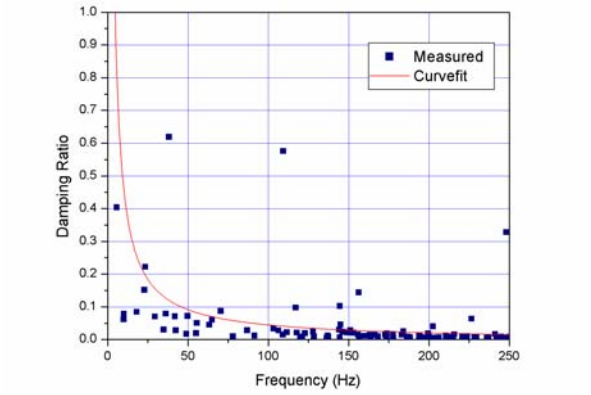

Figure 149. Modal Damping Ratio at Area 24, Vertical Direction (Original)

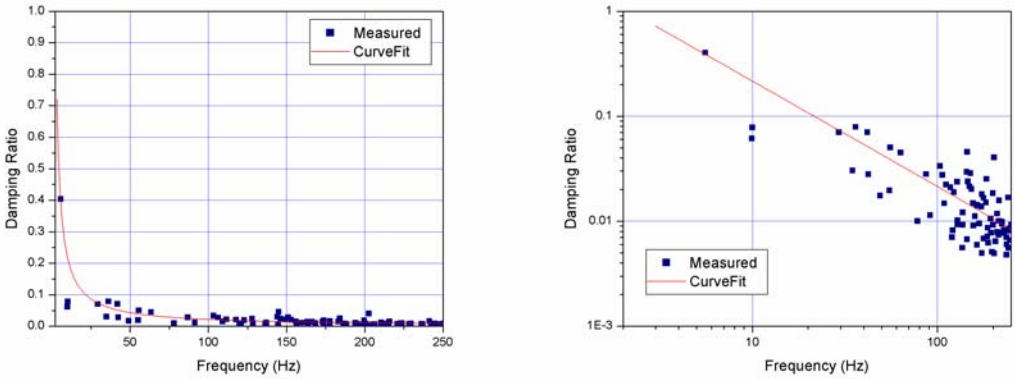

(in Linear Scale) (in Logarithmic Scale)

Figure 150. Modal Damping Ratio at Area 24, Vertical Direction (Modified)

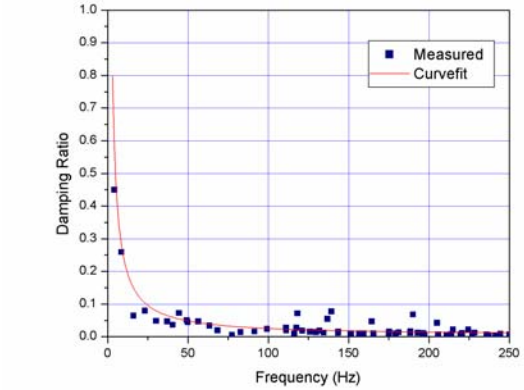

Figure 151. Modal Damping Ratio at Area 25, Vertical Direction (Original)

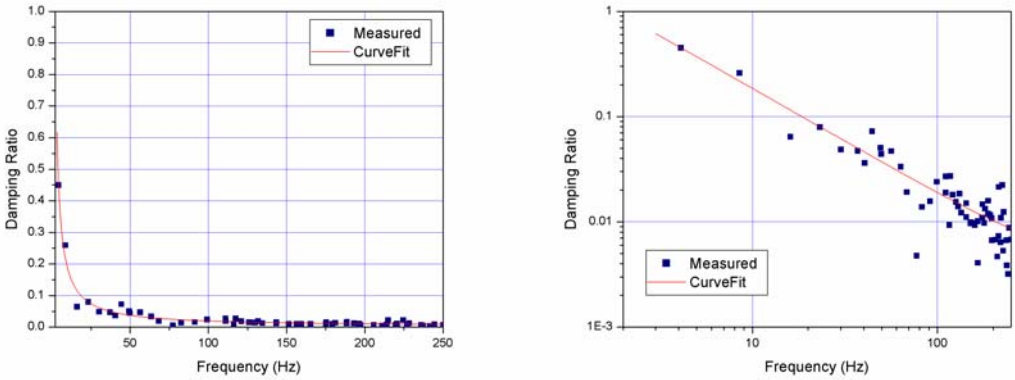

(in Linear Scale) (in Logarithmic Scale)

Figure 152. Modal Damping Ratio at Area 25, Vertical Direction (Modified)

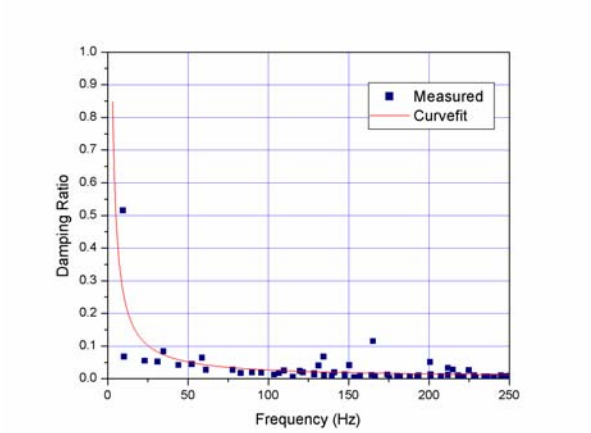

Figure 153. Modal Damping Ratio at Area 26, Vertical Direction (Original)

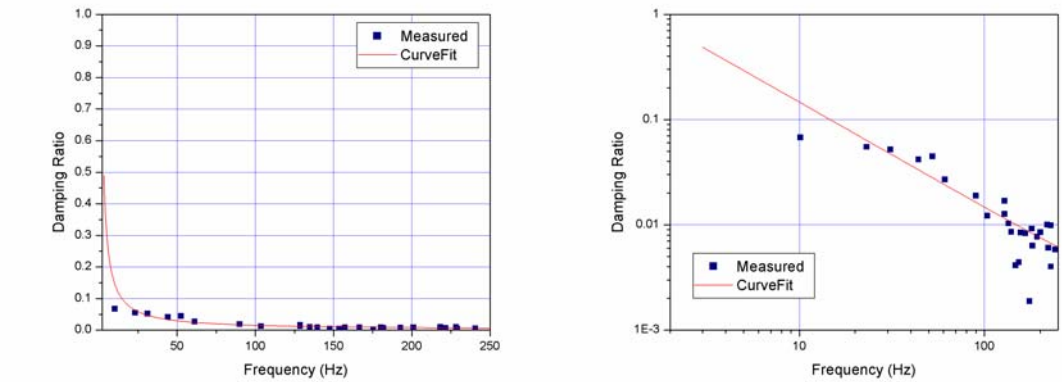

(in Linear Scale) (in Logarithmic Scale)

Figure 154. Modal Damping Ratio at Area 26, Vertical Direction (Modified)

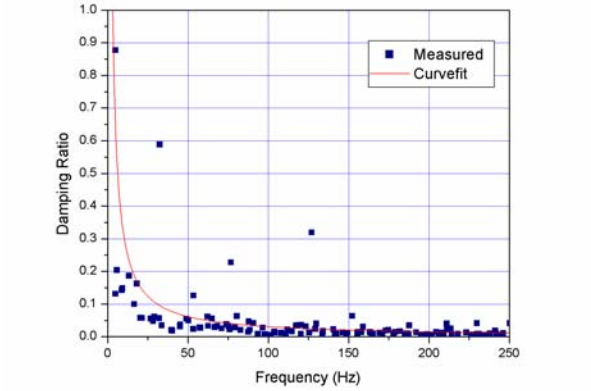

Figure 155. Modal Damping Ratio at Area 27, Vertical Direction (Original)

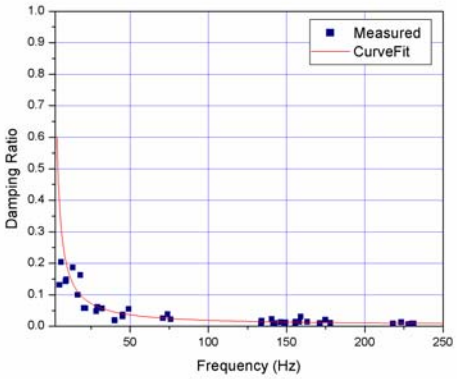

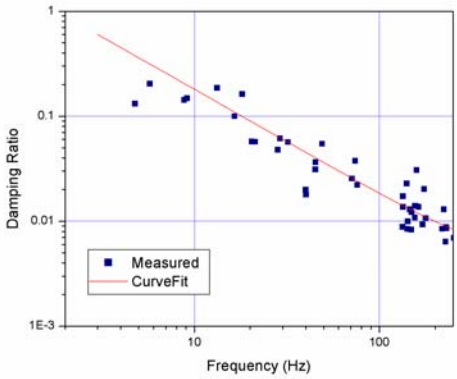

(in Linear Scale) (in Logarithmic Scale)

Figure 156. Modal Damping Ratio at Area 27, Vertical Direction (Modified)

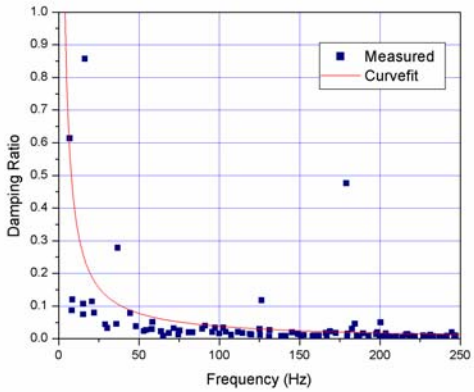

Figure 157. Modal Damping Ratio at Area 28, Vertical Direction (Original)

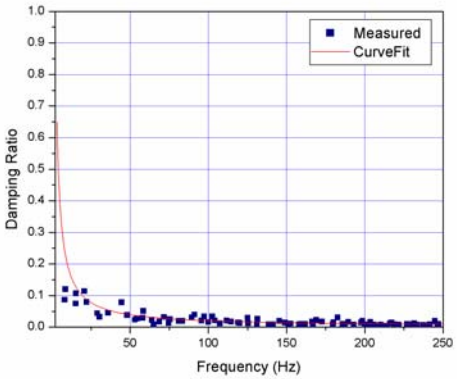

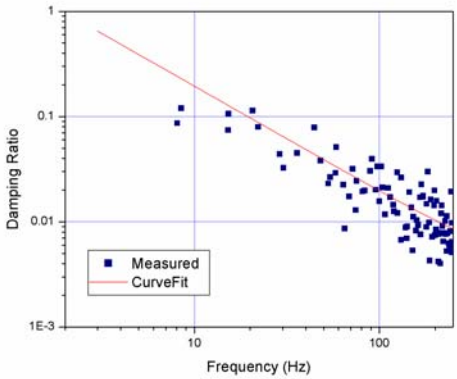

(in Linear Scale) (in Logarithmic Scale)

Figure 158. Modal Damping Ratio at Area 28, Vertical Direction (Modified)

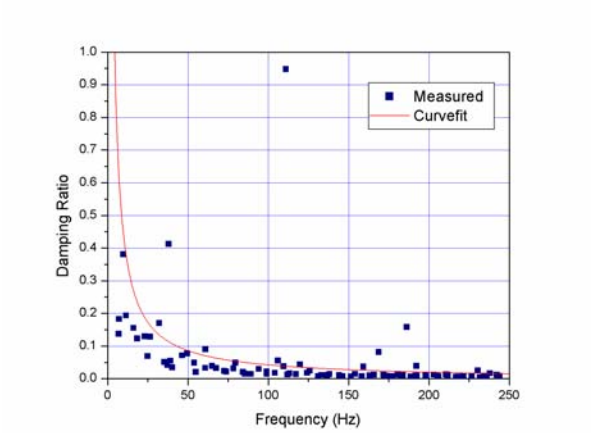

Figure 159. Modal Damping Ratio at Area 29, Vertical Direction (Original)

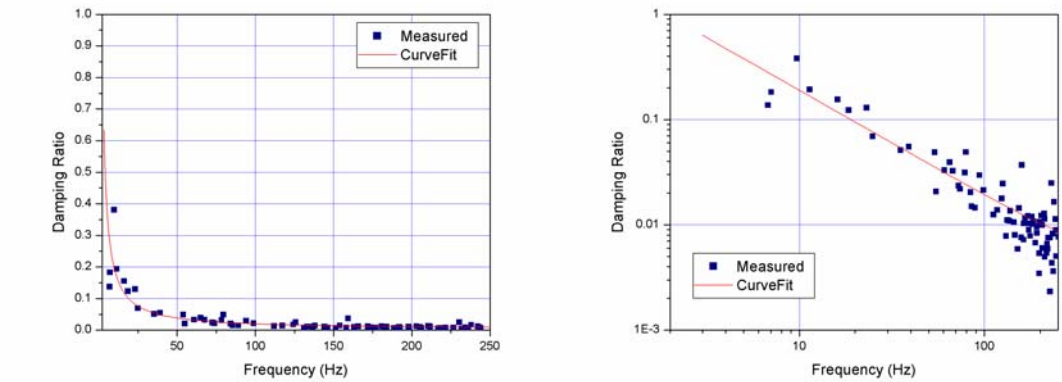

(in Linear Scale) (in Logarithmic Scale)

Figure 160. Modal Damping Ratio at Area 29, Vertical Direction (Modified)

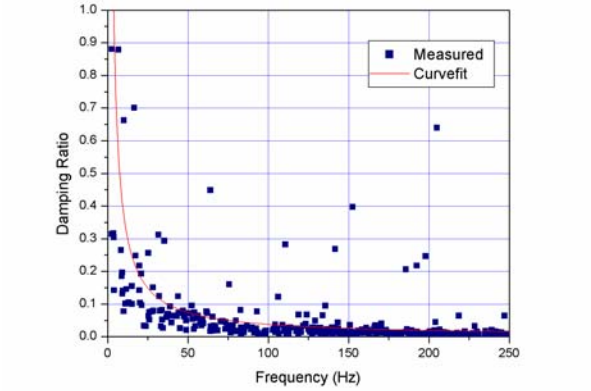

Figure 161. Modal Damping Ratio at Area 30, Vertical Direction (Original)

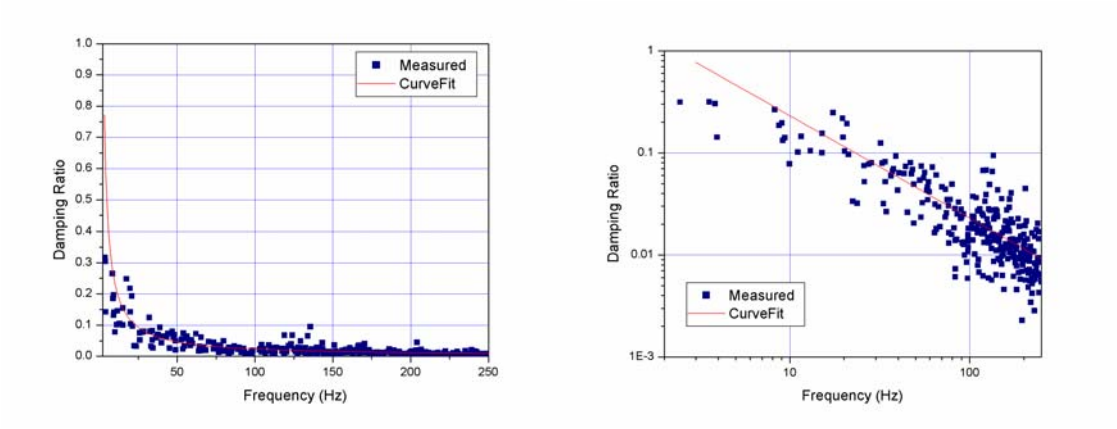

(in Linear Scale) (in Logarithmic Scale)

Figure 162. Modal Damping Ratio at Area 30, Vertical Direction (Modified)

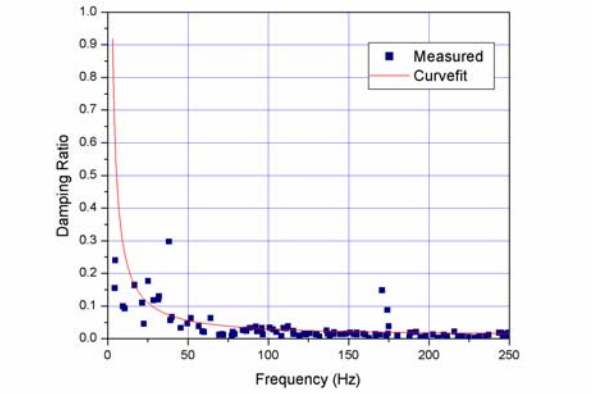

Figure 163. Modal Damping Ratio at Area 31, Vertical Direction (Original)

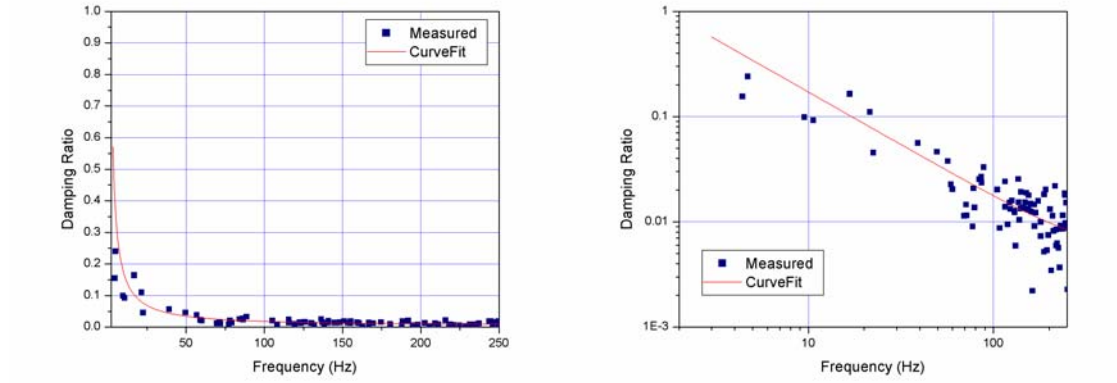

(in Linear Scale) (in Logarithmic Scale)

Figure 164. Modal Damping Ratio at Area 31, Vertical Direction (Modified)

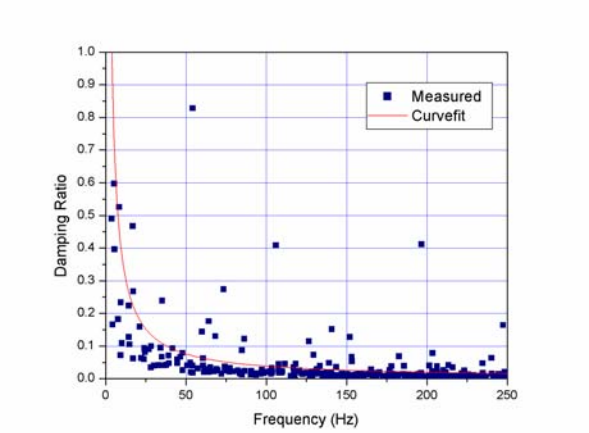

Figure 165. Modal Damping Ratio at Area 32, Vertical Direction (Original)

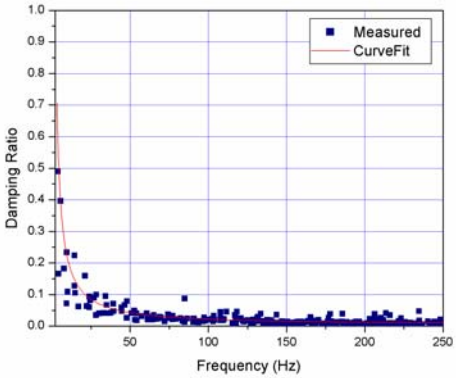

(in Linear Scale)

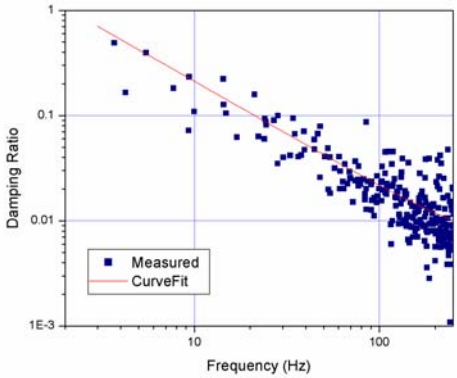

(in Logarithmic Scale)

Figure 166. Modal Damping Ratio at Area 32, Vertical Direction (Modified)

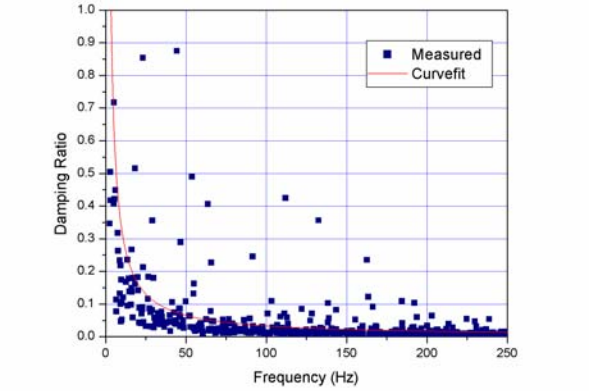

Figure 167. Modal Damping Ratio at Area 33, Vertical Direction (Original)

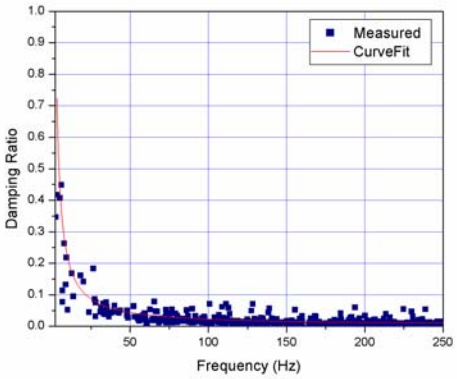

(in Linear Scale)

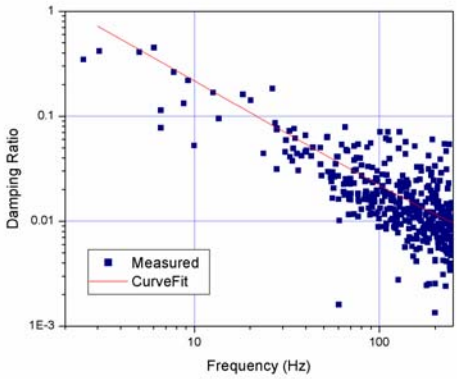

(in Logarithmic Scale)

Figure 168. Modal Damping Ratio at Area 33, Vertical Direction (Modified)

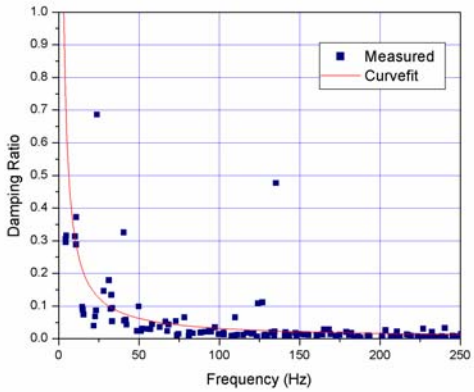

Figure 169. Modal Damping Ratio at Area 34, Vertical Direction (Original)

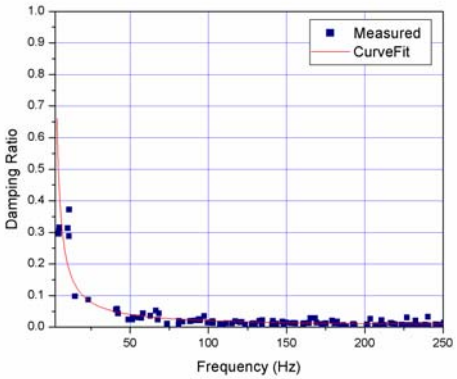

(in Linear Scale)

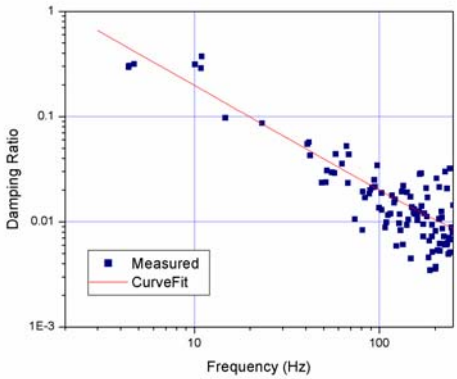

(in Logarithmic Scale)

Figure 170. Modal Damping Ratio at Area 34, Vertical Direction (Modified)

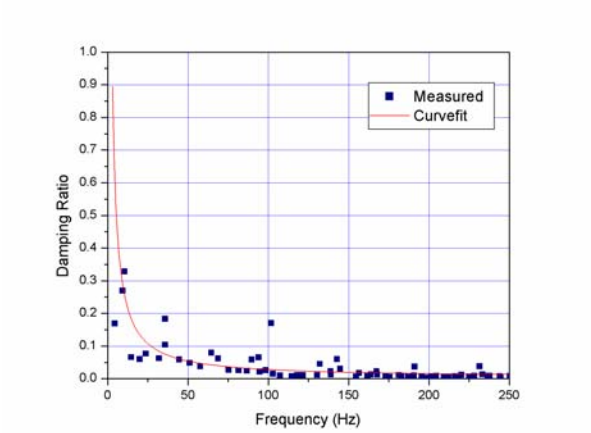

Figure 171. Modal Damping Ratio at Area 35, Vertical Direction (Original)

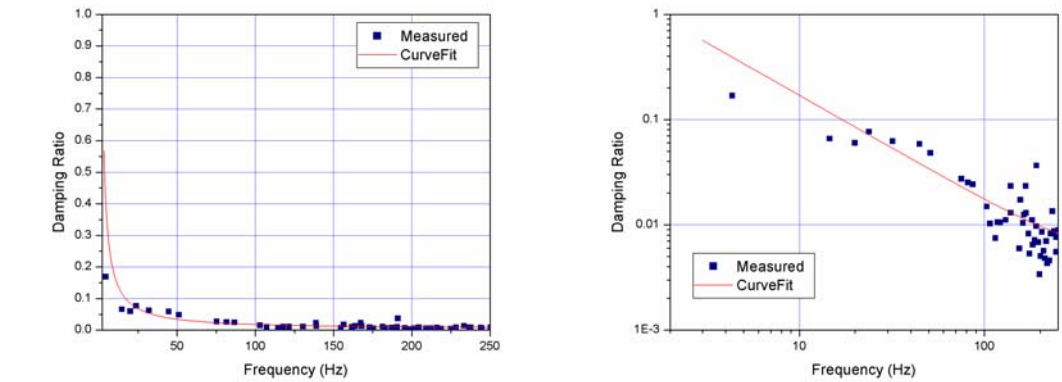

(in Linear Scale) (in Logarithmic Scale)

Figure 172. Modal Damping Ratio at Area 35, Vertical Direction (Modified)

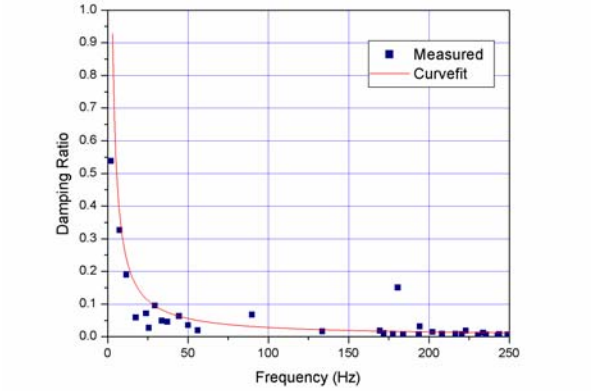

Figure 173. Modal Damping Ratio at Area 36, Vertical Direction (Original)

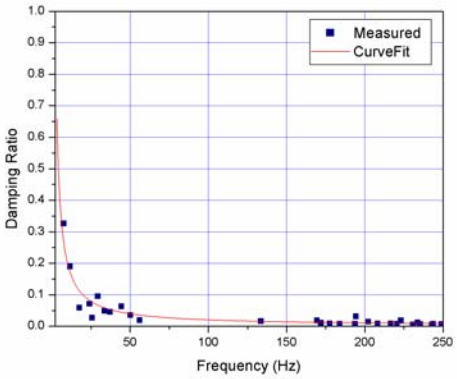

(in Linear Scale)

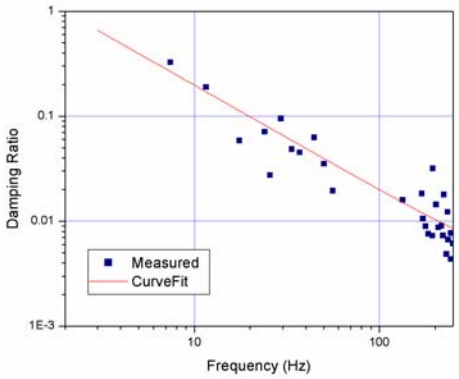

(in Logarithmic Scale)

Figure 174. Modal Damping Ratio at Area 36, Vertical Direction (Modified)

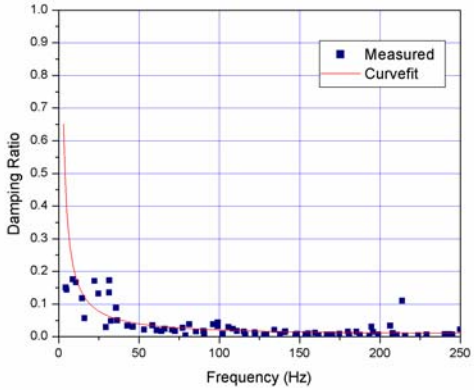

Figure 175. Modal Damping Ratio at Area 37, Vertical Direction (Original)

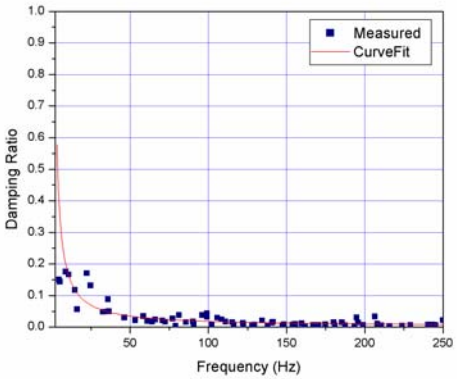

(in Linear Scale)

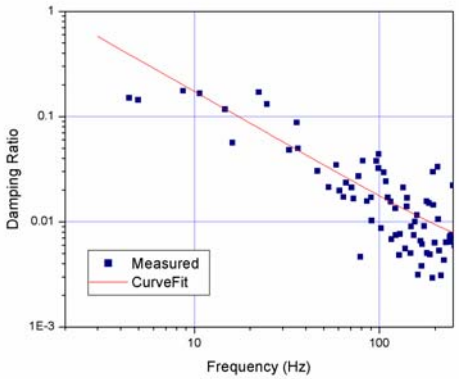

(in Logarithmic Scale)

Figure 176. Modal Damping Ratio at Area 37, Vertical Direction (Modified)

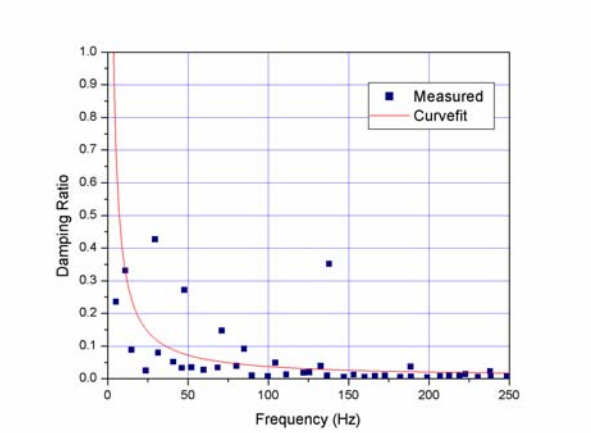

Figure 177. Modal Damping Ratio at Area 38, Vertical Direction (Original)

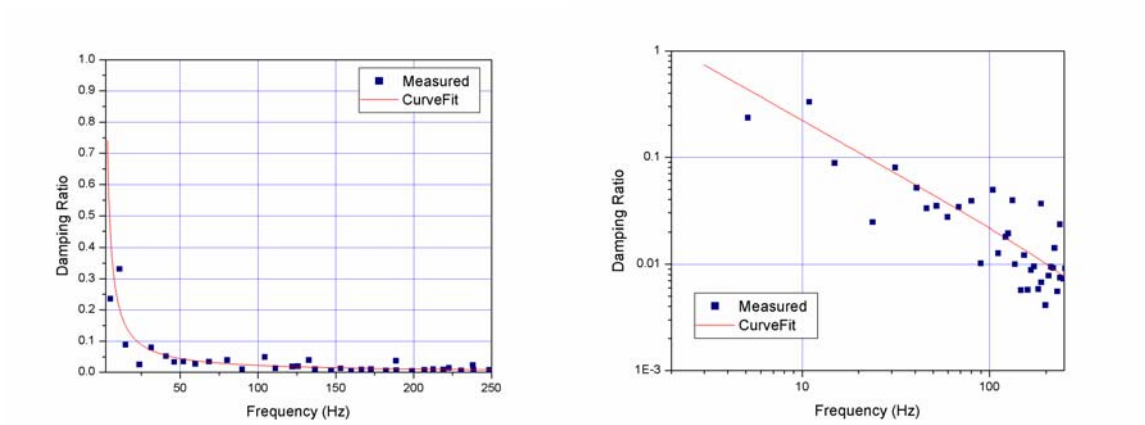

(in Linear Scale) (in Logarithmic Scale)

Figure 178. Modal Damping Ratio at Area 38, Vertical Direction (Modified)

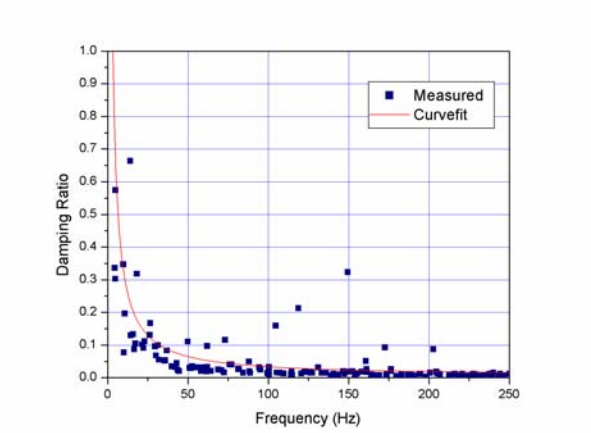

Figure 179. Modal Damping Ratio at Area 39, Vertical Direction (Original)

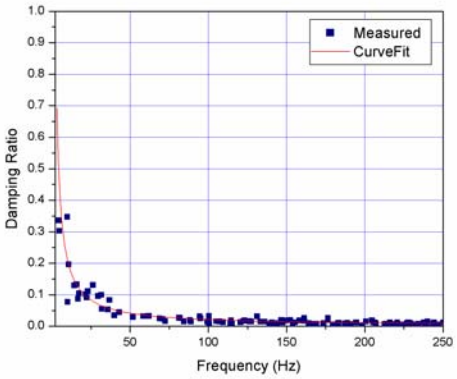

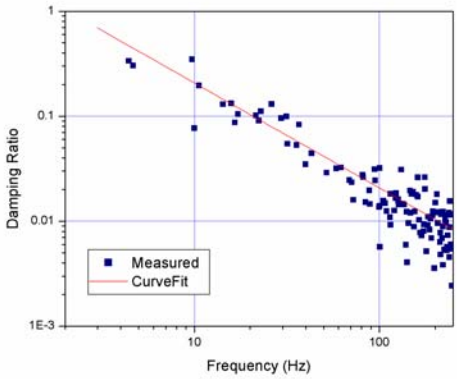

(in Linear Scale) (in Logarithmic Scale)

Figure 180. Modal Damping Ratio at Area 39, Vertical Direction (Modified)

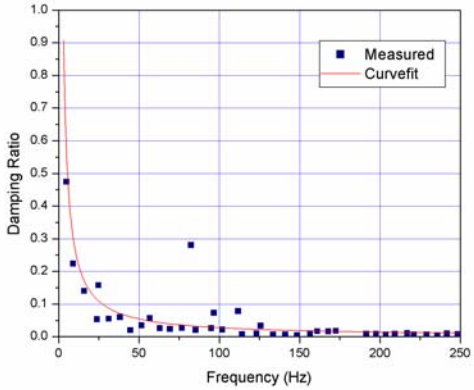

Figure 181. Modal Damping Ratio at Area 40, Vertical Direction (Original)

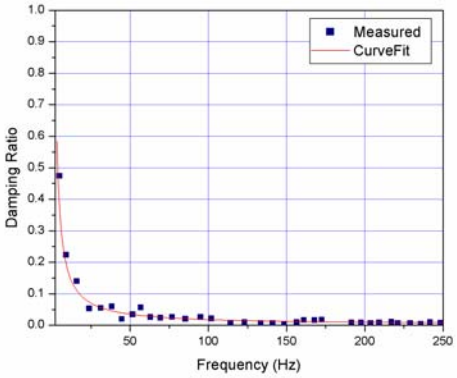

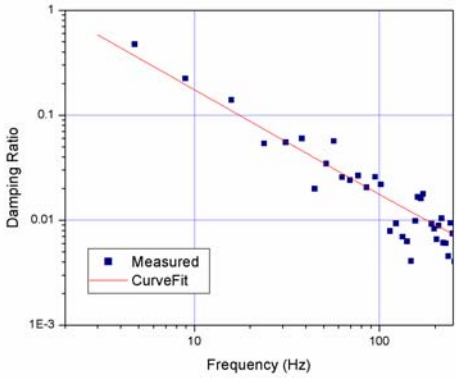

(in Linear Scale) (in Logarithmic Scale)

Figure 182. Modal Damping Ratio at Area 40, Vertical Direction (Modified)

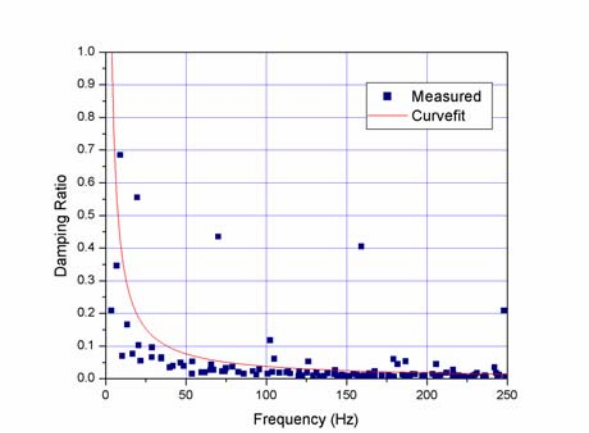

Figure 183. Modal Damping Ratio at Area 41, Vertical Direction (Original)

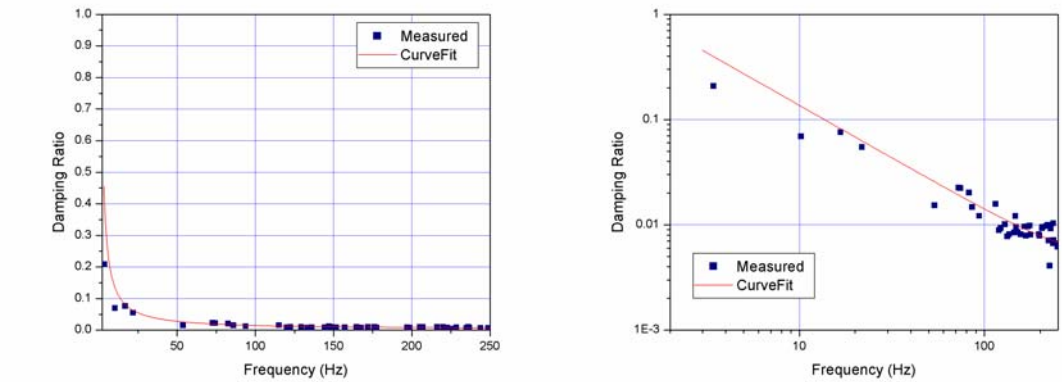

(in Linear Scale) (in Logarithmic Scale)

Figure 184. Modal Damping Ratio at Area 41, Vertical Direction (Modified)

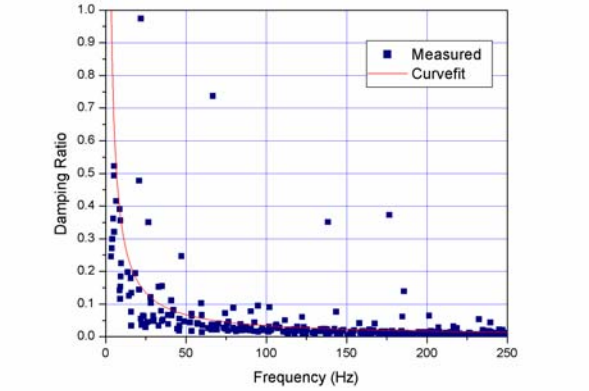

Figure 185. Modal Damping Ratio at Area 42, Vertical Direction (Original)

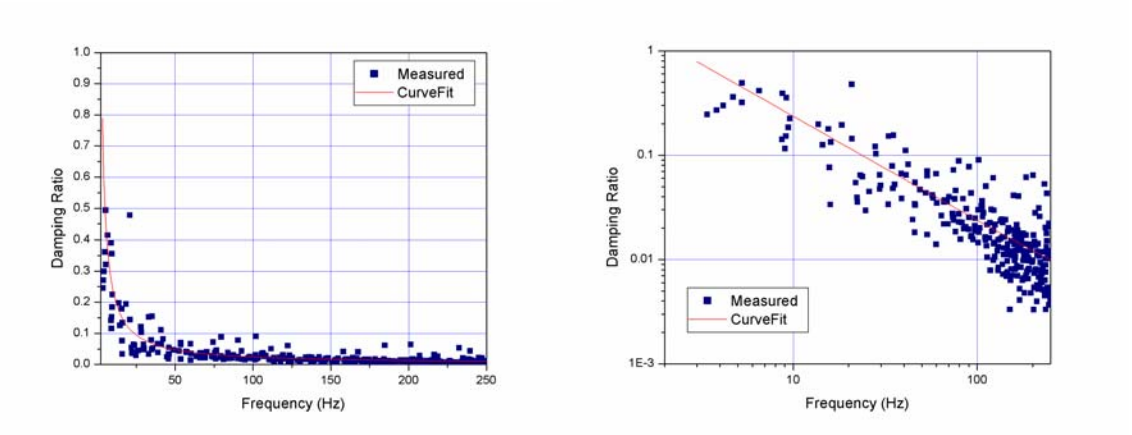

(in Linear Scale) (in Logarithmic Scale)

Figure 186. Modal Damping Ratio at Area 42, Vertical Direction (Modified)

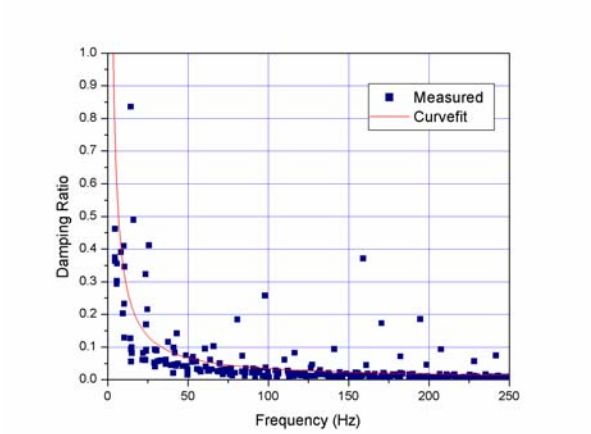

Figure 187. Modal Damping Ratio at Area 43, Vertical Direction (Original)

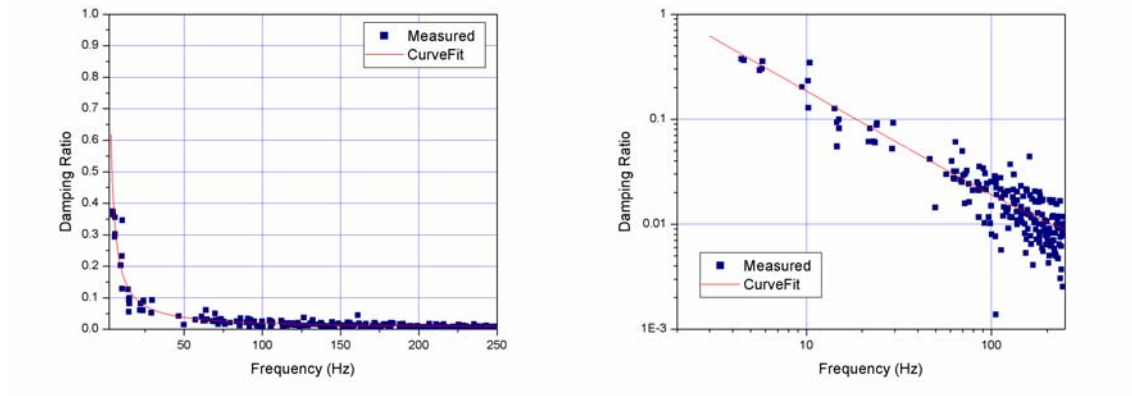

(in Linear Scale) (in Logarithmic Scale)

Figure 188. Modal Damping Ratio at Area 43, Vertical Direction (Modified)

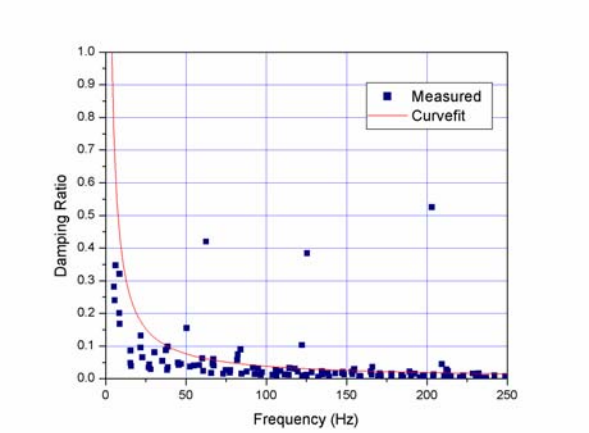

Figure 189. Modal Damping Ratio at Area 44, Vertical Direction (Original)

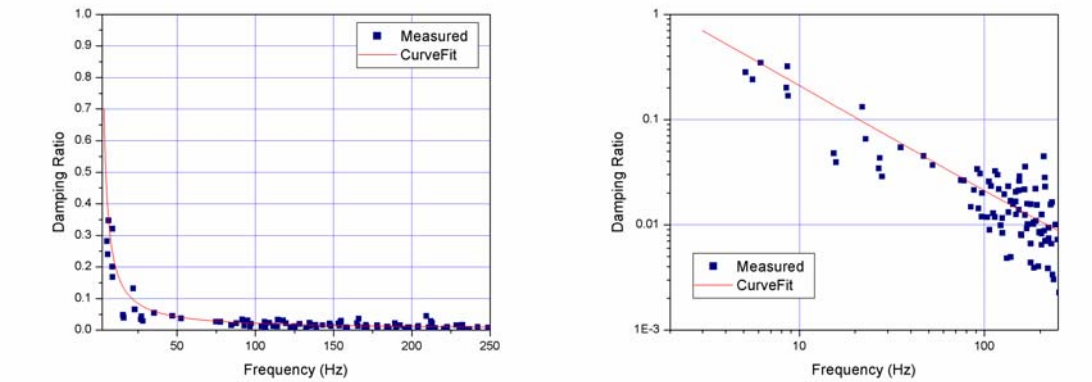

(in Linear Scale) (in Logarithmic Scale)

Figure 190. Modal Damping Ratio at Area 44, Vertical Direction (Modified)

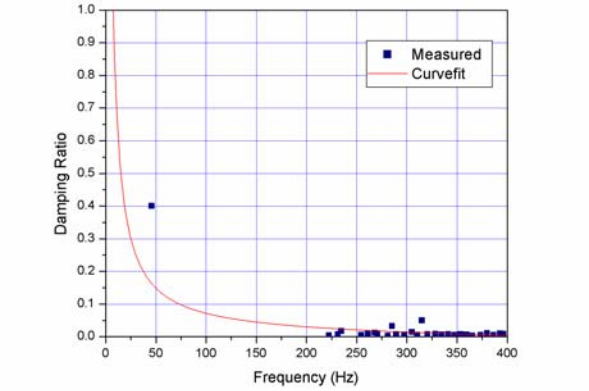

Figure 191. Modal Damping Ratio at Area 45, Vertical Direction (Original)

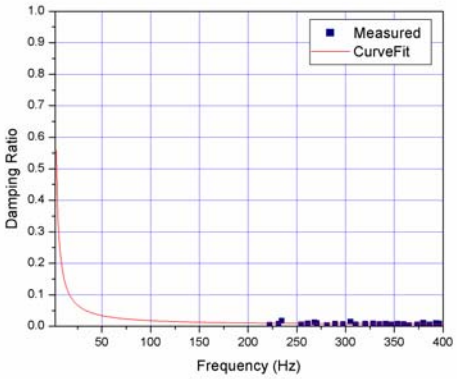

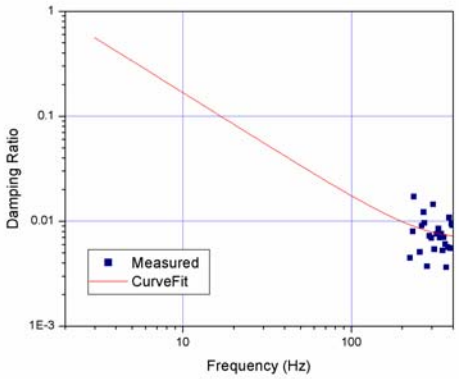

(in Linear Scale) (in Logarithmic Scale)

Figure 192. Modal Damping Ratio at Area 45, Vertical Direction (Modified)

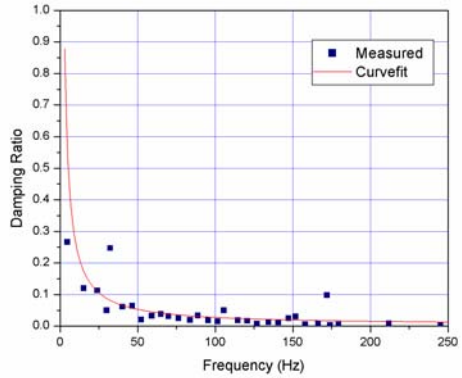

Figure 193. Modal Damping Ratio at Area 46, Vertical Direction (Original)

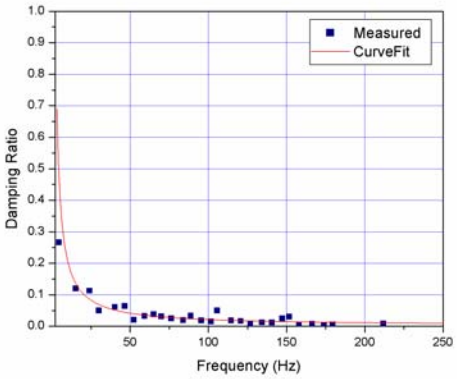

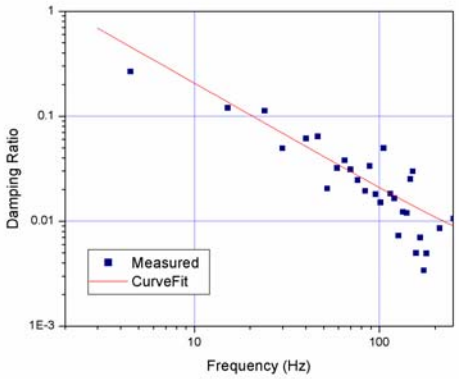

(in Linear Scale) (in Logarithmic Scale)

Figure 194. Modal Damping Ratio at Area 46, Vertical Direction (Modified)

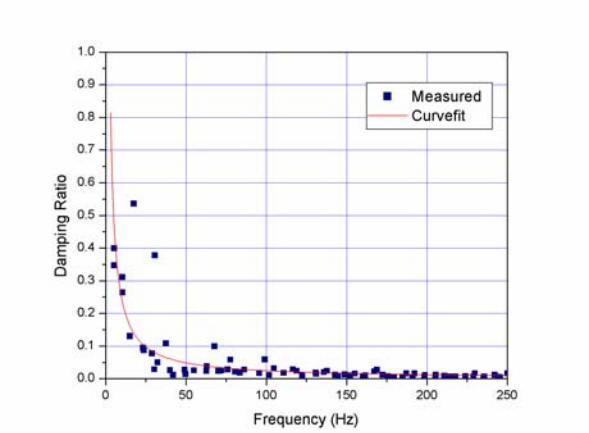

Figure 195. Modal Damping Ratio at Area 47, Vertical Direction (Original)

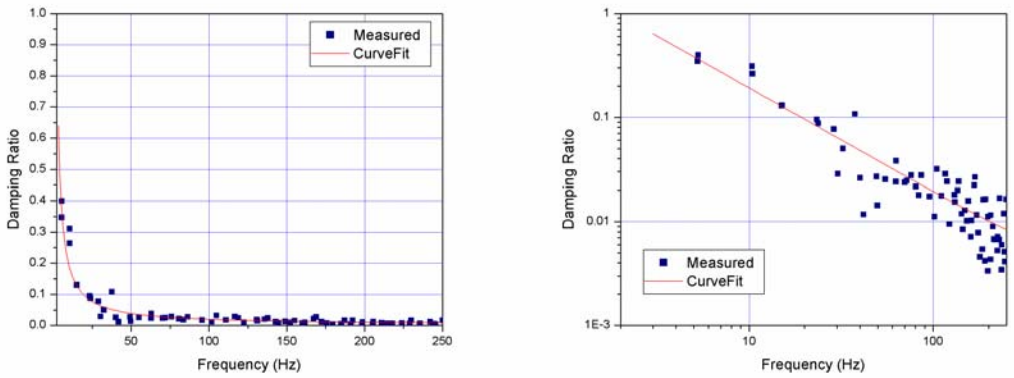

(in Linear Scale) (in Logarithmic Scale)

Figure 196. Modal Damping Ratio at Area 47, Vertical Direction (Modified)

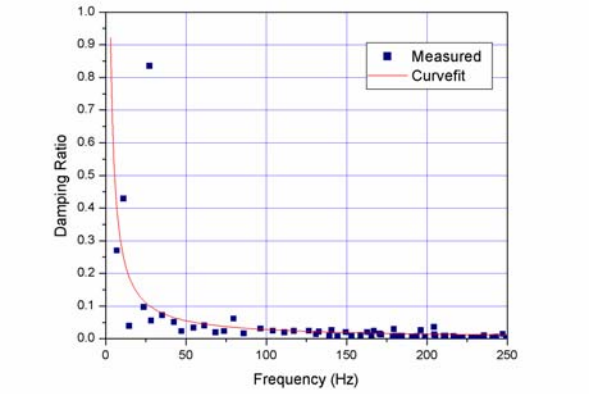

Figure 197. Modal Damping Ratio at Area 48, Vertical Direction (Original)

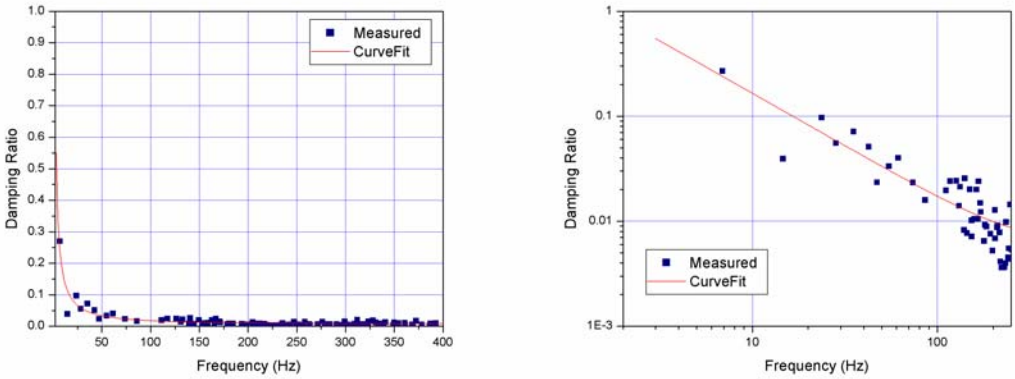

(in Linear Scale) (in Logarithmic Scale)

Figure 198. Modal Damping Ratio at Area 48, Vertical Direction (Modified)

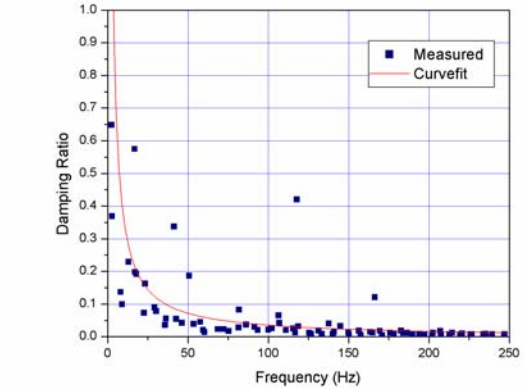

Figure 199. Modal Damping Ratio at Area 49, Vertical Direction (Original)

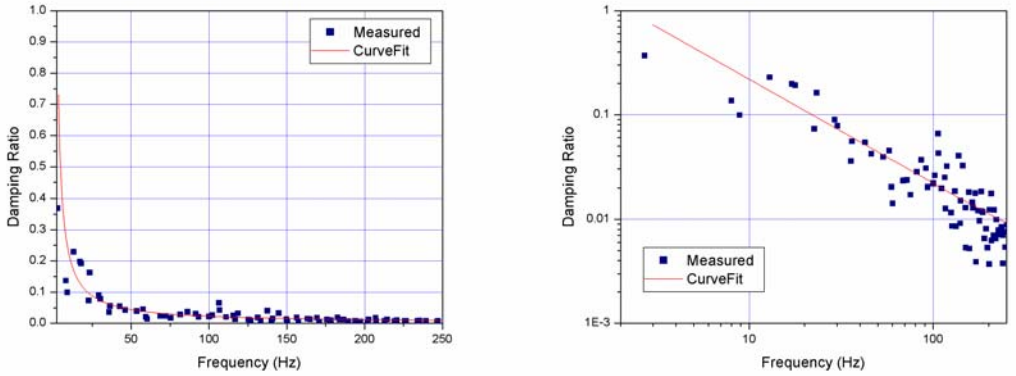

(in Linear Scale) (in Logarithmic Scale)

Figure 200. Modal Damping Ratio at Area 49, Vertical Direction (Modified)

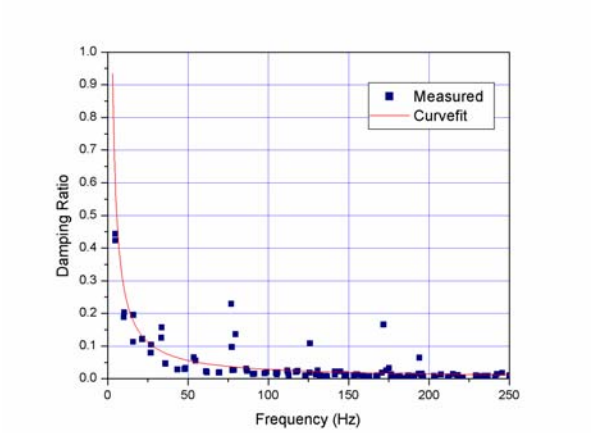

Figure 201. Modal Damping Ratio at Area 50, Vertical Direction (Original)

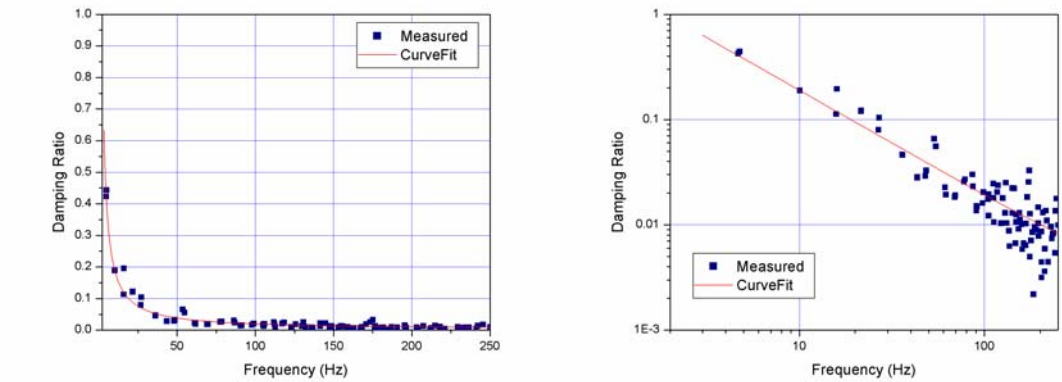

(in Linear Scale) (in Logarithmic Scale)

Figure 202. Modal Damping Ratio at Area 50, Vertical Direction (Modified)

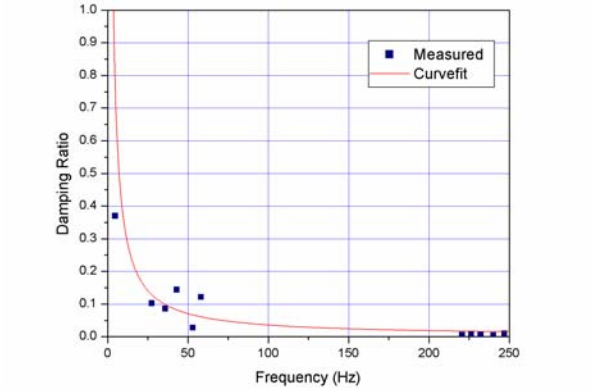

Figure 203. Modal Damping Ratio at Area 51, Vertical Direction (Original)

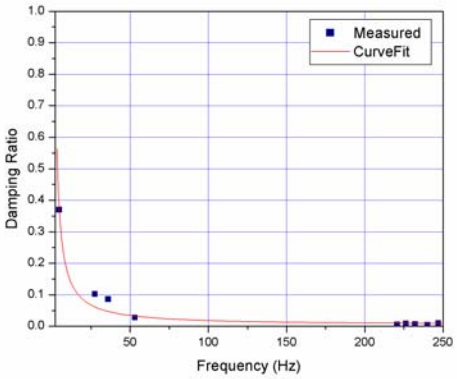

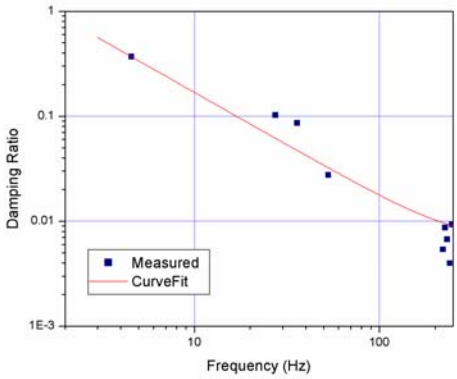

(in Linear Scale) (in Logarithmic Scale)

Figure 204. Modal Damping Ratio at Area 51, Vertical Direction (Modified)

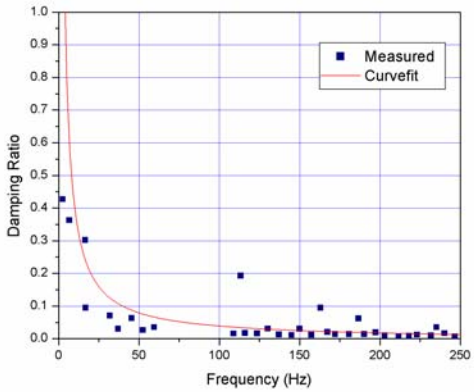

Figure 205. Modal Damping Ratio at Area 52, Vertical Direction (Original)

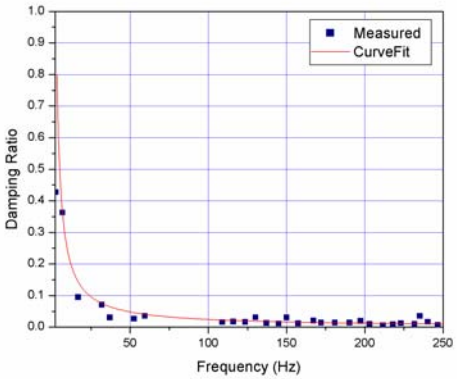

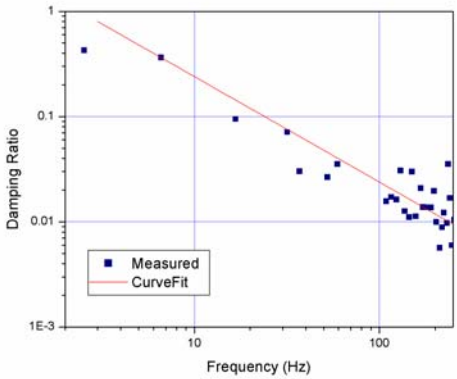

(in Linear Scale) (in Logarithmic Scale)

Figure 206. Modal Damping Ratio at Area 52, Vertical Direction (Modified)

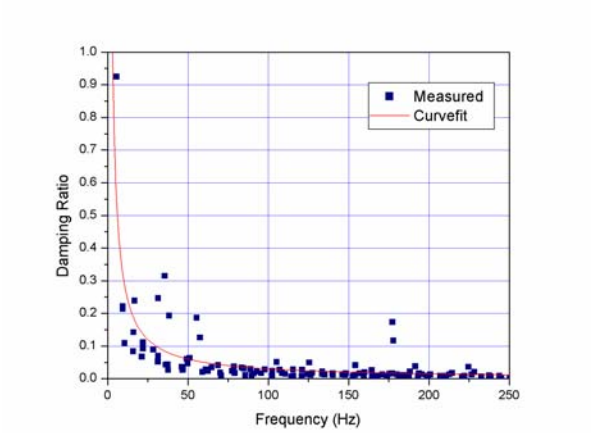

Figure 207. Modal Damping Ratio at Area 53, Vertical Direction (Original)

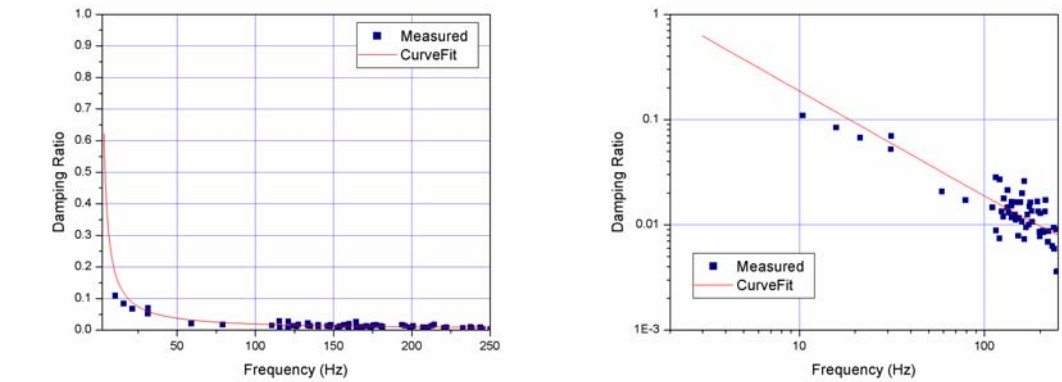

(in Linear Scale) (in Logarithmic Scale)

Figure 208. Modal Damping Ratio at Area 53, Vertical Direction (Modified)

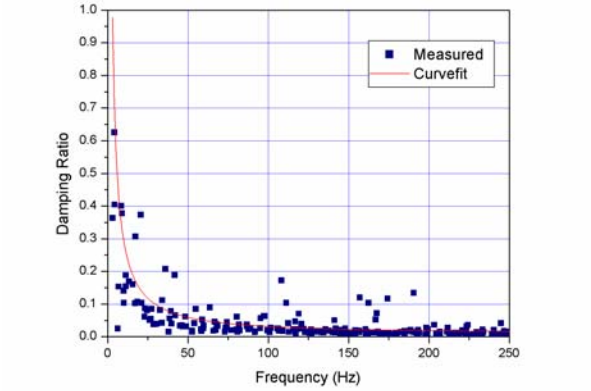

Figure 209. Modal Damping Ratio at Area 54, Vertical Direction (Original)

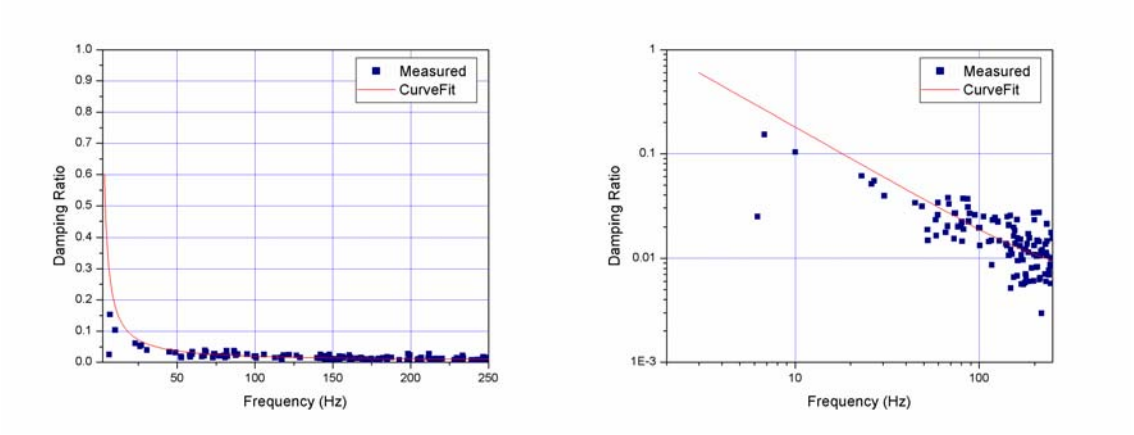

(in Linear Scale) (in Logarithmic Scale)

Figure 210. Modal Damping Ratio at Area 54, Vertical Direction (Modified)

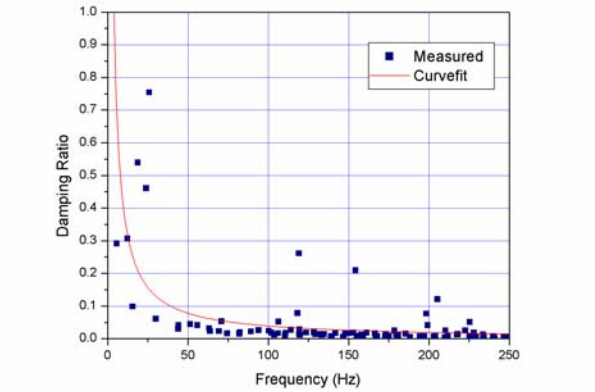

Figure 211. Modal Damping Ratio at Area 55, Vertical Direction (Original)

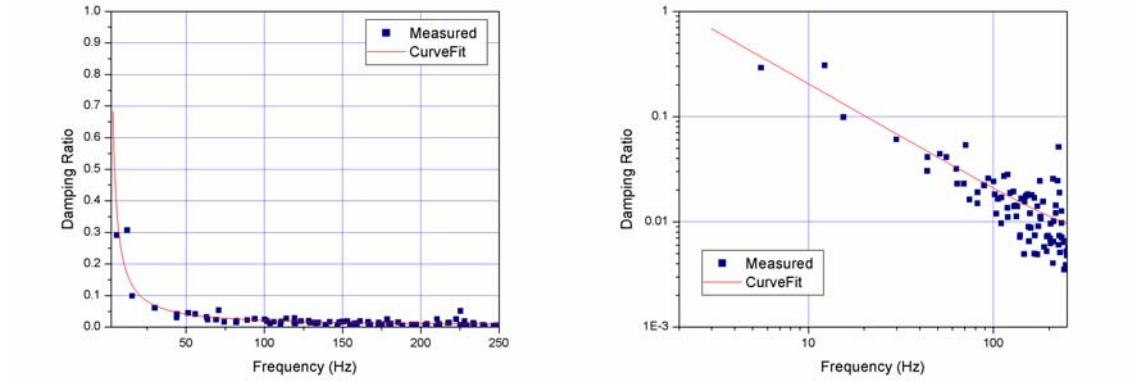

(in Linear Scale) (in Logarithmic Scale)

Figure 212. Modal Damping Ratio at Area 55, Vertical Direction (Modified)

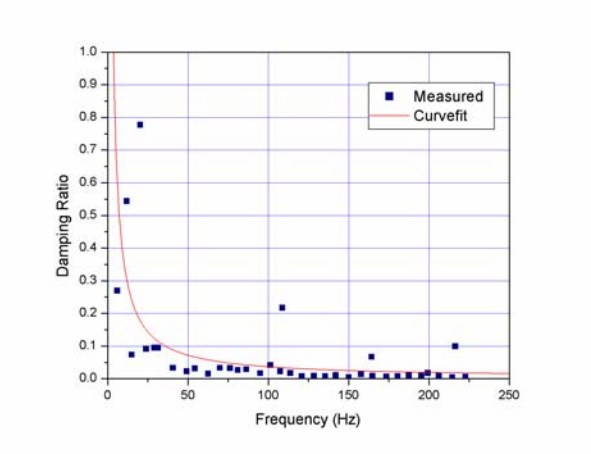

Figure 213. Modal Damping Ratio at Area 56, Vertical Direction (Original)

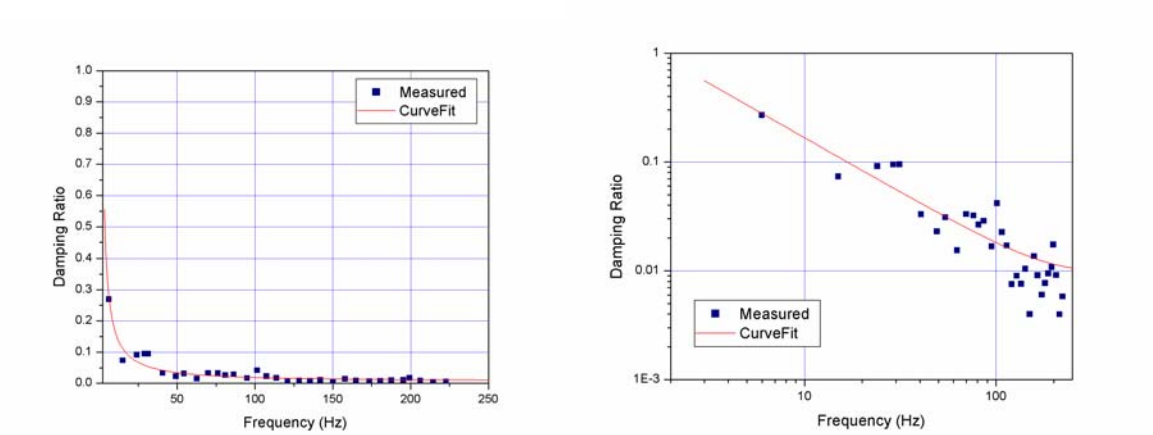

(in Linear Scale) (in Logarithmic Scale)

Figure 214. Modal Damping Ratio at Area 56, Vertical Direction (Modified)

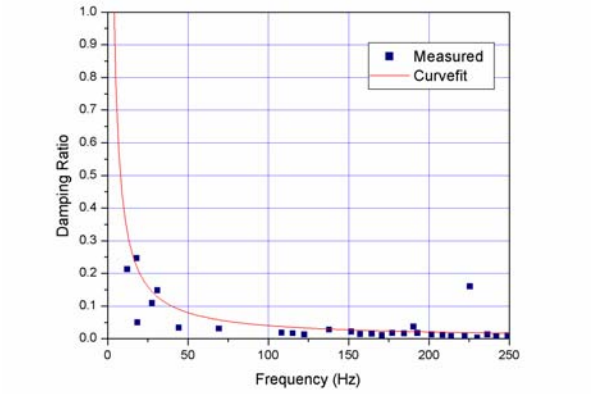

Figure 215. Modal Damping Ratio at Area 57, Vertical Direction (Original)

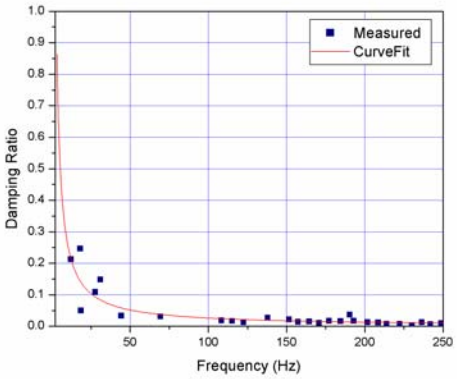

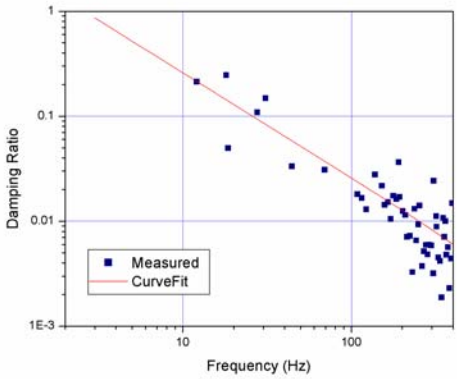

(in Linear Scale) (in Logarithmic Scale)

Figure 216. Modal Damping Ratio at Area 57, Vertical Direction (Modified)

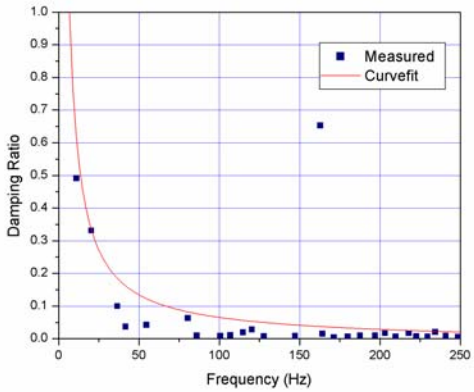

Figure 217. Modal Damping Ratio at Area 59, Vertical Direction (Original)

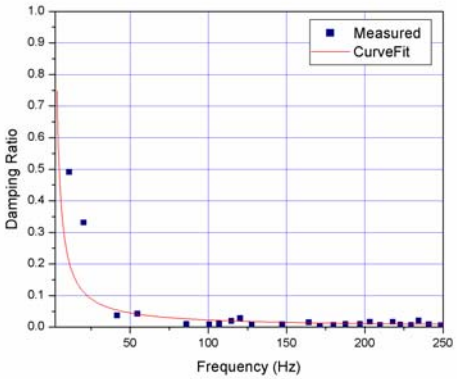

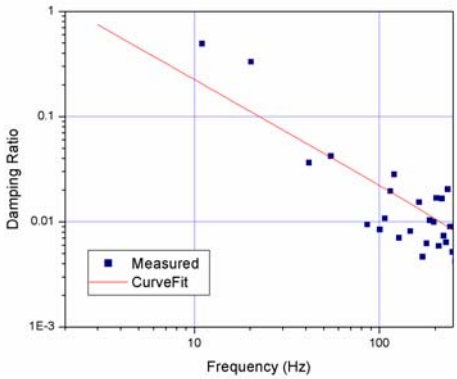

(in Linear Scale) (in Logarithmic Scale)

Figure 218. Modal Damping Ratio at Area 59, Vertical Direction (Modified)

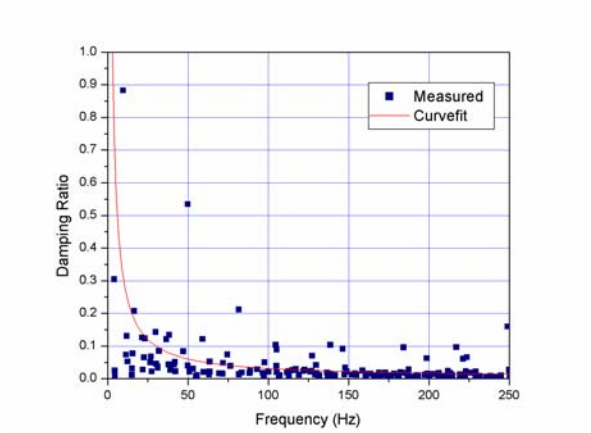

Figure 219. Modal Damping Ratio at Area 60, Vertical Direction (Original)

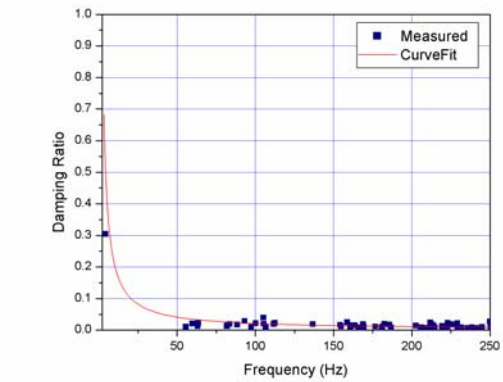

(in Linear Scale)

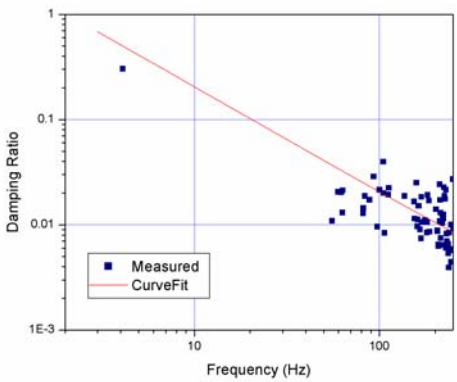

(in Logarithmic Scale)

Figure 220. Modal Damping Ratio at Area 60, Vertical Direction (Modified)

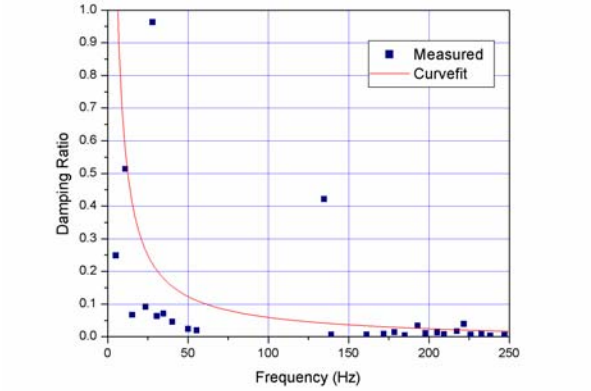

Figure 221. Modal Damping Ratio at Area 61, Vertical Direction (Original)

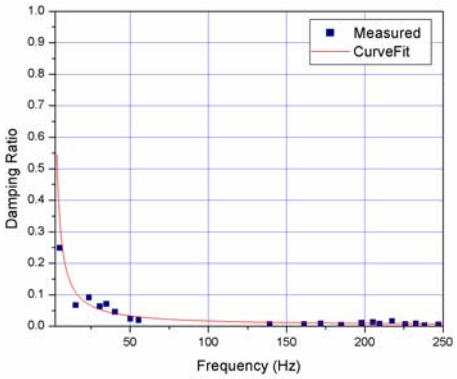

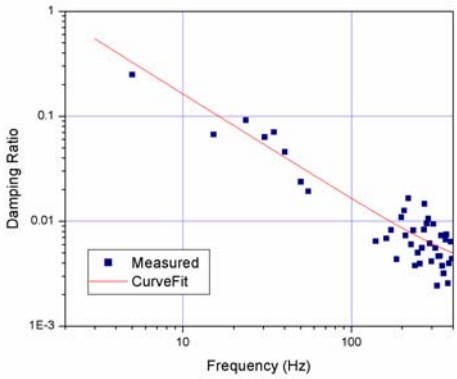

(in Linear Scale) (in Logarithmic Scale)

Figure 222. Modal Damping Ratio at Area 61, Vertical Direction (Modified)

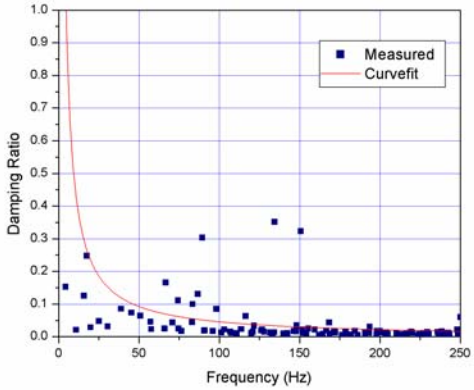

Figure 223. Modal Damping Ratio at Area 62, Vertical Direction (Original)

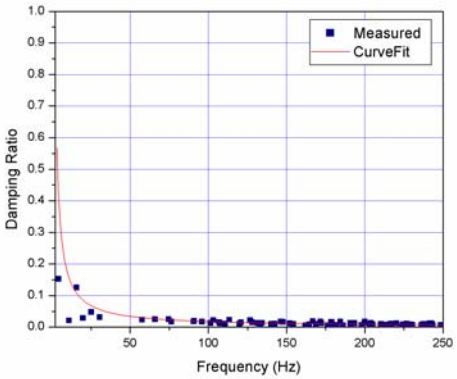

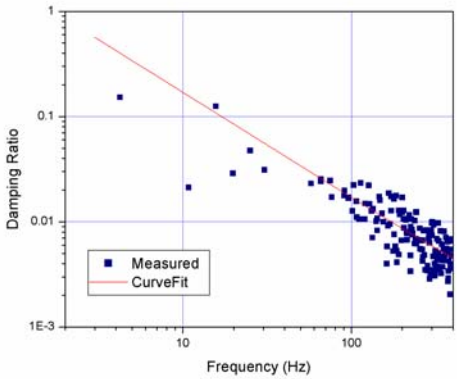

(in Linear Scale) (in Logarithmic Scale)

Figure 224. Modal Damping Ratio at Area 62, Vertical Direction (Modified)

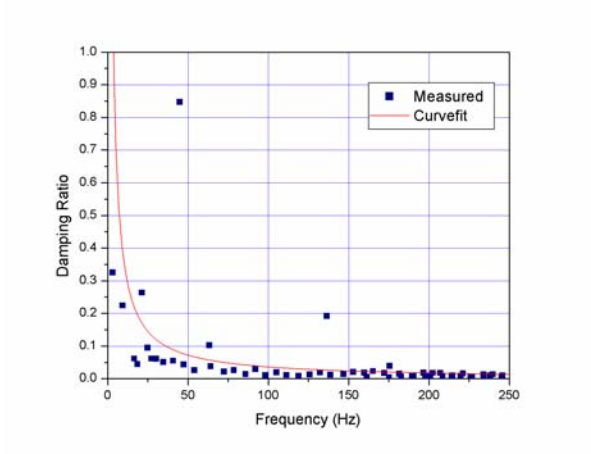

Figure 225. Modal Damping Ratio at Area 63, Vertical Direction (Original)

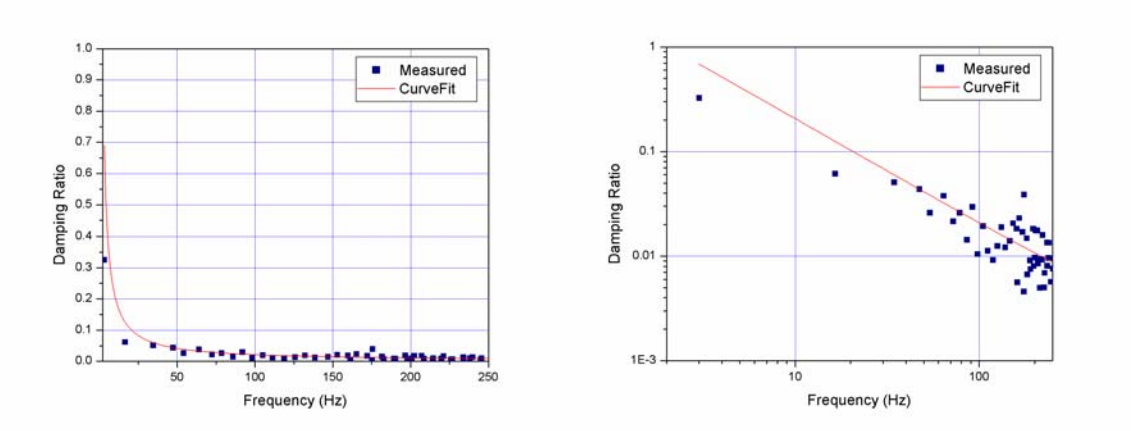

(in Linear Scale) (in Logarithmic Scale)

Figure 226. Modal Damping Ratio at Area 63, Vertical Direction (Modified)

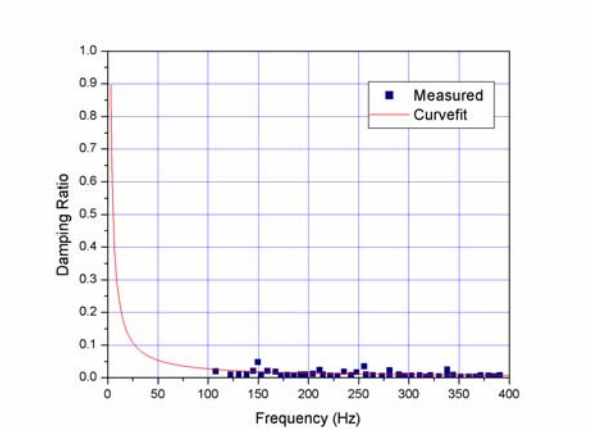

Figure 227. Modal Damping Ratio at Area 64, Vertical Direction (Original)

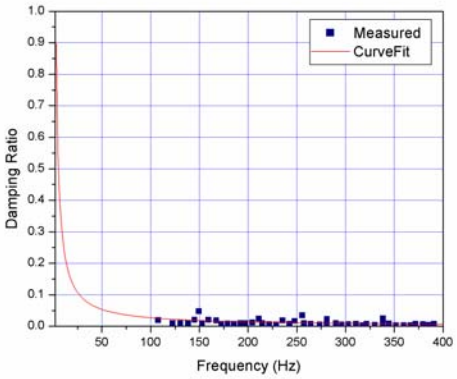

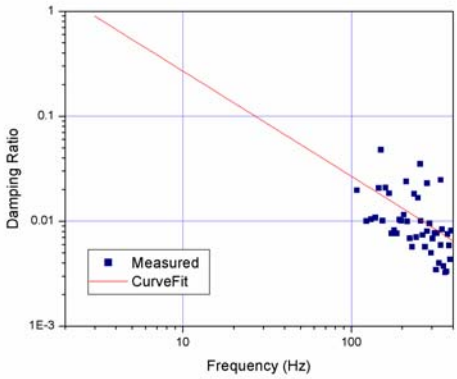

(in Linear Scale) (in Logarithmic Scale)

Figure 228. Modal Damping Ratio at Area 64, Vertical Direction (Modified)

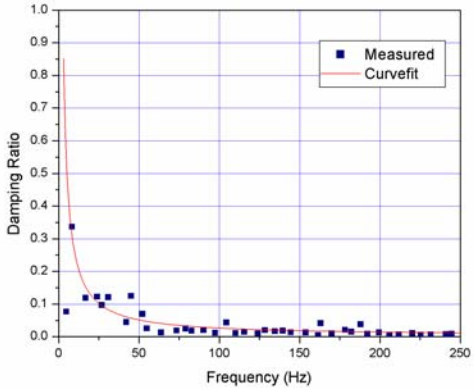

Figure 229. Modal Damping Ratio at Area 65, Vertical Direction (Original)

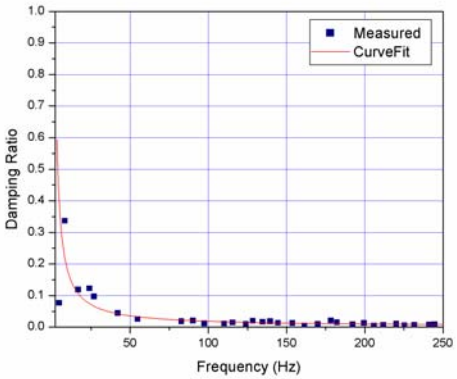

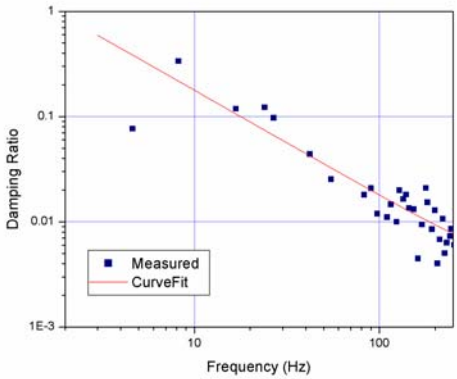

(in Linear Scale) (in Logarithmic Scale)

Figure 230. Modal Damping Ratio at Area 65, Vertical Direction (Modified)

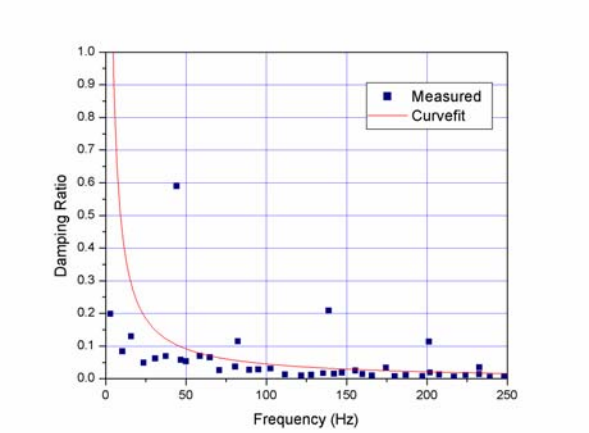

Figure 231. Modal Damping Ratio at Area 66, Vertical Direction (Original)

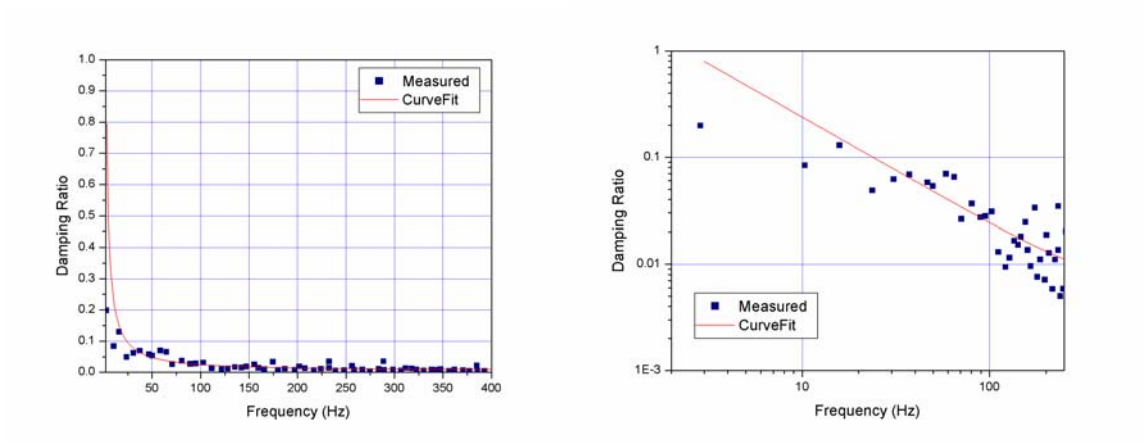

(in Linear Scale) (in Logarithmic Scale)

Figure 232. Modal Damping Ratio at Area 66, Vertical Direction (Modified)

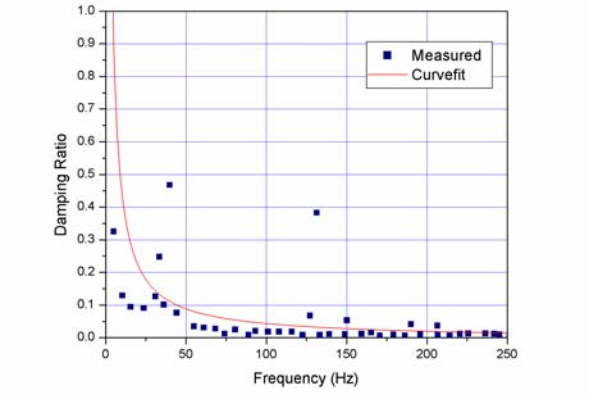

Figure 233. Modal Damping Ratio at Area 67, Vertical Direction (Original)

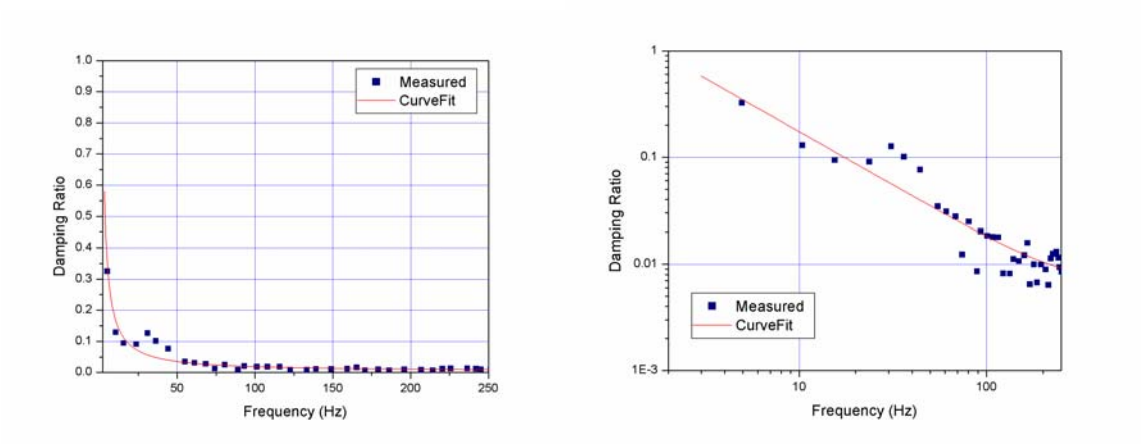

(in Linear Scale) (in Logarithmic Scale)

Figure 234. Modal Damping Ratio at Area 67, Vertical Direction (Modified)

APPENDIX B. MODAL PARAMETER EXTRACTION PROGRAM LIST IN TIME DOMAIN

This program uses IMSL libraries that are included in Microsoft Power Station.

```
use msimslmd
implicit double precision (a-h, o-z)
dimension tt(4000), vv(4000), hh(4000,200), hh2n(4000), betaq(201), coeff(201), &
          coefre(0:201), coefim(0:201), rootre(200), rootim(200)
dimension hht(200,4000),hhthh(200,200),hht2n(200)
double complex root(200), freg(6000), vvregm(6000)
dimension xr(200), wr(200), vvregr(4000), vvregi(4000)
dimension arn(200), nonq(1000)
double complex aaa(4000,200),aaat(200,4000),ah(4000),aaatah(200), &
               aaataaa(200,200), cmodal(201),sr(201),cw
character*25 ifiles(1000),pfiles(1000), gfiles(1000),sensor(1000), sensorid
LOGICAL COMPL
     pi=4.0d0*datan(1.0d0)
        tfinal=2000.0d0
     nf=773    ! no. of data sets 774
!     nq=170   ! total mode no. to be considered
     open(unit=1, file='modifieddat.lst')      ! input time data file list
     do 1881 ifl=1,nf
        read(1,*) sensor(ifl), nonq(ifl)
              ifiles(ifl)=trim(sensor(ifl))//'_2ms.dat'
        pfiles(ifl)=trim(sensor(ifl))//'_modal.dat'
        gfiles(ifl)=trim(sensor(ifl))//'_regen.dat'
1881 continue
     do 8888 ifl=467,nf
        mm=1500 ! data points to be used for calculation
           nq=nonq(ifl)
        write(*,*) ifl,' --> ', ifiles(ifl)
        open(unit=3, file=ifiles(ifl), err=8888)
        open(unit=4, file=pfiles(ifl))
        open(unit=6, file=gfiles(ifl))
!
! Velocity Data input, time is in miliseconds.
!
        do j=1,mm
           read(3,*) tt(j), vv(j)
           if(tt(j).ge.tfinal) goto 1788
        enddo
1788    mm=j-1
!
        dt=(tt(mm)-tt(1))/dfloat(mm-1)/1000.0d0     ! time interval in seconds
!             write(*,*) dt
!
! Calculate [H]{beta}={h}
!
        m2=mm-nq-1
        do i=1,m2
           ii=i-1
           hh2n(i)= -vv(ii+nq+1)
           do j=1,nq
              hh(i,j)=vv(ii+j)
              enddo
        enddo
```

```
              hht(1:nq,1:m2)=transpose(hh(1:m2,1:nq))
              hhthh(1:nq,1:nq)=matmul(hht(1:nq,1:m2),hh(1:m2,1:nq))
              hht2n(1:nq)=matmul(hht(1:nq,1:m2),hh2n(1:m2))
       CALL DLSARG (nq, hhthh, 200, hht2n, 1, betaq)
!
! Solve Polynomial Equation, and calculate {V}
!
       betaq(nq+1)=1.0d0
       compl=.FALSE.
       coefre(0:nq)=betaq(1:nq+1)
       CALL BAUPOL(coefre,coefim,nq,COMPL,ROOTRE,ROOTIM,NUMIT)
             root(1:nq)=dcmplx(rootre(1:nq), rootim(1:nq))
!
! Calculate modal frquencies and damping ratios from {V}
!
       do i=1,nq
          sr(i)=cdlog(root(i))/dt
                wr(i)=cdabs(sr(i))
                xr(i)= -dble(sr(i))/wr(i)
       enddo
!
! Calculate modal constants {Ar}
!
       cmodal=dcmplx(0.0d0,0.0d0)
             m2=mm-1
       do i=1,m2
          ah(i)=vv(i)
          do j=1,nq
            aaa(i,j)=root(j)**dfloat(i-1)
           enddo
       enddo
             aaat(1:nq,1:m2)=transpose(aaa(1:m2,1:nq))
             aaataaa(1:nq,1:nq)=matmul(aaat(1:nq,1:m2),aaa(1:m2,1:nq))
             aaatah(1:nq)=matmul(aaat(1:nq,1:m2),ah(1:m2))
       CALL DLSACG (nq, aaataaa, 200, aaatah, 1, cmodal)
!
       sensorid=sensor(ifl)
             do i=1,nq
                cmodal(i)=cmodal(i)/sr(i)
             enddo
!
       armax=0.0d0
       arn=0.0d0
       do i=1,nq
             if(cdabs(cmodal(i)).gt.armax) armax=cdabs(cmodal(i))
       enddo
       arn(1:nq)=cdabs(cmodal(1:nq))/armax
!
!  Calculate Spectrum using modal parameter to verify results
!
        fspan=1.0d0/dt/2.0d0
        wspan=2.0d0*pi*fspan
        dw=wspan/(dfloat(mm/2)-1.0d0)
        freg=dcmplx(0.0d0,0.0d0)
       do i=2,mm/2+1
             w=dfloat(i-1)*dw
                cw=dcmplx(0.0d0,w)
```

```
              do j=1,nq
                 freq(i)=freq(i)+cmodal(j)*cw/(cw-sr(j))
              enddo
        enddo
        do i=2, mm/2
                 ii=mm-i+2
           freq(ii)=dconjg(freq(i))
        enddo
        freq=freq*dw/(2.0d0*pi)
!
! Calculate synthesized time history by inverse FFT
!
        CALL DFFTCB (mm, freq, vvregm)
        vvregr=0.0
        do i=2,mm
            ii=mm-i+1
           vvregr(i)=dble(vvregm(i))
            vvregi(i)=dimag(vvregm(i))
        enddo
!
! Output synthesized time histories
!
        do i=2,mm/2
           write(6,200) tt(i), vvregr(i),vvregi(i), vv(i)
200        format(5(1x,e15.7))
        enddo
!
!  Sort and Output all modal parameters
!
        call sortmodal(nq, wr, xr, cmodal, arn)
        do i=1,nq
           write(4,100) i, wr(i)/(2.0d0*pi), xr(i), cmodal(i), arn(i)
100        format(1i5, 5(1x, e14.6))
        enddo
        close(unit=3)
        close(unit=4)
        close(unit=6)
8888 continue
877  format(5(1x,e15.7))
400  format(5(1x,e15.7))
     close(unit=1)
     close(unit=2)
     close(unit=5)
stop
end
!
!-------------------------------------------------------------------------
!  Subroutine to calculate damping curve and standard deviation
!-------------------------------------------------------------------------
!
Subroutine meansd(nto, totalfreq, totaldamp, rayleigh, raywgt, &
            ffreq, fdamp1, fdamp2, sdray, sdwgt)
implicit double precision (a-h,o-z)
dimension totalfreq(2000), totaldamp(2000), ffreq(250), fdamp1(250), &
          fdamp2(250)
dimension rayleigh(2), raywgt(2)
pi=4.0d0*datan(1.0d0)
```

```
sdray=0.0d0
sdwgt=0.0d0
do i=1,nto
   w=2.0d0*pi*totalfreq(i)
   x=rayleigh(1)/2.0d0/w+rayleigh(2)/2.0d0*w
   sdray=sdray+(totaldamp(i)-x)**2.0d0
   x=raywgt(1)/2.0d0/w+raywgt(2)/2.0d0*w
   sdwgt=sdwgt+(totaldamp(i)-x)**2.0d0
enddo
sdray=sdray/nto
sdwgt=sdwgt/nto
do i=1,250
   f=dfloat(i)
   ffreq(i)=f
   w=2.0d0*pi*f
   fdamp1(i)=rayleigh(1)/2.0d0/w+rayleigh(2)/2.0d0*w
   fdamp2(i)=raywgt(1)/2.0d0/w+raywgt(2)/2.0d0*w
enddo
return
end
!
!-------------------------------------------------------------------------
! Sort total
!-------------------------------------------------------------------------
!
subroutine sorttotal(itt, ffreq, ddamp, ar)
implicit double precision (a-h,o-z)
dimension ffreq(2000), ddamp(2000) , ar(2000)
ntt=itt
do i=1,ntt-1
   do j=i+1, ntt
         if(ffreq(i).gt.ffreq(j)) then
            ddum=ffreq(i)
               ffreq(i)=ffreq(j)
               ffreq(j)=ddum
               ddum=ddamp(i)
               ddamp(i)=ddamp(j)
               ddamp(j)=ddum
               ddum=ar(i)
               ar(i)=ar(j)
               ar(j)=ddum
         endif
   enddo
enddo
return
end
!
!-------------------------------------------------------------------------
subroutine sortmodal(nq, wr, xr, cmodal, arn)
!-------------------------------------------------------------------------
!
implicit double precision (a-h,o-z)
dimension wr(2000), xr(2000) , arn(2000)
double complex cmodal(2000), cdum
do i=1,nq-1
   do j=i+1, nq
         if(wr(i).gt.wr(j)) then
```

```
            ddum=wr(i)
               wr(i)=wr(j)
               wr(j)=ddum
               ddum=xr(i)
               xr(i)=xr(j)
               xr(j)=ddum
               ddum=arn(i)
               arn(i)=arn(j)
               arn(j)=ddum
               cdum=cmodal(i)
               cmodal(i)=cmodal(j)
               cmodal(j)=cdum
         endif
   enddo
enddo
return
end
!
!-------------------------------------------------------------------------
subroutine FindAr(nq,mm,dt,vv,sr,cmodal)
!-------------------------------------------------------------------------
! to find modal constants with frequency domain least square method
  implicit double precision (a-h,o-z)
  dimension vv(2000)
  double complex sr(201),cmodal(201),t(2000),ss(2000,200), &
                 st(200,2000),stf(200),sts(200,200),ff(2000),wi
  pi=4.0d0*datan(1.0d0)
  do i=1,mm
     t(i)=dcmplx(vv(i),0.0d0)
  enddo
  CALL DFFTCF (mm, t, ff)
  m=mm/2
  df=1.0d0/(dt*dfloat(mm-1))
  dw=2.0d0*pi*df
  ff(1:mm)=ff(1:mm)/dfloat(mm)
  do i=1,m+1
     w=dfloat(i-1)*dw
     wi=dcmplx(0.0d0,w)
        do j=1,nq
           ss(i,j)=wi/(wi-sr(j))*df
        enddo
  enddo
  do i=mm,m+2,-1
     w= dfloat(mm-i+1)*dw
     wi=dcmplx(0.0d0,-w)
        do j=1,nq
           ss(i,j)=wi/(wi-sr(j))*df
        enddo
  enddo
  st(1:nq,1:mm)=transpose(ss(1:mm,1:nq))
  stf(1:nq)=matmul(st(1:nq,1:mm),ff(1:mm))
  sts(1:nq,1:nq)=matmul(st(1:nq,1:mm),ss(1:mm,1:nq))
  CALL DLSACG (nq, sts, 100, stf, 1, cmodal)
return
end
!
!-------------------------------------------------------------------------
```

```
      SUBROUTINE BAUPOL(COEFRE,COEFIM,N,COMPL,ROOTRE,ROOTIM,NUMIT)
!C***********************************************************************
!C                                                                      *
!C  Without knowing any approximations of the roots, this               *
!C  SUBROUTINE finds N approximate values Z(I), I=1, ..., N for         *
!C  the N zeros of a polynomial PN of degree N with real or            *
!C  complex coefficients.                                              *
!C  The polynomial is described as follows:                            *
!C                                                                      *
!C     PN(Z)=COEF(0)+COEF(1)*Z+COEF(2)*Z**2+...+COEF(N)*Z**N,           *
!C                                                                      *
!C  with COEF(I) = (COEFRE(I),COEFIM(I)) for I=0, ..., N (complex       *
!C  coefficients).                                                      *
!C                                                                      *
!C  INPUT PARAMETERS:                                                  *
!C  ================                                                    *
!C  COEFRE   : (N+1)-vector COEFRE(0:N) containing the real             *
!C             part of each coefficient of the polynomial PN in         *
!C             DOUBLE PRECISION.                                        *
!C  COEFIM   : (N+1)-vector COEFIM(0:N) containing the imaginary        *
!C             part of each coefficient of the polynomial PN in         *
!C             DOUBLE PRECISION.                                        *
!C  N        : degree of the polynomial PN.                            *
!C  COMPL    : boolean variable :                                      *
!C             COMPL=.TRUE.  , if the coefficients are COMPLEX.         *
!C             COMPL=.FALSE. , if the coefficients are REAL.            *
!C                                                                      *
!C  OUTPUT PARAMETERS:                                                 *
!C  =================                                                   *
!C  ROOTRE   : N-vector ROOTRE(1:N) containing the approximate          *
!C             real parts of the computed zeros of PN in                *
!C             DOUBLE PRECISION.                                        *
!C  ROOTIM   : N-vector ROOTIM(1:N) containing the approximate          *
!C             imaginary parts of the computed zeros of PN in           *
!C             DOUBLE PRECISION.                                        *
!C  NUMIT    : maximum number of iteration steps.                      *
!C                                                                      *
!
      IMPLICIT DOUBLE PRECISION (a-h,o-z)
      DIMENSION COEFRE(0:201),COEFIM(0:201),E(201), &
                     ROOTRE(200),ROOTIM(200),A(500),B(500),C(500)
       DOUBLE PRECISION INFINY, MAX, MIN
      LOGICAL COMPL
!
!  Initializing the iteration step counter NUMIT and the error
! bound GAMMA.
!
      NUMIT=0
      GAMMA=5.0D-18
      IF(N .EQ. 1) THEN
!
! If the degree of PN is N=1, then the zero of the polynomial PN is
! Z=-COEF(0)/COEF(1), where COEF(I)=(COEFRE(I),COEFIM(I)) for I=0,1.
!
         CALL CDIV(-COEFRE(0),-COEFIM(0),COEFRE(1),COEFIM(1), &
                   ROOTRE(1),ROOTIM(1))
         RETURN
```

```
      ELSE
         N1=N+1
!
! Scaling via SCALFC.
!
         DO 10 I=1,N1
            E(I)=ABSCOM(COEFRE(N1-I),COEFIM(N1-I))
   10    CONTINUE
         CALL MCONST(FMACHP,INFINY,SMALNO,BASE)
         BND=SCALFC(N1,E,FMACHP,INFINY,SMALNO,BASE)
         IF(BND .EQ. 1.0D0) THEN
!
! Normalizing, in case scaling by SCALFC did not normalize the coefficients.
!
            MAX=0.0D0
            MIN=1.0D+300
            DO 20 I=N,0,-1
               X=ABSCOM(COEFRE(I),COEFIM(I))
               IF(X .GT. MAX) MAX=X
               IF(X .LT. MIN .AND. X .NE. 0.0D0) MIN=X
   20       CONTINUE
            BND=DSQRT(MAX*MIN)
            BND=1.0D0/BND
         END IF
         DO 30 K=1,N1
            B(2*K-1)=COEFRE(N1-K)*BND
            B(2*K)=0.0D0
            IF(COMPL) B(2*K)=COEFIM(N1-K)*BND
   30    CONTINUE
         X0=0.0D0
         Y0=0.0D0
         DO 40 I=1,N
            L=2*(N+2-I)
            DO 50 K=1,L
               A(K)=B(K)
   50       CONTINUE
!
! Calculating the I-th zero of PN.
!
            CALL BAUZRO(X0,Y0,N+1-I,GAMMA,XNEW,YNEW,NUMIT,A,B,C)
            ROOTRE(I)=XNEW
            ROOTIM(I)=YNEW
            X0=XNEW
            Y0=-YNEW
   40    CONTINUE
      END IF
      RETURN
      END
!

      SUBROUTINE BAUZRO(X0,Y0,N,GAMMA,XNEW,YNEW,NUMIT,A,B,C)
!
!*****************************************************************
!                                                                *
! This SUBROUTINE calculates a zero of a polynomial PN with      *
! complex coefficients.                                          *
! We solve the equation PN(Z)/PN'(Z)=0                           *
```

```
! via Newton's method with spiralization and extrapolation to   *
! improve convergence.                                          *
! The initial approximation (X0+I*Y0) can be chosen arbitrarily.*
!                                                               *
! INPUT PARAMETERS:                                             *
! ================                                              *
! X0       : real part of the initial approximation.            *
! Y0       : imaginary part of the initial approximation.       *
! N        : degree of the polynomial PN.                       *
! GAMMA    : error bound.                                       *
!                                                               *
! OUTPUT PARAMETERS:                                            *
! =================                                             *
! XNEW     : real part of the computed zero of PN.              *
! YNEW     : imaginary part of the zero of PN.                  *
! NUMIT    : maximum number of iteration steps.                 *
!                                                               *
!***************************************************************
!
      IMPLICIT DOUBLE PRECISION (a-h,o-z)
      DIMENSION A(500),B(500),C(500)
      LOGICAL ENDIT
!
      IF(N .EQ. 2) THEN
!
! Solving the remaining 2nd degree polynomial exactly.
!
         CALL CDIV(A(3),A(4),A(1),A(2),P1RE,P1IM)
         CALL CDIV(A(5),A(6),A(1),A(2),Q1RE,Q1IM)
         P12RE=-P1RE/2.0D0
         P12IM=-P1IM/2.0D0
         RA1RE=P12RE*P12RE-P12IM*P12IM
         RA1IM=2.0D0*P12RE*P12IM
         RARE=RA1RE-Q1RE
         RAIM=RA1IM-Q1IM
         IF(RAIM .EQ. 0.0D0) THEN
            IF(RARE .LT. 0.0D0) THEN
!
! Purely imaginary root.
!
               RTIM=DSQRT(-RARE)
               RTRE=0.0D0
               XNEW=P12RE
               YNEW=P12IM+RTIM
               RETURN
            ELSE
!
! Real root.
!
               RTRE=DSQRT(RARE)
               RTIM=0.0D0
               XNEW=P12RE+RTRE
               YNEW=P12IM
               RETURN
            END IF
         ELSE
!
```

```
! Complex root.
!
            RABE=ABSCOM(RARE,RAIM)
            IF(RARE .GT. 0.0D0) THEN
               RTRE=DSQRT(0.5D0*(RABE+RARE))
               IF(RAIM .LT. 0.0D0) RTRE=-RTRE
               RTIM=0.5D0*RAIM/RTRE
            ELSE
               RTIM=DSQRT(0.5D0*(RABE-RARE))
               RTRE=0.5D0*RAIM/RTIM
            END IF
            XNEW=P12RE+RTRE
            YNEW=P12IM+RTIM
            RETURN
         END IF
      ELSE IF(N .EQ. 1) THEN
!
! Polynomial of 1st degree.
!
         XNEW=P12RE-RTRE
         YNEW=P12IM-RTIM
         RETURN
      ELSE
         I=0
         ENDIT=.FALSE.
         RHO=DSQRT(GAMMA)
         BETA=10.0D0*GAMMA
         QR=0.1D0
         QI=0.9D0
         XNEW=X0
         YNEW=Y0
         CALL COMHOR(XNEW,YNEW,N,GAMMA,UNEW,VNEW,UDNEW,VDNEW, &
                     UDDNEW,VDDNEW,BD,BDD,A,B,C)
         NUMIT=NUMIT+1
         PBNEW=ABSCOM(UNEW,VNEW)
         IF(PBNEW .LE. BD) THEN
            RETURN
         ELSE
            PBOLD=2.0D0*PBNEW
            DZMIN=BETA*(RHO+ABSCOM(XNEW,YNEW))
   10       PSBNEW=ABSCOM(UDNEW,VDNEW)
!
! Spiralization.
!
            IF(PBNEW .LT. PBOLD) THEN
               DZMAX=1.0D0+ABSCOM(XNEW,YNEW)
               NUMIT=NUMIT+1
               H1=UDNEW*UDNEW-VDNEW*VDNEW-UNEW*UDDNEW+VNEW*VDDNEW
               H2=2.0D0*UDNEW*VDNEW-UNEW*VDDNEW-VNEW*UDDNEW
               IF(PSBNEW .GT. 10.0D0*BDD .AND. &
                 ABSCOM(H1,H2) .GT. 100.0D0*BDD*BDD) THEN
!
! Applying Newton's method.
!
                  I=I+1
                  IF(I .GT. 2) I=2
                  U=UNEW*UDNEW-VNEW*VDNEW
```

```
                  V=UNEW*VDNEW+VNEW*UDNEW
                  CALL CDIV(-U,-V,H1,H2,DX,DY)
                  IF(ABSCOM(DX,DY) .GT. DZMAX) THEN
                     H=DZMAX/ABSCOM(DX,DY)
                     DX=DX*H
                     DY=DY*H
                     I=0
                  END IF
                  IF(I .EQ. 2 .AND. ABSCOM(DX,DY) .LT. DZMIN/RHO .AND. &
                                    ABSCOM(DX,DY) .GT. 0.0D0) THEN
!
! Extrapolation.
!
                     I=0
                     CALL CDIV(XNEW-XOLD,YNEW-YOLD,DX,DY,H3,H4)
                     H3=1.0D0+H3
                     H1=H3*H3-H4*H4
                     H2=2.0D0*H3*H4
                     CALL CDIV(DX,DY,H1,H2,H3,H4)
                     IF(ABSCOM(H3,H4) .LT. 50.0D0*DZMIN) THEN
                        DX=DX+H3
                        DY=DY+H4
                     END IF
                  END IF
                  XOLD=XNEW
                  YOLD=YNEW
                  PBOLD=PBNEW
               ELSE
!
! In a neighborhood of a saddle point.
!
                  I=0
                  H=DZMAX/PBNEW
                  DX=H*UNEW
                  DY=H*VNEW
                  XOLD=XNEW
                  YOLD=YNEW
                  PBOLD=PBNEW
   20             CALL COMHOR(XNEW+DX,YNEW+DY,N,GAMMA,U,V,H,H1, &
                              H2,H3,H4,H5,A,B,C)
                  IF(DABS(ABSCOM(U,V)/PBNEW-1.0D0) .LE. RHO) THEN
                     DX=2.0D0*DX
                     DY=2.0D0*DY
                     GOTO 20
                  END IF
               END IF
            ELSE
               I=0
               NUMIT=NUMIT+1
               H=QR*DX-QI*DY
               DY=QR*DY+QI*DX
               DX=H
            END IF
            IF(ENDIT) THEN
               IF(ABSCOM(DX,DY) .LT. 0.1D0*BDZE) THEN
                  XNEW=XNEW+DX
                  YNEW=YNEW+DY
```

```
               END IF
               CALL COMHOR(XNEW,YNEW,N,GAMMA,UNEW,VNEW,UDNEW, &
                           VDNEW,UDDNEW,VDDNEW,BD,BDD,A,B,C)
               RETURN
            ELSE
               XNEW=XOLD+DX
               YNEW=YOLD+DY
               DZMIN=BETA*(RHO+ABSCOM(XNEW,YNEW))
               CALL COMHOR(XNEW,YNEW,N,GAMMA,UNEW,VNEW,UDNEW, &
                           VDNEW,UDDNEW,VDDNEW,BD,BDD,A,B,C)
               PBNEW=ABSCOM(UNEW,VNEW)
               IF(PBNEW .EQ. 0.0D0) THEN
                  RETURN
               ELSE IF(ABSCOM(DX,DY) .GT. DZMIN .AND. &
                      PBNEW .GT. BD) THEN
                  GOTO 10
               ELSE
                  ENDIT=.TRUE.
                  BDZE=ABSCOM(DX,DY)
                  GOTO 10
               END IF
            END IF
         END IF
      END IF
      END
!
!
      SUBROUTINE COMHOR(X,Y,N,GAMMA,U,V,UD,VD,UDD,VDD,BDP,BDPD,A,B,C)
!
!*****************************************************************
!                                                                *
! This SUBROUTINE calculates the complex functional value        *
! PN(X+I*Y)=(U+I*V), the complex valued derivatives              *
! PN'(X+I*Y)=(UD+I*VD) and PN''(X+I*Y)=(UDD+I*VDD) of a polymial*
! PN(Z) of degree N (N>0) with complex coefficients by using     *
! the Horner-scheme.                                             *
! Additionally bounds BDP and BDPD are computed for the          *
! rounding errors in computing DABS(PN(Z)) and DABS(PN'(Z)).     *
! The complex coefficients of PN are stored in a 2-dimensional   *
! array A(1:2*(N+1)), arranged in descending order of the        *
! powers (they will remain unchanged by this subroutine).        *
! The complex coefficients of the polynomial Q(Z) of degree N-1  *
! are stored in the array B(1:2*(N+1)), arranged in descending   *
! order. Here Q(Z) is defined by PN(Z)=Q(Z)*(Z-Z0)+PN(Z0).       *
! The array C(1:2*N) is used as an auxiliary array.              *
!                                                                *
!                                                                *
! INPUT PARAMETERS:                                              *
! ================                                               *
! X        : real part of the value for which the functional     *
!            value and its 1st and 2nd derivatives are to be     *
!            computed for the polynomial PN.                     *
! Y        : imaginary part of the value for which the           *
!            functional value and its 1st and 2nd derivatives    *
!            are to be computed for the polynomial PN.           *
! GAMMA    : error bound.                                        *
```

```
!                                                                      *
!                                                                      *
! OUTPUT PARAMETERS:                                                   *
! ==================                                                   *
! U        : real part of PN(X+I*Y).                                   *
! V        : imaginary part of PN(X+I*Y).                              *
!                                                                      *
! UD       : real part of PN'(X+I*Y).                                  *
! VD       : imaginary part of PN'(X+I*Y).                             *
!                                                                      *
! UDD      : real part of PN''(X+I*Y).                                 *
! VDD      : imaginary part of PN''(X+I*Y).                            *
!                                                                      *
! BDP      : bound for the rounding error of DABS(PN(Z)).              *
! BDPD     : bound for the rounding error of DABS(PN'(Z)).             *
!                                                                      *
!
      IMPLICIT DOUBLE PRECISION (a-h,o-z)
      DIMENSION A(500),B(500),C(500)
      C(1)=A(1)
      B(1)=A(1)
      C(2)=A(2)
      B(2)=A(2)
      BDPD=ABSCOM(A(1),A(2))
      BDP=BDPD
      MS=N-1
      M=N
      J=N
      NM2P1=N*2+1
      DO 10 K=3,NM2P1,2
         J=J-1
         H1=X*B(K-2)-Y*B(K-1)
         H2=Y*B(K-2)+X*B(K-1)
         B(K)=A(K)+H1
         B(K+1)=A(K+1)+H2
         H3=ABSCOM(A(K),A(K+1))
         H4=ABSCOM(H1,H2)
         H=H3
         IF(H3 .LT. H4) H=H4
         IF(H .GT. BDP) THEN
            BDP=H
            M=J
         END IF
         IF(K .EQ. NM2P1) THEN
            GOTO 20
         ELSE
            H1=X*C(K-2)-Y*C(K-1)
            H2=Y*C(K-2)+X*C(K-1)
            C(K)=B(K)+H1
            C(K+1)=B(K+1)+H2
            H3=ABSCOM(B(K),B(K+1))
            H4=ABSCOM(H1,H2)
            H=H3
            IF(H3 .LT. H4) H=H4
            IF(BDPD .LT. H) THEN
               BDPD=H
               MS=J-1
```

```
            END IF
         END IF
   10 CONTINUE
   20 CONTINUE
      U=B(2*N+1)
      V=B(2*N+2)
      UD=C(2*N-1)
      VD=C(2*N)
      H=ABSCOM(X,Y)
      IF(H .NE. 0.0D0) THEN
         BDP=BDP*FLOAT(M+1)*H**M
         BDPD=BDPD*FLOAT(MS+1)*H**MS
      ELSE
         BDP=ABSCOM(U,V)
         BDPD=ABSCOM(UD,VD)
      END IF
      BDP=BDP*GAMMA
      BDPD=BDPD*GAMMA
      IF(N .GT. 1) THEN
         H1=C(1)
         H2=C(2)
         NM2M3=N*2-3
         DO 30 K=3,NM2M3,2
            H=C(K)+X*H1-Y*H2
            H2=C(K+1)+Y*H1+X*H2
            H1=H
   30    CONTINUE
         UDD=2.0D0*H1
         VDD=2.0D0*H2
         RETURN
      ELSE
         UDD=0.0D0
         VDD=0.0D0
         RETURN
      END IF
      END
!
!

      DOUBLE PRECISION FUNCTION ABSCOM(X,Y)
!
!*****************************************************************
!                                                                *
! This FUNCTION-subroutine calculates the absolute value of a    *
! complex number (X+I*Y).                                        *
!                                                                *
!                                                                *
! INPUT PARAMETERS:                                              *
! =================                                              *
! X        : real part of the complex number.                    *
! Y        : imaginary part of the complex number.               *
!                                                                *
!                                                                *
! OUTPUT PARAMETER:                                              *
! =================                                              *
! ABSCOM   : absolute value of the complex number.               *
!                                                                *
```

```
!
      IMPLICIT DOUBLE PRECISION (a-h,o-z)
      IF(X .NE. 0.0D0 .OR. Y .NE. 0.0D0) THEN
         IF(DABS(X) .GE. DABS(Y)) THEN
            ABSCOM=DABS(X)*DSQRT(Y/X*Y/X+1.0D0)
            RETURN
         ELSE
            ABSCOM=DABS(Y)*DSQRT(X/Y*X/Y+1.0D0)
            RETURN
         END IF
      ELSE
         ABSCOM=0.0D0
         RETURN
      END IF
      END
!
!


      SUBROUTINE MCONST(FMACHP,INFINY,SMALNO,BASE)
!
!*****************************************************************
!                                                                *
! This subroutine sets up some constants that are machine        *
! dependent.                                                     *
!                                                                *
!                                                                *
! OUTPUT PARAMETERS:                                             *
! ==================                                             *
! FMACHP   : machine constant for DOUBLE PRECISION.              *
! INFINY   : largest representable floating-point number.        *
! SMALNO   : smallest representable floating-point number.       *
! BASE     : base of the floating-point number system used to    *
!            represent machine numbers.                          *
!                                                                *
!                                                                *
! Description of the auxiliary variables:                        *
! ========================================                       *
! I        : number of digits of the floating-point mantissa     *
!            of DOUBLE PRECISION numbers.                        *
! M        : largest allowed exponent.                           *
! N        : smallest allowed exponent.                          *
!                                                                *
!
      IMPLICIT DOUBLE PRECISION (a-h,o-z)
       DOUBLE PRECISION INFINY
      BASE=8.0D0
      I=29
      M=322
      N=-293
      FMACHP=1.0D0
   10 FMACHP=0.5D0*FMACHP
      IF(1.0D0 .LT. 1.0D0+FMACHP) GOTO 10
      FMACHP=2.0D0*FMACHP
      INFINY=BASE*(1.0D0-BASE**(-I))*BASE**(M-1)
      SMALNO=(BASE**(N+3))/BASE**3
      RETURN
      END
```

```
!
!
      DOUBLE PRECISION FUNCTION SCALFC(NN,PT,FMACHP,INFINY,SMALNO, &
                                       BASE)
!
!*****************************************************************
!                                                                *
! This FUNCTION-subroutine calculates a scaling factor which     *
! is used to scale the polynomial coefficients.                  *
!                                                                *
!                                                                *
! INPUT PARAMETERS:                                              *
! ================                                               *
! NN       : 1 + the degree of the polynomial.                   *
! PT       : nn-vector PT(1:NN) containing the absolute          *
!            values of the polynomial's coefficients.            *
! FMACHP   : machine constant for DOUBLE PRECISION.              *
! INFINY   : largest representable floating-point number.        *
! SMALNO   : smallest representable floating-point number.       *
! BASE     : base for the floating-point number system used by   *
!            the machine.                                        *
!                                                                *
!                                                                *
! OUTPUT PARAMETER:                                              *
! ================                                               *
! SCALFC  : scaling factor.                                      *
!                                                                *
!
      IMPLICIT DOUBLE PRECISION (a-h,o-z)
      DIMENSION PT(NN)
       DOUBLE PRECISION MAX, MIN    ,INFINY
      HI=DSQRT(INFINY)
      LO=SMALNO/FMACHP
      MAX=0.0D0
      MIN=INFINY
      DO 10 I=1,NN
         X=PT(I)
         IF(X .GT. MAX) MAX=X
         IF(X .NE. 0.0D0 .AND. X .LT. MIN) MIN=X
   10 CONTINUE
      SCALFC=1.0D0
      IF(MIN .GE. LO .AND. MAX .LE. HI) THEN
         RETURN
      ELSE
         X=LO/MIN
         IF(X .GT. 1.0D0) THEN
            SC=X
            IF(INFINY/SC .GT. MAX) SC=1.0D0
         ELSE
            SC=1.0D0/(DSQRT(MAX)*DSQRT(MIN))
         END IF
         L=DLOG(SC)/DLOG(BASE)+0.5D0
         SCALFC=BASE**L
      END IF
      RETURN
      END
!
```

```
!
      SUBROUTINE CDIV(A,B,C,D,X,Y)
!
!*****************************************************************
!                                                                *
! This SUBROUTINE performs a complex division                    *
!          (X+I*Y) := (A+I*B)/(C+I*D).                           *
!                                                                *
!                                                                *
! INPUT PARAMETERS:                                              *
! ================                                               *
! A        : real part of the numerator.                         *
! B        : imaginary part of the numerator.                    *
!                                                                *
! C       : real part of the denominator.                        *
!  D        : imaginary part of the denominator.                 *
!                                                                *
!                                                                *
!  OUTPUT PARAMETERS:                                            *
!  =================                                             *
!  X        : real part of the quotient.                         *
!  Y        : imaginary part of the quotient.                    *
!                                                                *
!                                                                *
!  NOTE: If the denominator's real and imaginary parts are both  *
!        equal to zero, the program is aborted with a detailed   *
!        error message.                                          *
!                                                                *
!*****************************************************************
!
      IMPLICIT DOUBLE PRECISION (a-h,o-z)
      IF(C .NE. 0.0D0 .OR. D .NE. 0.0D0) THEN
         IF(A .NE. 0.0D0 .OR. B .NE. 0.0D0) THEN
            IF(DABS(A) .GT. DABS(B)) THEN
               U=A
               AM=1.0D0
               AN=B/A
            ELSE
               U=B
               AM=A/B
               AN=1.0D0
            END IF
            IF(DABS(C) .GT. DABS(D)) THEN
               V=C
               P=1.0D0
               Q=D/C
            ELSE
               V=D
               P=C/D
               Q=1.0D0
            END IF
            F=U/V
            V=P*P+Q*Q
            U=(AM*P+AN*Q)/V
            X=U*F
            U=(-AM*Q+AN*P)/V
            Y=U*F
```

```
      RETURN
   ELSE
      X=0.0D0
      Y=0.0D0
      RETURN
   END IF
ELSE
   WRITE(*,*)'DIVISION BY ZERO IN SUBROUTINE CDIV'
   STOP
END IF
END
```

INITIAL DISTRIBUTION LIST

1.	Defense Technical Information Center 8725 John J. Kingman Rd., STE 0944 Ft. Belvoir, VA 22060-6218	2
2.	Dudley Knox Library Naval Postgraduate School Monterey, CA 93943	2
3.	Mechanical Engineering Department Chairman, Code ME Naval Postgraduate School Monterey, CA 93943	1
4.	Naval/Mechanical Engineering Curriculum Code 34 Naval Postgraduate School Monterey, CA 93943	1
5.	Professor Young S. Shin, Code ME/Sg Department of Mechanical Engineering Naval Postgraduate School Monterey, CA 93943 yshin@nps.navy.mil	2
6.	Visiting Professor Ilbae Ham Department of Mechanical Engineering Naval Postgraduate School Monterey, CA 93943	1
7.	Frederick A. Costanzo Underwater Explosion Research Department (UERD) Naval Surface Warfare Center - Carderock Division 9500 MacArthur Blvd. West Bethesda, MD 20817 - 5700 CostanzoFA@nswccd.navy.mil	1
8.	Steven E. Rutgerson Underwater Explosion Research Department (UERD) Naval Surface Warfare Center - Carderock Division 9500 MacArthur Blvd. West Bethesda, MD 20817 - 5700 RutgersonSE@nswccd.navy.mil	1

9. Greg Harris 1
Code 440A
Indian Head Division
Naval Surface Warfare Center
101 Strauss Ave
Indian Head MD 20640-5035
HarrisGS@ih.navy.mil